*Supporting Information for*

## Copper Catalyzed Benzylic sp³ C-H Alkenylation

Ting-An Chen,[a,b] Richard J. Staples,[b] and Timothy H. Warren[b,*]

[a]Department of Chemistry, Georgetown University, Washington, DC 20057

[b]Department of Chemistry, Michigan State University, East Lansing, MI 48824

### Table of Contents for Supporting Information

## 1. General Procedures and Instrumentation

All catalytic reactions were carried out in a nitrogen-filled glovebox. Molecular sieves (4A, 4–8 mesh beads) were obtained from Fisher Scientific and activated in vacuo at 310 °C for 48 h. Extra dry solvents (≥99.5%) with Acroseal® and deuterated solvents were purchased from Acros Organics and Cambridge Isotope Laboratories, respectively. Both anhydrous and deuterated solvents were sparged with nitrogen and stored over activated 4A molecular sieves under a nitrogen atmosphere. All reagents were purchased from Sigma, TCI, Oakwood, Combi-Block, and Strem and sparged with nitrogen and stored over 4A molecular sieves before use without further purification. $\beta$-diketiminato copper catalysts [Cl$_2$NN]Cu,[1] [Me$_3$NN]Cu,[2] [$^i$Pr$_2$NN]Cu,[3] [$^i$Pr$_2$NN$_{F6}$]Cu,[4] [(MeO)$_2$NN]Cu,[5] and [Cl$_2$NN$_{F6}$]Cu[5] were synthesized and characterized according to literature procedures.

NMR spectra were recorded on a Varian 500 MHz spectrometer at r.t. unless otherwise noted. The chemical shift ($\delta$) values are expressed in ppm relative to tetramethylsilane, whereas the residual $^1$H signal of deuterated solvent served as an internal standard. Boron trifluoride diethyl etherate serves as an external reference for $^{11}$B NMR ($\delta$ = 0.0 ppm). UV−vis spectra were recorded on an Agilent 8454 Diode Array spectrometer equipped with a stirrer and Unisoku USP−203 cryostat for variable temperature (−40 to 40 °C) experiments. GC−MS analyses of the reaction mixtures were performed on a Shimadzu GCMS-QP2010 SE. Identification of products was carried out by comparing their GC retention times, electron ionization (EI) mass spectra, and NMR spectra with those of the authentic compounds. Elemental analysis was performed on FlashSmar Elemental Analyzer, FlashSmart NC SOIL. HRMS analysis of new organic molecules were performed on Thermo Scientific Q Exactive™ Plus Hybrid Quadrupole-Orbitrap™ Mass Spectrometer with an electrospray Ionization (ESI) interface in the positive ionization mode at full scan mode and Leco GC-HRT+ GC/Time-of-Flight MS.
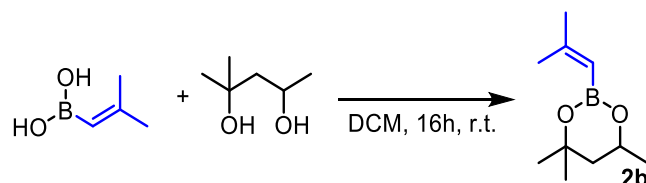
## 2. Optimization of Catalytic C-H Alkenylation

**Synthesis of 2-(2-methylprop-1-en-1-yl)-1,3,2-dioxaborinane (2a)**
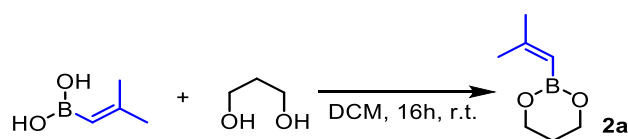


2-(2-methylprop-1-en-1-yl)-1,3,2-dioxaborinane (**2a**) was synthesized according to a literature procedure.[6] 2,2-Dimethylethenylboronic acid (1.0 g, 8.6 mmol) was mixed with 1,3-propanediol (0.72 g, 9.5 mmol) in 50 mL dichloromethane (DCM) for 16 h at r.t. The DCM solution was then washed with NaHCO$_3$, brine, dried over MgSO$_4$ and concentrated before transferring to glovebox. Yield: 63 %. ^{1}H NMR (500 MHz, CDCl$_3$): δ 4.99 (p, $J$ = 1.2 Hz, 1H), 4.03 (t, 4H), 1.99 – 1.90 (m, 5H), 1.83 (d, $J$ = 1.3 Hz, 3H). ^{13}C{^{1}H} NMR (126 MHz, CDCl$_3$): δ 156.65, 61.72, 29.32, 27.58, 22.09 (missing α-C to boron due to broadening by [10/11]B nuclei). ^{11}B NMR (160 MHz, CDCl$_3$): δ 26.25. HRMS (CI) m/z calcd. For C$_7$H$_{14}$BO$_2^+$ 141.1081, found 141.1080.

**Synthesis of 4,4,6-trimethyl-2-(2-methylprop-1-en-1-yl)-1,3,2-dioxaborinane (2b)**



4,4,6-trimethyl-2-(2-methylprop-1-en-1-yl)-1,3,2-dioxaborinane (**2b**) was synthesized according to a literature procedure.[6] 2,2-Dimethylethenylboronic acid (1.0 g, 8.6 mmol) was mixed with 1,3-propanediol (0.72 g, 9.5 mmol) in 50 mL DCM for 16 h at r.t. The DCM solution was further washed with NaHCO$_3$, brine, dried over MgSO$_4$ and concentrated before transferring to glovebox. Yield: 74 %. ^{1}H NMR (500 MHz, CDCl$_3$): δ 5.03 (p, J = 1.3 Hz, 1H), 4.21 (ddd, J = 4.9, 3.6, 2.4 Hz, 1H), 1.94 (d, J = 1.3 Hz, 3H), 1.82 (d, J = 1.4 Hz, 3H), 1.77 (ddd, J = 13.8, 3.0, 1.2 Hz, 1H), 1.49 (dd, J = 13.8, 11.6 Hz, 1H), 1.30 (t, J = 1.5 Hz, 6H), 1.26 (dd, J = 6.2, 1.3 Hz, 3H). ^{13}C{^{1}H} NMR NMR (126 MHz, CDCl$_3$): δ 155.97, 70.72, 64.72, 46.07, 31.52, 29.29, 28.35, 23.42, 21.99 (missing α-C to boron due to broadening by [10/11]B nuclei). ^{11}B NMR (160 MHz, CDCl$_3$): δ 25.88. HRMS (CI) m/z calcd. For C$_{10}$H$_{20}$BO$_2^+$ 183.1551, found 183.1544.

**Synthesis of prenylbenzene (3a) and 2-methyl-4-phenyl-2-pentene (3j) via Wittig reaction**
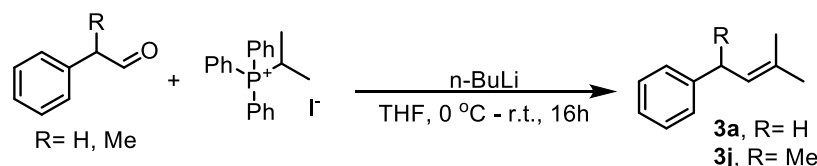


To enable determination of the C-H alkenylation yield by GCMS, the C-H alkenylation products **3a** and **3j** were synthesized via a Wittig reaction.[7] Under a nitrogen atmosphere in a glovebox, n-

butyl lithium (2.0 M in hexane, 1.0 mL, 2.0 mmol) was slowly added dropwise to a THF solution (6 mL) containing isopropyltriphenylphosphonium iodide (0.86 g, 2.0 mmol, obtained from Sigma) at 0 °C and stirred for 2 h. Subsequently, aldehyde (1.0 mmol) in THF (1.6 mL) was introduced to the reaction mixture at r.t. and stirred for 16 h. The mixture of the crude was extracted to ethyl acetate and washed with brine. The products were isolated via flash column chromatography (diethyl ether/ethyl acetate). **3a** Yield: 62%. **3a**: $^1$H NMR (500 MHz, CDCl$_3$) δ 7.28 (m, 2H), 7.19 (d, J = 6.9 Hz, 3H), 5.34 (m, 1H), 3.35 (d, J = 7.3 Hz, 2H), 1.74 (d, J = 12.5 Hz, 6H).$^{13}$C{$^1$H} NMR (126 MHz, CDCl$_3$) δ 141.98, 132.66, 128.49, 128.45, 125.83, 123.33, 34.51, 25.90, 17.97. **3j** Yield: 52%. **3j**: $^1$H NMR (500 MHz, CDCl$_3$) δ 7.30 (t, J = 7.5 Hz, 2H), 7.25 (m, 2H), 7.18 (t, J = 7.2 Hz, 1H), 5.30 (m, 1H), 3.67 (m, 1H), 1.70 (d, J = 14.0 Hz, 5H), 1.32 (d, J = 7.0 Hz, 2H). $^{13}$C{$^1$H} NMR (126 MHz, CDCl$_3$) δ 147.43, 130.63, 130.29, 128.48, 127.01, 125.84, 38.27, 25.96, 22.58, 18.09. NMR characterization details of isolated **3a** and **3j** were in good agreement with data reported for these compound in the literature.[7,8]

**Independent synthesis of benzyl *t*-butyl ether: a side product in toluene C-H alkenylation**
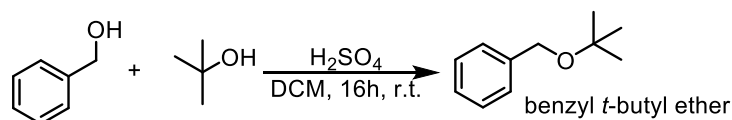


Benzyl *t*-butyl ether (PhCH$_2$-O$^t$Bu) was prepared through acid-catalyzed etherification following a literature procedure.[9] Sulfuric acid (0.55 mL, 10 mmol) and magnesium sulfate (4.8 g, 40 mmol) were combined in DCM (30 mL) and stirred for 15 min. The mixture of benzyl alcohol (10 mmol, 1.0 mL) and *t*-butanol (4.8 mL, 50 mmol) in DCM (10 mL) was subsequently added to the solution and stirred for 16 h at r.t. The reaction was further neutralized by saturated NaHCO$_3$ and concentrated on rotovap. The product was isolated via flash column chromatography (hexane/DCM). Yield: 63 %. $^1$H NMR (500 MHz, CDCl$_3$): δ 7.38 – 7.30 (m, 4H), 7.24 (m, 1H), 4.45 (s, 2H), 1.30 (s, 9H). $^1$H NMR characterization details of isolated benzyl *t*-butyl ether were in good agreement with data reported for this compound in the literature.[10]

**Examination of alkenyl boronate substrates for C-H alkenylation**
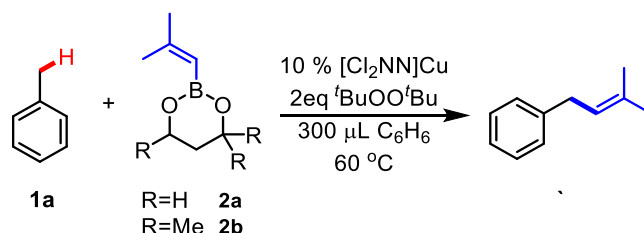


Since the boronate ester backbone could influence the yield in copper-catalyzed sp$^3$ C-H arylation with aryl boronate esters, we examined a couple of different alkenyl boronate esters for this sp$^3$ C-H alkenylation protocol. For example, 4,4,6-trimethyl-2-phenyl-1,3,2-dioxaborinane exhibited a higher yield in sp$^3$ C-H arylation compared to phenylboronic acid pinacol ester.[6] Therefore, we

chose to use the 4,4,6-trimethyl-1,3,2-dioxaborinane and 1,3,2-dioxaborinane backbones as the model substrates for alkenylation.

In a nitrogen filled glovebox, the alkenyl boronate ester (**2a** or **2b**) (0.38 mmol, 1 equiv.) and [Cl$_2$NN]Cu (16 mg, 0.038 mmol, 10 mol%) was dissolved in dry toluene (760 μL, 7.2 mmol, 20 equiv.) and benzene (300 μL) in a 5 mL thick-walled pressure vessel. $^t$BuOO$^t$Bu (132 μL, 0.72 mmol, 2 equiv.) was added and the solution was immediately sealed and heated to 60 °C. After 3 h, the reaction was allowed to cool to r.t. and quenched by exposure to air. 1,2,4,5-tetrachlorobenzene was added to the product mixture as an internal standard and yields were determined by GCMS analysis based on response factors determined between the internal standard and an authentic sample of the product **3a** prepared via independent synthesis.

Under the same reaction conditions, alkenylation of **2a** yielded prenylbenzene (**3a**) in 63% yield, while **2b** produced 15% of **3a** along with 30% of the etherification product (benzyl *t*-butyl ether). These products were identified and quantified by GCMS employing authentic standards. This outcome suggested that the transmetalation rate of [Cu$^{II}$]-O$^t$Bu with alkenyl boronate ester **2b** is slower than with **2a** to form the key [Cu$^{II}$]-CH=CMe$_2$ intermediate. The benzyl radical (PhCH$_2$•) (generated via H-atom abstraction from the substrate PhCH$_2$-H via $^t$BuO•) couples with [Cu$^{II}$]-O$^t$Bu rather than the anticipated [Cu$^{II}$]-C=CMe$_2$ intermediate (**Scheme S1**).
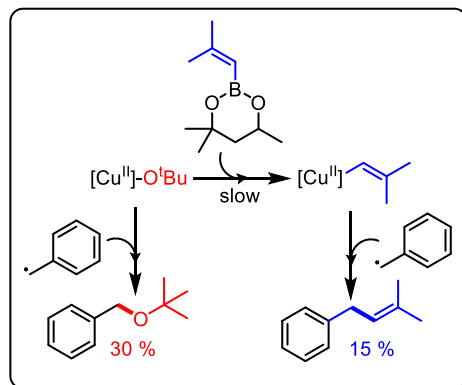


**Scheme S1.** Slow transmetalation to form the key [Cu$^{II}$]-CH=CMe$_2$ intermediate can lead to undesired C-H etherification of the benzylic radical formed during the reaction.

**Method for quantitative analysis of C-H alkenylation products via GCMS**

The GC yields of alkenylation products presented in Table 2 were determined using calibration curves prepared from authentic products and 1,2,4,5-tetrachlorobenzene as an internal standard.

*Example of calibration curve construction for GCMS analysis*: Mixtures containing various molar ratios of **3a** and the internal standard (0:1, 0.1:1, 0.5:1, and 1:1) were prepared for $^1$H NMR analysis in deuterated solvents such as C$_6$D$_6$ or CDCl$_3$. The $^1$H NMR integrations of **3a** and the internal standard enhance the accuracy of determining the mole ratio. Subsequently, these $^1$H NMR samples were diluted 100 times with DCM for GCMS analysis. The calibration curve was generated by analyzing solutions with different molar ratios of **3a** to the internal standard and plotting their respective area ratios from GCMS

(Figure S1). This calibration curve enables the determination of the yield of **3a** directly from C-H alkenylation reaction mixtures.
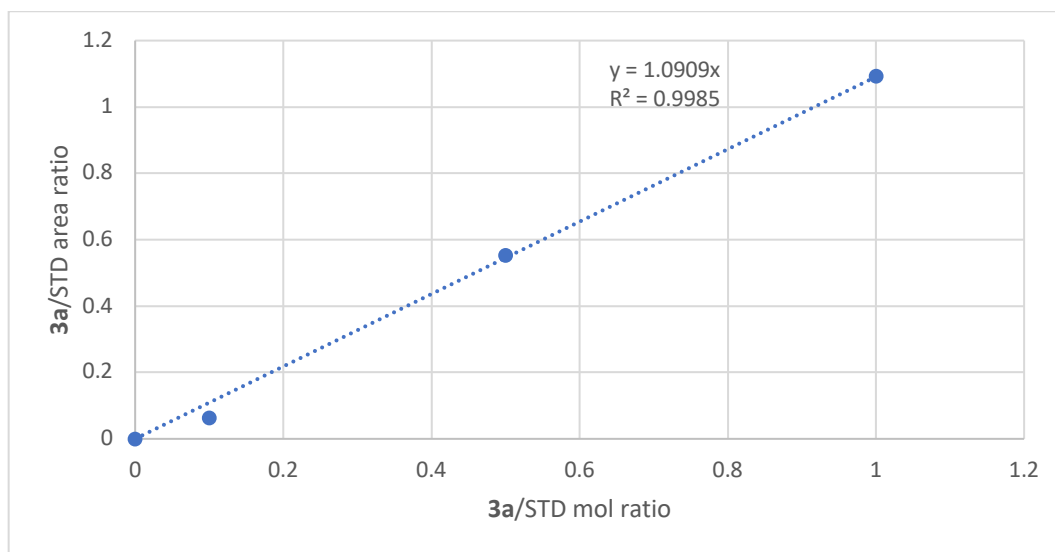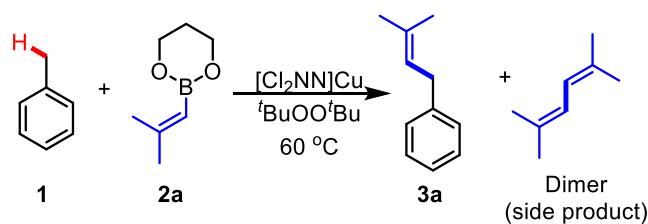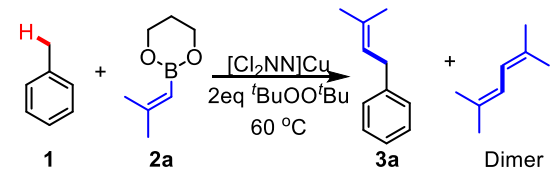


**Figure S1.** GCMS calibration curve of **3a** to the 1,2,4,5-tetrachlorobenzene standard.


**Examining 2,5-dimethyl-2,4-hexadiene (alkenyl dimer) formation in C-H alkenylation with 2a**
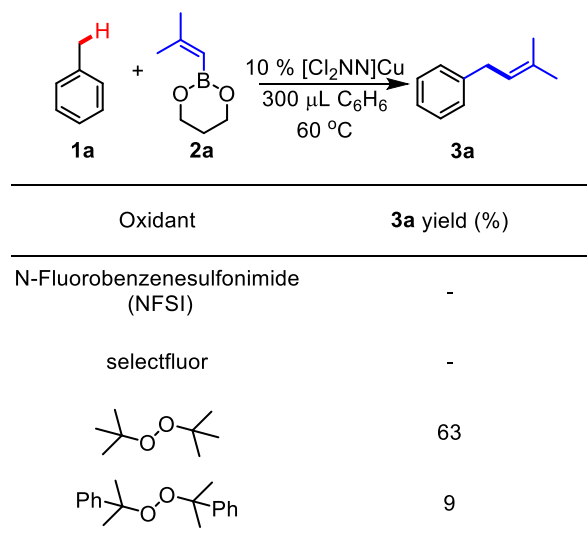


Because of the radical nature of the [Cu$^{II}$]-CH=CMe$_2$ intermediate, we expected the formation of 2,5-dimethyl-2,4-hexadiene (alkene dimer) through self-coupling. Therefore, for alkenylation optimization, we adjusted the catalyst loading and solvent volume to reduce dimerization. In a nitrogen filled glovebox, **2a** (58 μL, 0.38 mmol, 1 equiv.), [Cl$_2$NN]Cu (5, 10, and 20 mol%) were dissolved in dry toluene (760 μL, 7.2 mmol, 10 equiv.) and benzene (0, 100, and 300 μL) in a 5 mL thick-walled pressure vessel. $^t$BuOO$^t$Bu (132 μL, 0.72 mmol, 2 equiv.) was added, and the solution was immediately sealed and heated to 60 °C. After 1 h, the reaction was allowed to cool to r.t. and quenched by exposure to air. 1,2,4,5-tetrachlorobenzene was added to the reaction mixture as an internal standard and yields were determined by GCMS analysis.

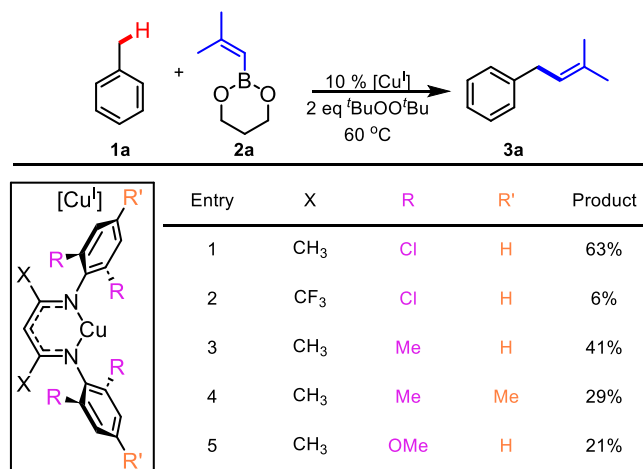**Table S1.** C-H alkenylation and alkenyl dimer formation.



| Benzene | Equiv. R-H | Catalyst loading (%) | 3a yield (%) | Dimer (%) |
|---------|-----------|----------------------|--------------|-----------|
| - | 10 | 10 | 17 | 20 |
| 100 μL | 10 | 10 | 19 | 11 |
| 300 μL | 10 | 10 | 20 | 4 |
| 300 μL | 10 | 5 | 13 | 40 |
| 300 μL | 10 | 20 | 19 | 2 |
| - | 20 | 10 | 36 | 27 |
| 100 μL | 20 | 10 | 39 | 18 |
| 300 μL | 20 | 10 | 63 | 4 |

## Oxidant optimization for C-H alkenylation with 2a

In a nitrogen filled glovebox, **2a** (58 μL, 0.38 mmol, 1 equiv.), [Cl$_2$NN]Cu (16 mg, 0.038 mmol, 10 mol%) was dissolved in dry toluene (760 μL, 7.2 mmol, 20 equiv.) and benzene (300 μL) in a 5 mL thick-walled pressure vessel. The corresponding oxidant (0.72 mmol, 2 equiv.) was added, and the solution was immediately sealed and heated to 60 °C. After 16 h, the reaction was allowed to cool to r.t. and quenched by exposure to air. 1,2,4,5-tetrachlorobenzene was added to the reaction mixture as an internal standard and yields of **3a** were determined by GCMS analysis.

**Table S2.** Oxidant optimization.



| Oxidant | 3a yield (%) |
|---|---|
| N-Fluorobenzenesulfonimide (NFSI) | - |
| selectfluor | - |
| (tBuOOtBu structure) | 63 |
| (Ph-peroxide structure) | 9 |

## Catalyst optimization for C-H alkenylation with 2a

In a nitrogen filled glovebox, **2a** (58 μL, 0.38 mmol, 1 equiv.) and the β-diketiminatio copper(I) catalyst [Cu] (0.038 mmol, 10 mol%) were dissolved in dry toluene (760 μL, 7.2 mmol, 20 equiv.) and benzene (300 μL) in a 5 mL thick-walled pressure vessel. $^t$BuOO$^t$Bu (132 μL, 0.72 mmol, 2 equiv.) was added and the solution was immediately sealed and heated to 60 °C. After 1 h, the reaction was allowed to cool to r.t. and quenched by exposure to air. 1,2,4,5-tetrachlorobenzene was added to the reaction mixture as an internal standard and yields of **3a** were determined by GCMS analysis.

**Table S3.** Catalyst optimization. (Also appears as Table 1 in the manuscript).



| Entry | X | R | R' | Product |
|---|---|---|---|---|
| 1 | CH$_3$ | Cl | H | 63% |
| 2 | CF$_3$ | Cl | H | 6% |
| 3 | CH$_3$ | Me | H | 41% |
| 4 | CH$_3$ | Me | Me | 29% |
| 5 | CH$_3$ | OMe | H | 21% |

## Temperature, R-H loading and oxidant loading optimization

In a nitrogen filled glovebox, **2a** (58 μL, 0.38 mmol, 1 equiv.) and [Cl$_2$NN]Cu (16 mg, 0.038 mmol, 10 mol%) were dissolved in dry toluene (10, 20, and 40 equiv.) along with benzene (300 μL) in a

5 mL thick-walled pressure vessel. $^tBuOO^tBu$ (1.5, 2, 3, and 5 equiv.) was added and the solution was immediately sealed and heated to the corresponding temperature. After 16 h, the reaction was allowed to cool to r.t. and quenched by exposure to air. 1,2,4,5-tetrachlorobenzene was added to the reaction mixture as an internal standard and the yield of **3a** was determined by GCMS analysis.

**Table S4.** Temperature, R-H loading, and oxidant loading optimization.
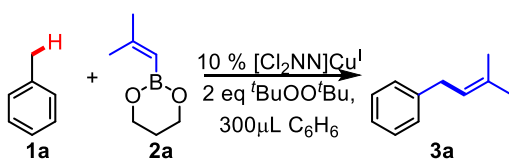


| Equiv. R-H | Temp (°C) | Equiv. $^tBuOO^tBu$ | 3a yield (%) |
|---|---|---|---|
| 40 | 50 | 2 | 49 |
| 40 | 60 | 2 | 63 |
| 40 | 70 | 2 | 52 |
| 40 | 90 | 2 | 45 |
| 40 | 60 | 5 | 52 |
| 40 | 60 | 3 | 54 |
| 40 | 60 | 1.5 | 54 |
| 20 | 60 | 2 | 63 |
| 10 | 60 | 2 | 22 |

## 3. C-H Alkenylation of a Range of C-H Substrates with Alkenylboronate (2a)
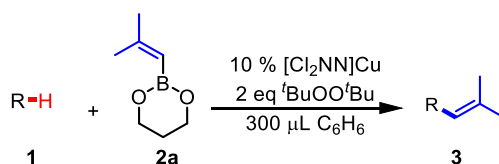
**Table 2, entry 3a: (3-methylbut-2-en-1-yl)benzene.**
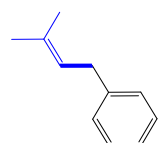
In a nitrogen filled glovebox, **2a** (58 μL, 0.36 mmol, 1 equiv.) and [Cl$_2$NN]Cu (16 mg, 0.038 mmol, 10 mol%) were dissolved in dry toluene substrate (760 μL, 7.2 mmol, 20 equiv.) with benzene (300 μL) in a 5 mL thick-walled pressure vessel. $^t$BuOO$^t$Bu (132 μL, 0.72 mmol, 2 equiv.) was added and the solution was immediately sealed and heated to 60 °C. After 1 h, the reaction was allowed to cool to r.t. and quenched by exposure to air. The yield determined by GCMS analysis of the reaction mixture was 63 %. The authentic sample of **3a** synthesized from a Wittig reaction and from C-H alkenylation have the same retention times and fragmentation pattern as analyzed by GCMS. **3a**: $^1$H NMR (500 MHz, CDCl$_3$) δ 7.28 (m, 2H), 7.19 (d, J = 6.9 Hz, 3H), 5.34 (m, 1H), 3.35 (d, J = 7.3 Hz, 2H), 1.74 (d, J = 12.5 Hz, 6H).$^{13}$C{$^1$H} NMR (126 MHz, CDCl$_3$) δ 141.98, 132.66, 128.49, 128.45, 125.83, 123.33, 34.51, 25.90, 17.97. Full characterization details are given in the entry for this compound as synthesized via a Wittig reaction (page S3).

**Table 2, entry 3b: 1-methyl-4-(3-methylbut-2-en-1-yl)benzene.**
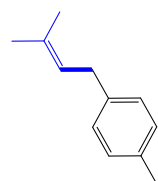
In a nitrogen filled glovebox, **2a** (58 μL, 0.36 mmol, 1 equiv.) and [Cl$_2$NN]Cu (16 mg, 0.038 mmol, 10 mol%) were dissolved in dry *p*-xylene substrate (886 μL, 7.2 mmol, 20 equiv.) with benzene (300 μL) in a 5 mL thick-walled pressure vessel. $^t$BuOO$^t$Bu (132 μL, 0.72 mmol, 2 equiv.) was added and the solution was immediately sealed and heated to 60 °C. After 1 h, the reaction was allowed to cool to r.t. and quenched by exposure to air. The yield determined by GCMS analysis of the reaction mixture was 64 %. The target product **3b** was isolated via flash column chromatography on 10 % silver nitrate-impregnated silica gel (100 % hexane). The isolation yield was 40 % as a colorless oil. $^1$H NMR (500 MHz, CDCl$_3$) δ 7.09 (dd, J = 7.9, 4.0 Hz, 4H), 5.31 (m, 1H), 3.30 (d, J = 7.4 Hz, 2H), 2.31 (s, 3H), 1.73 (d, J = 10.7 Hz, 6H). $^{13}$C{$^1$H} NMR (126 MHz, CDCl$_3$) δ 138.90, 135.27, 132.39, 129.19, 128.32, 123.62, 34.07, 25.90, 21.13, 17.95. NMR characterization details of isolated **3b** were in good agreement with data reported for this compound in the literature.[7]
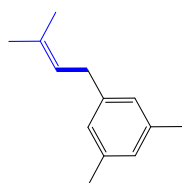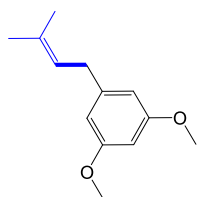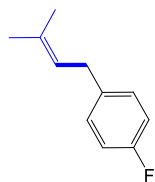
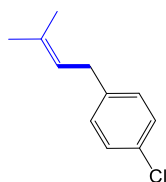**Table 2, entry 3c: 1-(tert-butyl)-4-(3-methylbut-2-en-1-yl)benzene.**
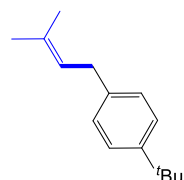
In a nitrogen filled glovebox, **2a** (58 μL, 0.36 mmol, 1 equiv.) and [Cl$_2$NN]Cu (16 mg, 0.038 mmol, 10 mol%) were dissolved in dry 1-(tert-butyl)-4-methylbenzene substrate (1.2mL, 7.2 mmol, 20 equiv.) with benzene (300 μL) in a 5 mL thick-walled pressure vessel. $^t$BuOO$^t$Bu (132 μL, 0.72 mmol, 2 equiv.) was added and

the solution was immediately sealed and heated to 60 °C. After 1 h, the reaction was allowed to cool to r.t. and quenched by exposure to air. The yield determined by GCMS analysis of the reaction mixture was 51 %. The target product **3c** was isolated via flash column chromatography on 10 % silver nitrate-impregnated silica gel (100 % hexane). The isolation yield was 21 % as a colorless oil. $^1$H NMR (500 MHz, CDCl$_3$): δ 7.31 (d, J = 8.2 Hz, 2H), 7.12 (d, J = 8.1 Hz, 2H), 5.34 (m, 1H), 3.32 (d, J = 7.4 Hz, 2H), 1.74 (d, J = 11.5 Hz, 6H), 1.31 (s, 9H). $^{13}$C{$^1$H} NMR (126 MHz, CDCl$_3$): δ 148.63, 138.89, 132.43, 128.09, 125.40, 123.52, 34.48, 33.95, 31.56, 25.91, 17.95. NMR characterization details of isolated **3c** were in good agreement with that reported for this compound in the literature.[11]

**Table 2, entry 3d: 1,3-dimethyl-5-(3-methylbut-2-en-1-yl)benzene.**

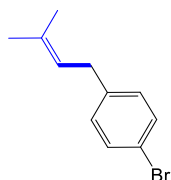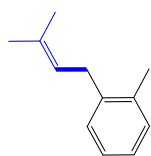In a nitrogen filled glovebox, **2a** (58 μL, 0.36 mmol, 1 equiv.) and [Cl$_2$NN]Cu (16 mg, 0.038 mmol, 10 mol%) were dissolved in dry mesitylene substrate (993 μL, 7.2 mmol, 20 equiv.) with benzene (300 μL) in a 5 mL thick-walled pressure vessel. $^t$BuOO$^t$Bu (132 μL, 0.72 mmol, 2 equiv.) was added and the solution was immediately sealed and heated to 60 °C. After 1 h, the reaction was allowed to cool to r.t. and quenched by exposure to air. The yield determined by GCMS analysis of the reaction mixture was 92 %. The target product **3d** was isolated via flash column chromatography on silica gel (100% hexane). The isolation yield was 75 % as a colorless oil. $^1$H NMR (500 MHz, CDCl$_3$) δ 6.81 (d, J = 11.8 Hz, 3H), 5.30 (m, 1H), 3.26 (d, J = 7.2 Hz, 3H), 2.29 (s, 6H), 1.73 (d, J = 10.6 Hz, 6H). $^{13}$C{$^1$H} NMR (126 MHz, CDCl$_3$): δ 141.89, 138.01, 132.30, 127.51, 126.26, 123.60, 34.38, 25.94, 21.43, 17.97. HRMS (CI) m/z calcd. For C$_{13}$H$_{17}$$^+$ 173.1325, found 173.1324.

**Table 2, entry 3e: 1,3-dimethoxy-5-(3-methylbut-2-en-1-yl)benzene.**

In a nitrogen filled glovebox, **2a** (58 μL, 0.36 mmol, 1 equiv.) and [Cl$_2$NN]Cu (16 mg, 0.038 mmol, 10 mol%) were dissolved in dry 1,3-dimethoxy-5-methylbenzene substrate (1.0 mL, 7.2 mmol, 20 equiv.) with benzene (300 μL) in a 5 mL thick-walled pressure vessel. $^t$BuOO$^t$Bu (132 μL, 0.72 mmol, 2 equiv.) was added and the solution was immediately sealed and heated to 60 °C. After 1 h, the reaction was allowed to cool to r.t. and quenched by exposure to air. The yield determined by GCMS analysis of the reaction mixture was 69 %. The target product **3e** was isolated via flash column chromatography (100 % hexane) for qualitative and quantitative analysis on GCMS. Due to the separation challenges, a significant amount of R-H substrate (1,3-dimethoxy-5-methylbenzene) could not be removed in $^1$H NMR. $^1$H NMR (500 MHz, CDCl$_3$): δ 6.36 (s, 2H), 5.31 (s, 1H), 3.80 (s, 6H), 3.28 (d, J = 7.2 Hz, 2H), 2.25 (s, 3H), 2.06 (s, 3H). The $^1$H NMR of partially isolated **3e** was in good agreement with previous literature.[12] HRMS (CI) m/z calcd. For C$_{13}$H$_{19}$O$_2$$^+$ 207.1385, found 207.1373.

**Table 2, entry 3f: 1-fluoro-4-(3-methylbut-2-en-1-yl)benzene.**

In a nitrogen filled glovebox, **2a** (58 μL, 0.36 mmol, 1 equiv.) and [Cl₂NN]Cu (16 mg, 0.038 mmol, 10 mol%) were dissolved in dry 1-fluoro-4-methylbenzene substrate (792 μL, 7.2 mmol, 20 equiv.) with benzene (300 μL) in a 5 mL thick-walled pressure vessel. ${}^{t}$BuOO${}^{t}$Bu (132 μL, 0.72 mmol, 2 equiv.) was added and the solution was immediately sealed and heated to 60 °C. After 1 h, the reaction was allowed to cool to r.t. and quenched by exposure to air. The yield determined by GCMS analysis of the reaction mixture was 50 %. The target product **3f** was isolated via flash column chromatography on 10 % silver nitrate-impregnated silica gel (100 % hexane) for qualitative and quantitative analysis on GCMS. Due to the low volatility of **3f**, trace amount of hexane could not be removed completely in ${}^{1}$H and ${}^{13}$C NMR. ${}^{1}$H NMR (500 MHz, CDCl₃): δ 7.11 (m, 2H), 6.95 (s, 2H), 5.29 (m, 1H), 3.31 (d, $J$ = 7.3 Hz, 2H), 1.75 (d, $J$ = 1.4 Hz, 3H), 1.71 (d, $J$ = 1.2 Hz, 3H). ${}^{13}$C{${}^{1}$H} NMR (126 MHz, CDCl₃): δ 161.34 (d, J = 243.2 Hz), 137.52, 132.93, 129.68, 123.16, 115.15, 33.64, 25.89, 17.94. NMR characterization details of **3f** were in good agreement with that reported for this compound in the literature.[7]

**Table 2, entry 3g: 1-chloro-4-(3-methylbut-2-en-1-yl)benzene.**

In a nitrogen filled glovebox, **2a** (58 μL, 0.36 mmol, 1 equiv.) and [Cl₂NN]Cu (16 mg, 0.038 mmol, 10 mol%) were dissolved in dry 1-chloro-4-methylbenzene substrate (848 μL, 7.2 mmol, 20 equiv.) with benzene (300 μL) in a 5 mL thick-walled pressure vessel. ${}^{t}$BuOO${}^{t}$Bu (132 μL, 0.72 mmol, 2 equiv.) was added and the solution was immediately sealed and heated to 60 °C. After 1 h, the reaction was allowed to cool to r.t. and quenched by exposure to air. The yield determined by GCMS analysis of the reaction mixture was 52 %. The target product **3g** was isolated via flash column chromatography on 10 % silver nitrate-impregnated silica gel (100 % hexane). The isolation yield was 38 % as a colorless oil. ${}^{1}$H NMR (500 MHz, CDCl₃): δ 7.23(d, $J$ = 8.3 Hz, 2H), 7.10 (dd, $J$ = 7.8, 1.3 Hz, 2H), 5.28 (m, 1H), 3.30 (d, $J$ = 7.4 Hz, 2H), 1.74 (q, $J$ = 1.3 Hz, 3H), 1.70 (d, $J$ = 1.3 Hz, 3H). ${}^{13}$C{${}^{1}$H} NMR (126 MHz, CDCl₃): δ 140.39, 129.78, 128.54, 122.73, 33.81, 25.89, 17.98 (2 resonances either coincident or missing). NMR characterization details of isolated **3g** were in good agreement with that reported for this compound in the literature.[7]

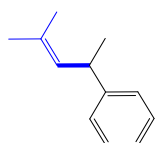**Table 2, entry 3h: 1-bromo-4-(3-methylbut-2-en-1-yl)benzene.**

In a nitrogen filled glovebox, **2a** (58 μL, 0.36 mmol, 1 equiv.) and [Cl₂NN]Cu (16 mg, 0.038 mmol, 10 mol%) were dissolved in dry 1-bromo-4-methylbenzene substrate (886 μL, 7.2 mmol, 20 equiv.) with benzene (300 μL) in a 5 mL thick-walled pressure vessel. ${}^{t}$BuOO${}^{t}$Bu (132 μL, 0.72 mmol, 2 equiv.) was added and the solution was immediately sealed and hea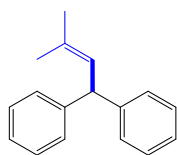ted to 60 °C. After 1 h, the reaction was allowed to cool to r.t. and quenched by exposure to air. The yield determined by GCMS analysis of the reaction mixture was 43 %. The target product **3h** was isolated via flash column chromatography on 10 % silver nitrate-impregnated silica gel (100 % hexane). The isolation yield was 34 % as a

colorless oil. ^{1}H NMR (500 MHz, CDCl$_3$): δ 7.38 (d, $J$ = 8.3 Hz, 2H), 7.04 (d, $J$ = 8.6 Hz, 2H), 5.27 (m, 1H), 3.29 (d, $J$ = 7.4 Hz, 2H), 1.75 (t, $J$ = 1.4 Hz, 3H), 1.71 (d, $J$ = 1.3 Hz, 3H). ^{13}C{^{1}H} NMR (126 MHz, CDCl$_3$): δ 140.91, 133.33, 131.48, 130.21, 122.62, 119.53, 33.87, 25.89, 17.98. NMR characterization details of isolated **3h** were in good agreement with data reported for this compound in the literature.[7]

**Table 2, entry 3i: 1-methyl-2-(3-methylbut-2-en-1-yl)benzene.**
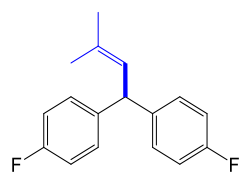
In a nitrogen filled glovebox, **2a** (58 µL, 0.36 mmol, 1 equiv.) and [Cl$_2$NN]Cu (16 mg, 0.038 mmol, 10 mol%) were dissolved in o-xylene substrate (872 µL, 7.2 mmol, 20 equiv.) with benzene (300 µL) in a 5 mL thick-walled pressure vessel. [t]BuOO[t]Bu (132 µL, 0.72 mmol, 2 equiv.) was added and the solution was immediately sealed and heated to 60 °C. After 1 h, the reaction was allowed to cool to r.t. and quenched by exposure to air. The yield determined by GCMS analysis of the reaction mixture is 70 %. The target product **3i** was isolated via flash column chromatography on silica gel (100 % hexane). The isolation yield was 22 % as a colorless oil. ^{1}H NMR (500 MHz, CDCl$_3$) δ 7.13 (m, 4H), 5.24 (m, 1H), 3.30 (d, J = 7.1 Hz, 2H), 2.29 (s, 3H), 1.73 (d, J = 8.5 Hz, 6H). ^{13}C{^{1}H} NMR (126 MHz, CDCl$_3$) δ 140.09, 136.28, 132.51, 130.18, 128.72, 126.09, 126.04, 122.67, 32.32, 25.88, 19.61, 18.00. NMR characterization details of isolated **3i** were in good agreement with that reported for this compound in the literature.[7]
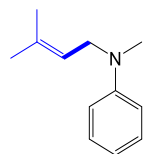
**Table 2, entry 3k: 1-chloro-2-(3-methylbut-2-en-1-yl)benzene.**
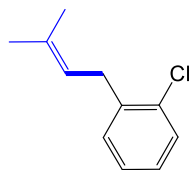
In a nitrogen filled glovebox, **2a** (58 µL, 0.36 mmol, 1 equiv.) and [Cl$_2$NN]Cu (16 mg, 0.038 mmol, 10 mol%) were dissolved in dry 1-chloro-2-methylbenzene substrate (836 µL, 7.2 mmol, 20 equiv.) with benzene (300 µL) in a 5 mL thick-walled pressure vessel. [t]BuOO[t]Bu (132 µL, 0.72 mmol, 2 equiv.) was added and the solution was immediately sealed and heated to 80 °C. After 1 h, the reaction was allowed to cool to r.t. and quenched by exposure to air. The yield determined by GCMS analysis of the reaction mixture is 53 %. The target product **3j** was isolated via flash column chromatography on silica gel (100 % hexane). The isolation yield was 31 % as a colorless oil. ^{1}H NMR (500 MHz, CDCl$_3$) δ 7.34 (d, J = 7.8 Hz, 1H), 7.17 (m, 3H), 5.28 (m, 1H), 3.44 (d, J = 7.1 Hz, 2H), 1.74 (d, J = 16.5 Hz, 6H). ^{13}C{^{1}H} NMR (126 MHz, CDCl$_3$) δ 139.40, 134.07, 133.67, 130.12, 129.47, 127.28, 126.87, 121.43, 32.22, 25.91, 18.05. NMR characterization details of isolated **3j** were in good agreement with that reported for this compound in the literature.[7]
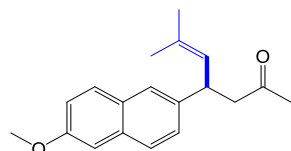
**Table 2, entry 3k: 1-methyl-4-(3-methylbut-2-en-1-yl)benzene.**
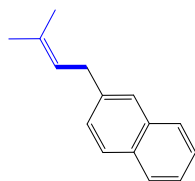
In a nitrogen filled glovebox, **2a** (58 µL, 0.36 mmol, 1 equiv.) and [Cl$_2$NN]Cu (16 mg, 0.038 mmol, 10 mol%) were dissolved in dry 2-methylnaphthalene substrate (1g, 7.2 mmol, 20 equiv.) with benzene (300 µL) in a 5 mL thick-walled pressure vessel. [t]BuOO[t]Bu (132 µL, 0.72 mmol, 2 equiv.) was added and the solution was immediately sealed and heated to 80 °C. After 1 h, the reaction was allowed to

cool to r.t. and quenched by exposure to air. The yield determined by GCMS analysis of the reaction mixture is 42 %. The target product **3k** was isolated via flash column chromatography on silica gel (100 % hexane). The isolation yield was 28 % as a colorless oil. $^1$H NMR (500 MHz, CDCl$_3$) δ 7.78 (dd, J = 16.4, 8.5 Hz, 3H), 7.60 (s, 1H), 7.43 (m, 2H), 7.33 (m, 1H), 5.41 (m, 1H), 3.51 (d, J = 7.3 Hz, 2H), 1.78 (d, J = 3.9 Hz, 6H). $^{13}$C{$^1$H} NMR (126 MHz, CDCl$_3$) δ 139.48, 133.81, 133.01, 132.10, 128.01, 127.73, 127.57, 127.52, 126.21, 125.98, 125.20, 123.15, 34.68, 25.96, 18.06. NMR characterization details of isolated **3k** were in good agreement with that reported for this compound in the literature.[13]

**Table 2, entry 3l: (4-methylpent-3-en-2-yl)benzene.**

In a nitrogen filled glovebox, **2a** (58 µL, 0.36 mmol, 1 equiv.) and [Cl$_2$NN]Cu (16 mg, 0.038 mmol, 10 mol%) were dissolved in dry ethylbenzene substrate (877 µL, 7.2 mmol, 20 equiv.) with benzene (300 µL) in a 5 mL thick-walled pressure vessel. $^t$BuOO$^t$Bu (132 µL, 0.72 mmol, 2 equiv.) was added and the solution was immediately sealed and heated to 60 °C. After 1 h, the reaction was allowed to cool to r.t. and quenched by exposure to air. The yield determined by GCMS analysis of the reaction mixture is 39 %. An authentic sample of the product **3l** was synthesized via a Wittig reaction for qualitative and quantitative analysis on GCMS. **3l**: $^1$H NMR (500 MHz, CDCl$_3$) δ 7.30 (t, J = 7.5 Hz, 2H), 7.25 (m, 2H), 7.18 (t, J = 7.2 Hz, 1H), 5.30 (m, 1H), 3.67 (m, 1H), 1.70 (d, J = 14.0 Hz, 5H), 1.32 (d, J = 7.0 Hz, 2H). $^{13}$C{$^1$H} NMR (126 MHz, CDCl$_3$) δ 147.43, 130.63, 130.29, 128.48, 127.01, 125.84, 38.27, 25.96, 22.58, 18.09. Full characterization details are given in the entry for this compound as synthesized via a Wittig reaction (page S3).

**Table 2, entry 3m: (3-methylbut-2-ene-1,1-diyl)dibenzene.**

In a nitrogen filled glovebox, **2a** (58 µL, 0.36 mmol, 1 equiv.) and [Cl$_2$NN]Cu (16 mg, 0.038 mmol, 10 mol%) were dissolved in dry diphenylmethane substrate (604 µL, 3.6 mmol, 10 equiv.) with benzene (300 µL) in a 5 mL thick-walled pressure vessel. $^t$BuOO$^t$Bu (132 µL, 0.72 mmol, 2 equiv.) was added and the solution was immediately sealed and heated to 60 °C. After 1 h, the reaction was allowed to cool to r.t. and quenched by exposure to air. The yield determined by GCMS analysis of the reaction mixture is 65 %. The target product **3m** was isolated via flash column chromatography on silica gel (100 % hexane). The isolation yield was 19 % as a colorless oil. $^1$H NMR (500 MHz, CDCl$_3$) δ 7.28 (m, 4H), 7.19 (m, 6H), 5.62 (d, J = 9.6 Hz, 1H), 4.89 (d, J = 9.5 Hz, 2H), 1.79 (s, 3H), 1.72 (s, 3H). $^{13}$C{$^1$H} NMR (126 MHz, CDCl$_3$) δ 131.44, 130.11, 129.47, 127.28, 126.87, 121.41, 32.22, 25.92, 18.05. NMR characterization details of isolated **3m** were in good agreement with data reported for this compound in the literature.[7]

**Table 2, entry 3n: 4,4'-(3-methylbut-2-ene-1,1-diyl)bis(fluorobenzene).**

In a nitrogen filled glovebox, **2a** (58 μL, 0.36 mmol, 1 equiv.) and [Cl$_2$NN]Cu (16 mg, 0.038 mmol, 10 mol%) were dissolved in dry 4,4'-difluorodiphenylmethane substrate (1.28 mL, 7.2 mmol, 20 equiv.) with benzene (300 μL) in a 5 mL thick-walled pressure vessel. $^t$BuOO$^t$Bu (132 μL, 0.72 mmol, 2 equiv.) was added and the solution was immediately sealed and heated to 60 °C. After 1 hour, the reaction was allowed to cool to r.t. and quenched by exposure to air. The yield determined by GCMS analysis of the reaction mixture is 64 %. The target product **3n** was isolated via flash column chromatography on 10 % silver nitrate-impregnated silica gel (100 % hexane). The isolation yield was 25 % as a colorless oil. $^1$H NMR (500 MHz, CDCl$_3$): δ 7.11 (dd, J = 8.6, 5.7 Hz, 4H), 6.96 (t, J = 8.7 Hz, 4H), 5.52 (d, J = 9.4 Hz, 1H), 4.83 (d, J = 9.3 Hz, 1H), 1.79 (d, J = 1.1 Hz, 3H), 1.70 (d, J = 1.2 Hz, 3H). $^{13}$C{$^1$H} NMR (126 MHz, CDCl$_3$): δ 162.44, 160.49, 133.18, 129.70 (d, J = 7.8 Hz), 127.18, 115.31 (d, J = 21.1 Hz), 48.05, 26.04, 18.21. $^{19}$F{$^1$H} NMR (470 MHz, CDCl$_3$): δ -117.30. HRMS (CI) m/z calcd. For C$_{17}$H$_{16}$F$_2$$^+$ 258.1220, found 258.1205.

**Table 2, entry 3o: N-methyl-N-(3-methylbut-2-en-1-yl)aniline.**

In a nitrogen filled glovebox, **2a** (58 μL, 0.36 mmol, 1 equiv.) and [Cl$_2$NN]Cu (16 mg, 0.038 mmol, 10 mol%) were dissolved in dry N,N-dimethylaniline substrate (455 μL, 3.6 mmol, 10 equiv.) with benzene (300 μL) in a 5 mL thick-walled pressure vessel. $^t$BuOO$^t$Bu (132 μL, 0.72 mmol, 2 equiv.) was added and the solution was immediately sealed and heated to 60 °C. After 1 h, the reaction was allowed to cool to r.t. and quenched by exposure to air. The yield determined by GCMS analysis of the reaction mixture is 22 %. The target product **3o** was isolated via flash column chromatography (70 % hexane and 30 % DCM) for quantitative analysis on GCMS. Due to the separation challenge of **3o**, a significant amount of R-H substrate (N,N-dimethylaniline) could not be removed completely in $^1$H NMR. $^1$H NMR (500 MHz, CDCl$_3$): δ 7.25 (m), 6.75 (m), 5.20 (d, J = 6.9 Hz, 1H), 3.89 (d, J = 6.4 Hz, 2H), 2.89 (s, 3H), 1.72 (s, 3H). $^1$H NMR characterization details of **3o** was in good agreement with data reported for this compound in the literature.[14]

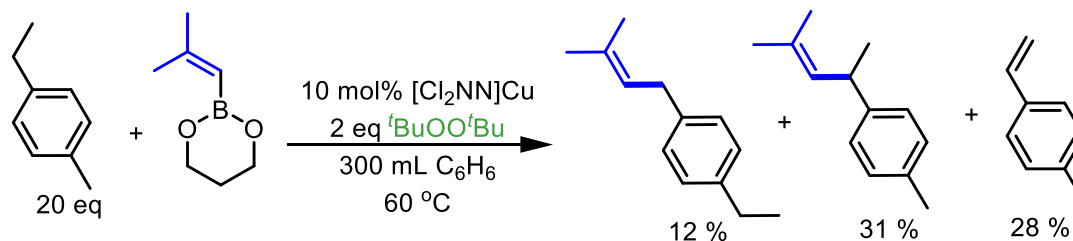**Table 2, entry 3p: 4-(6-methoxynaphthalen-2-yl)-6-methylhept-5-en-2-one.**

In a nitrogen filled glovebox, **2a** (58 μL, 0.36 mmol, 1 equiv.) and [Cl$_2$NN]Cu (16 mg, 0.038 mmol, 10 mol%) were dissolved in dry 4-(6-methoxynaphthalen-2-yl)butan-2-one (nabumetone) substrate (0.82 g, 3.6 mmol, 10 equiv.) with benzene (300 μL) in a 5 mL thick-walled pressure vessel. $^t$BuOO$^t$Bu (132 μL, 0.72 mmol, 2 equiv.) was added and the solution was immediately sealed and heated to 60 °C. After 1 h, the reaction was allowed to cool to r.t. and quenched by exposure to air. The yield determined by GCMS analysis of the reaction mixture is 35 %. The target product **3p** was isolated via flash column chromatography (95 % hexane and 5 % EA). The isolation yield was 15 % as a white solid. 70 % of Nabumetone was recovered. $^1$H NMR (500 MHz, CDCl$_3$): δ 7.69 – 7.65 (m, 2H), 7.56 (d, J = 1.8 Hz, 1H), 7.32 (dd, J = 8.5, 1.8 Hz, 1H), 7.12

(dd, $J$ = 8.9, 2.6 Hz, 1H), 7.09 (d, $J$ = 2.5 Hz, 1H), 5.32 (m, 1H), 4.20 (m, 1H), 3.90 (s, 3H), 2.88 (dd, $J$ = 15.6, 6.6 Hz, 1H), 2.80 (dd, $J$ = 15.6, 8.0 Hz, 1H), 2.08 (s, 3H), 1.71 (dd, $J$ = 11.7, 1.4 Hz, 6H).$^{13}$C{$^1$H} NMR (126 MHz, CDCl$_3$): δ 207.89, 157.47, 139.96, 133.31, 132.96, 129.26, 129.18, 127.27, 127.17, 126.57, 125.17, 118.92, 105.72, 55.45, 51.02, 40.07, 30.92, 26.03, 18.34. HRMS (CI) m/z calcd. For C$_{19}$H$_{23}$O$_2^+$ 283.1698, found 283.1693.

**Table 2, entry 3q: 6-(3-methylbut-2-en-1-yl)-2H-chromen-2-one.**



In a nitrogen filled glovebox, **2a** (58 μL, 0.36 mmol, 1 equiv.) and [Cl$_2$NN]Cu (16 mg, 0.038 mmol, 10 mol%) were dissolved in dry 6-methylcoumarin (0.57 g, 3.6 mmol, 10 equiv.) with benzene (300 μL) in a 5 mL thick-walled pressure vessel. $^t$BuOO$^t$Bu (132 μL, 0.72 mmol, 2 equiv.) was added and the solution was immediately sealed and heated to 100 °C. After 1 hour, the reaction was allowed to cool to r.t. and quenched by exposure to air. The yield determined by GCMS analysis of the reaction mixture is 29 %. The target product **3q** was isolated via flash column chromatography (90 % hexane and 10 % EA). The isolation yield was 6 % as a white solid. 85 % of 6-methylcoumarin was recovered. $^1$H NMR (500 MHz, CD$_2$Cl$_2$): δ 7.69 (d, $J$ = 9.7 Hz, 1H), 7.36 (dd, $J$ = 8.5, 2.2 Hz, 1H), 7.29 (d, $J$ = 2.1 Hz, 1H), 7.23 (d, $J$ = 8.5 Hz, 1H), 6.35 (d, $J$ = 9.5 Hz, 1H), 3.39 (d, $J$ = 7.4 Hz, 2H), 1.76 (d, $J$ = 1.3 Hz, 3H), 1.73 (d, $J$ = 1.4 Hz, 3H). $^{13}$C{$^1$H} NMR (126 MHz, CD$_2$Cl$_2$): δ 161.26, 152.96, 144.00, 138.75, 134.09, 132.57, 127.55, 122.85, 119.28, 117.02, 117.00, 33.93, 25.99, 18.09. HRMS (CI) m/z calcd. For C$_{14}$H$_{15}$O$_2^+$ 215.1072, found 215.1072.

**Table 2, entry 3r: 8-(3-methylbut-2-en-1-yl)-2H-chromen-2-one.**



In a nitrogen filled glovebox, **2a** (58 μL, 0.36 mmol, 1 equiv.) and [Cl$_2$NN]Cu (16 mg, 0.038 mmol, 10 mol%) were dissolved in dry 8-methylcoumarin substrate (0.57 g, 3.6 mmol, 10 equiv.) with benzene (300 μL) in a 5 mL thick-walled pressure vessel. $^t$BuOO$^t$Bu (132 μL, 0.72 mmol, 2 equiv.) was added and the solution was immediately sealed and heated to 100 °C. After 1 hour, the reaction was allowed to cool to r.t. and quenched by exposure to air. Isolation yield was 8 % as white solid. 73 % of R-H (8-methylcoumarin) substrate was recovered. The target product **3r** was isolated via flash column chromatography (95 % hexane and 5 % EA). $^1$H NMR (500 MHz, CDCl$_3$): δ 7.71 (dd, $J$ = 9.5, 1.1 Hz, 1H), 7.40 (d, $J$ = 7.5 Hz, 1H), 7.33 (d, $J$ = 7.6 Hz, 1H), 7.21 (m, 1H), 6.43 (dd, $J$ = 9.5, 1.1 Hz, 1H), 5.35 (m, $J$ = 7.5, 6.0, 2.9, 1.4 Hz, 1H), 3.57 (d, $J$ = 7.5 Hz, 2H), 1.77 (s, 6H). $^{13}$C{$^1$H} NMR (126 MHz, CDCl$_3$): δ 161.11, 152.03, 144.01, 134.27, 132.04, 130.07, 125.76, 124.27, 120.93, 118.78, 116.47, 27.71, 25.94, 18.04. $^1$H NMR characterization details of isolated **3r** was in good agreement with data reported for this compound in the literature.[15]

## 4. Dehydrogenation of Ethylbenzene to Styrene and Competition Study of 2° and 1° Benzylic C-H Bonds

Ethylbenzene exhibits a lower yield than toluene in C-H alkenylation because styrene forms in 20% yield during the C-H alkenylation of ethylbenzene as determined by GCMS analysis employing authentic standards.



37 %          23 %

Styrene formation likely occurs via β-H atom abstraction from the PhCH(•)Me radical as outlined in Scheme S5.

To compare the reactivities of benzylic CH$_2$ and CH$_3$ groups, 4-ethyltoluene was used as a model substrate in the competition study. The results show that the secondary benzylic CH$_2$ is more reactive towards alkenylation (31 %) compared to the primary benzylic CH$_3$ (12 %). However, the secondary benzylic CH$_2$ radical can also undergo a second HAT at the β-H position. As a result, 4-methylstyrene was observed as a side product (28 %). Yields were determined by GCMS analysis of the reaction mixture.



20 eq          12 %          31 %          28 %

An additional competition study was performed by conducting a one-pot experiment involving the alkenylation of toluene and ethylbenzene. The findings indicated that the secondary benzylic CH$_2$ is more reactive towards alkenylation (29%) compared to the primary benzylic CH$_3$ (16%). Similar to 4-ethyltoluene, ethylbenzene can also undergo a HAT at the β-H position, resulting in the formation of styrene as a side product (20%). The yield determined by GCMS analysis of the reaction mixture.



20 eq     20 eq          16 %          29 %          20 %

## 5. Interaction of [Cl₂NN]Cu($\eta^2$-benzene) with Alkenylboronate (2a), 6-Methylcoumarin (1q), and 2,5-Dimethyl-2,4-hexadiene (alkenyl dimer)



### [Cl₂NN]Cu($\eta^2$-alkenylboronate) adduct [Cuᴵ]($\eta^2$-2a)

In a nitrogen filled glovebox, [Cl₂NN]Cu catalyst (0.33 mmol, 170 mg) and **2a** (0.43 mmol, 69 μL) were mixed in 5 mL of fluorobenzene for 0.5 h. The mixture was further dried under vacuum and redissolved back to pentane. X-ray quality crystals were grown by slow evaporation at -40 °C. $^1$H NMR (500 MHz, C₆D₆): δ 7.14 (dd, $J$ = 8.1, 1.5 Hz, 2H), 7.05 (dd, $J$ = 8.1, 1.4 Hz, 2H), 6.46 (t, $J$ = 8.0 Hz, 2H), 5.04 (s, 1H), 3.53 - 3.49 (m, 2H), 3.46 – 3.41 (m, 2H), 3.30 (s, 1H), 1.77 (s, 6H), 1.57 (d, $J$ = 0.6 Hz, 3H), 1.29 (s, 3H). $^{13}$C{$^1$H} NMR (126 MHz, C₆D₆): δ 164.56, 148.13, 131.68, 130.80, 124.31, 113.97, 95.87, 61.25, 28.87, 27.15, 23.38, 21.35. Anal. Calcd for C₂₄H₂₆BCl₄CuN₂O₂: C, 48.81; H,4.44; N,4.74. Found: C, 48.64; H, 4.53; N, 5.03.

### Calculation of the equilibrium constant for 2a binding in benzene: v'ant Hoff plot

Pure crystals of [Cl₂NN]Cu($\eta^2$-**2a**) (2.7 mg, 4.6 mmol) dissolved in 0.6 mL of C₆D₆ with 6.3 mg (0.0293 mmol) of internal standard, 1,2,4,5-tetrachlorobenzene (δ 6.8 ppm). Variable temperature $^1$H NMR spectra were acquired from 10 °C to 60 °C, equilibrating at each temperature for 15 min before each collection. A delay time of 25s was used between $^1$H NMR scans to ensure accurate integration. Benzene concentration was needed to calculate [Cuᴵ]-($\eta^2$-**2a**) binding ΔG. [Benzene]= 0.87 (g/mL) ÷ 78 (g/mol) = 0.01123 mol/mL = 11.23 M.



[A]      [Benzene]= 11.23 M      [B]      [C]

**Figure S2.** The temperature variation staking $^1H$ NMR spectra of $[Cl_2NN]Cu(\eta^2\text{-}\textbf{2a})$ in $C_6D_6$.

**Table S5.** The summary of integration results, the equilibrium constants (K), and the free energies ($\Delta G$) at various temperatures.

| | 10 °C | 20 °C | 25 °C | 40 °C | 50 °C | 60 °C |
|---|---|---|---|---|---|---|
| STD integration | 2 | 2 | 2 | 2 | 2 | 2 |
| Ha integration | 1.61 | 1.47 | 1.98 | 1.38 | 1.34 | 1.21 |
| Hb integration | 0.11 | 0.16 | 0.24 | 0.27 | 0.39 | 0.49 |
| Hc integration | 0.16 | 0.20 | 0.28 | 0.32 | 0.49 | 0.52 |
| [A] (mM) | 6.864341 | 6.267442 | 8.44186 | 5.883721 | 5.713178 | 5.158915 |
| [B] (mM) | 0.468992 | 0.682171 | 1.023256 | 1.151163 | 1.662791 | 2.089147 |
| [C] (mM) | 0.682 | 0.853 | 1.194 | 1.364 | 2.089 | 2.217 |
| K | 4.150E-06 | 8.265E-06 | 1.289E-05 | 2.377E-05 | 5.414E-05 | 7.995E-05 |
| Ln(K) | -12.392 | -11.704 | -11.259 | -10.647 | -9.824 | -9.434 |
| $\Delta G$ (kcal/mol) | 6.975 | 6.821 | 6.674 | 6.628 | 6.311 | 6.249 |

$$\ln K = -\Delta H/RT + \Delta S/R$$
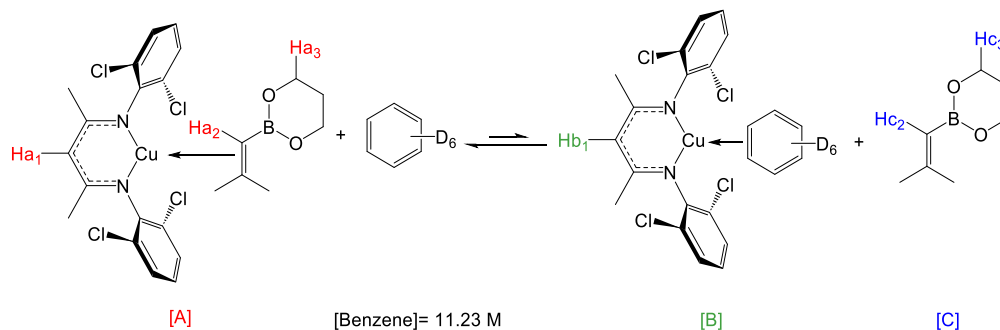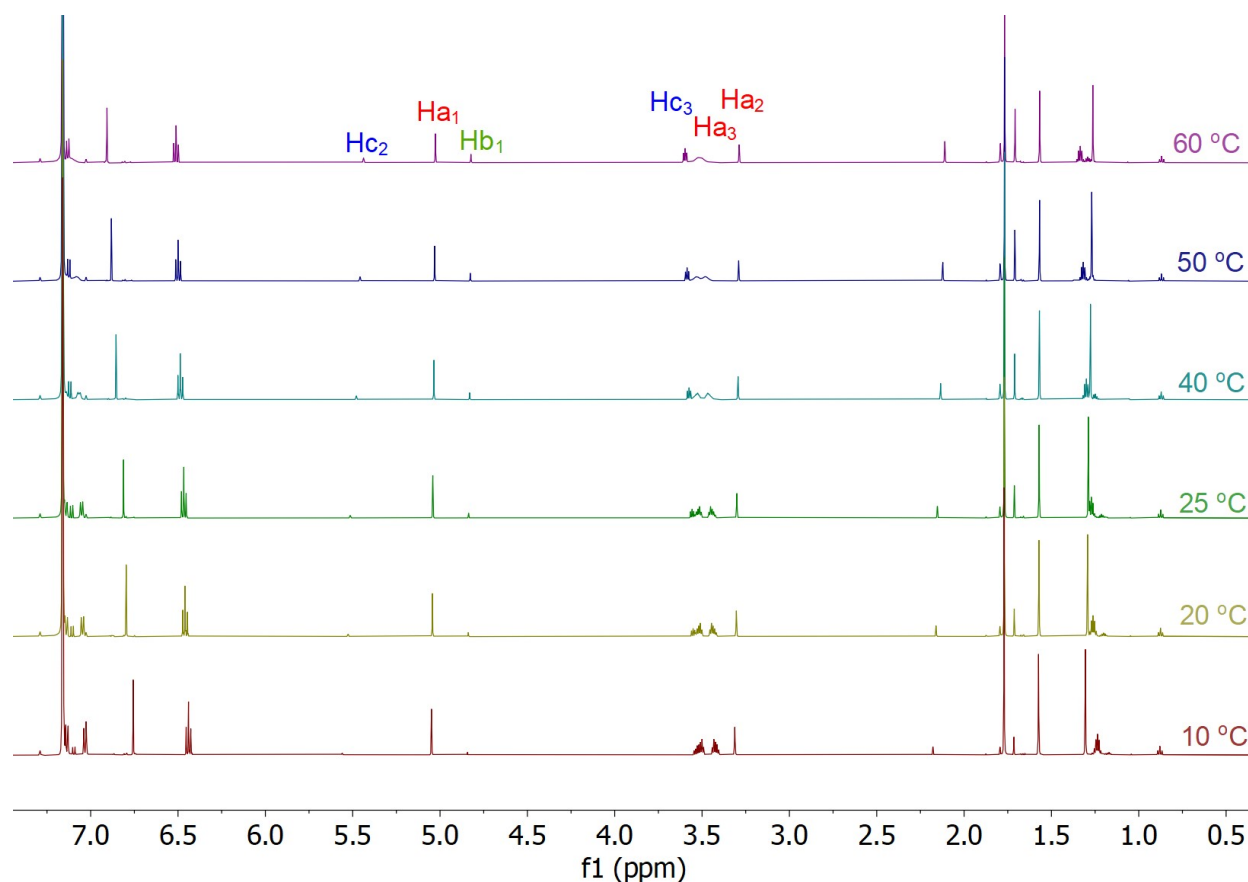
y = -5559x + 7.2791
R² = 0.9916
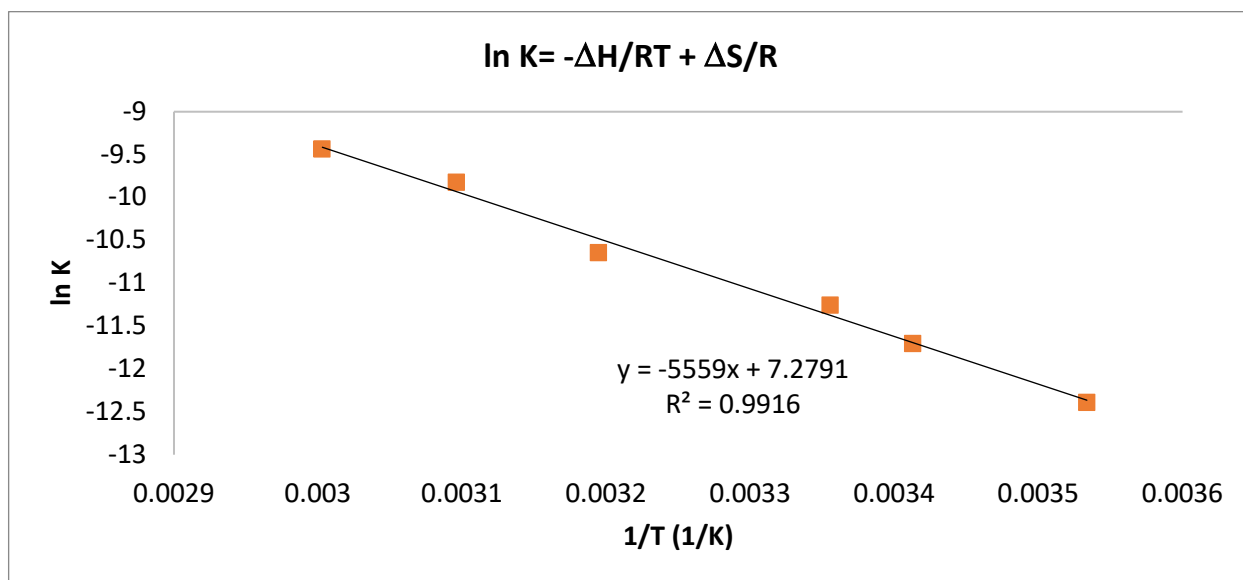
**Figure S3.** van't Hoff plot analysis for the binding of **2a** to catalyst $[Cl_2NN]Cu(\eta^2\text{-benzene})$ in benzene. $\Delta G^o_{exp}(298K) = 6.7 \pm 1.0$ kcal/mol, $\Delta H^o_{exp} = 11.1 \pm 0.5$ kcal/mol, and $\Delta S^o_{exp} = 14.4 \pm 1.6$ e.u. (cal/mol•K). (Also appears as Figure 3c in the manuscript.)

## ^{1}H NMR study of binding affinity of 6-methylcoumarin (1q) to [Cl₂NN]Cu

To initiate alkenylation in the catalytic reaction involving substrates **1q** and **1r**, elevated reaction temperatures are necessary. We hypothesize that strong binding of C-H substrates **1q** and **1r** to the $[Cl_2NN]Cu$ catalyst impeeds reaction with $^tBuOO^tBu$ to form $[Cl_2NN]Cu\text{-}O^tBu$.[16]
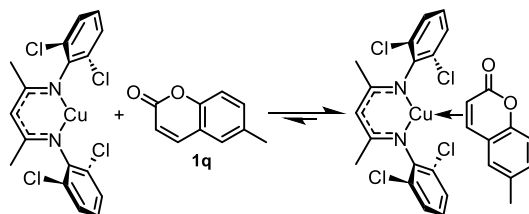


**Scheme S2**. Reversible **1q** binding to [Cuᴵ] catalyst.

To investigate this phenomenon, we used ^{1}H NMR to monitor the interaction between **1q** and $[Cl_2NN]Cu$ in benzene-$d_6$. We prepared two NMR samples: *1:1 sample*, $[Cl_2NN]Cu$ (5.0 mg, 0.0095 mmol, 1 equiv.) and **1q** (1.5 mg, 0.0095 mmol, 1 equiv.) in 0.6 mL $C_6D_6$. *1:8 sample*, $[Cl_2NN]Cu$ (5 mg, 0.0095 mmol, 1 equiv.) and **1q** (12 mg, 0.076 mmol, 8 equiv.) in 0.6 mL $C_6D_6$. In the 1:1 solution, only trace amount of $[Cl_2NN]Cu(\eta^2\text{-benzene})$ was present. Upon the addition of [Cuᴵ], the $H_1$ signal of **1q** upfield shifted to 4.5 ppm. The upfield shift of H* suggests the backbonding interaction of $[Cl_2NN]Cu$ and $C_\alpha = C_\beta$ of **1q**. In the 8:1 soution, no ^{1}H NMR signal for $[Cl_2NN]Cu(\eta^2\text{-}$ benzene) was present. Thus, arene solutions of catalyst $[Cl_2NN]Cu$ with a large excess of C-H substrate **1q** exclusively contain $[Cl_2NN]Cu(\mathbf{1q})$. It requires higher temperatures to dissociate $[Cl_2NN]Cu(\mathbf{1q})$.
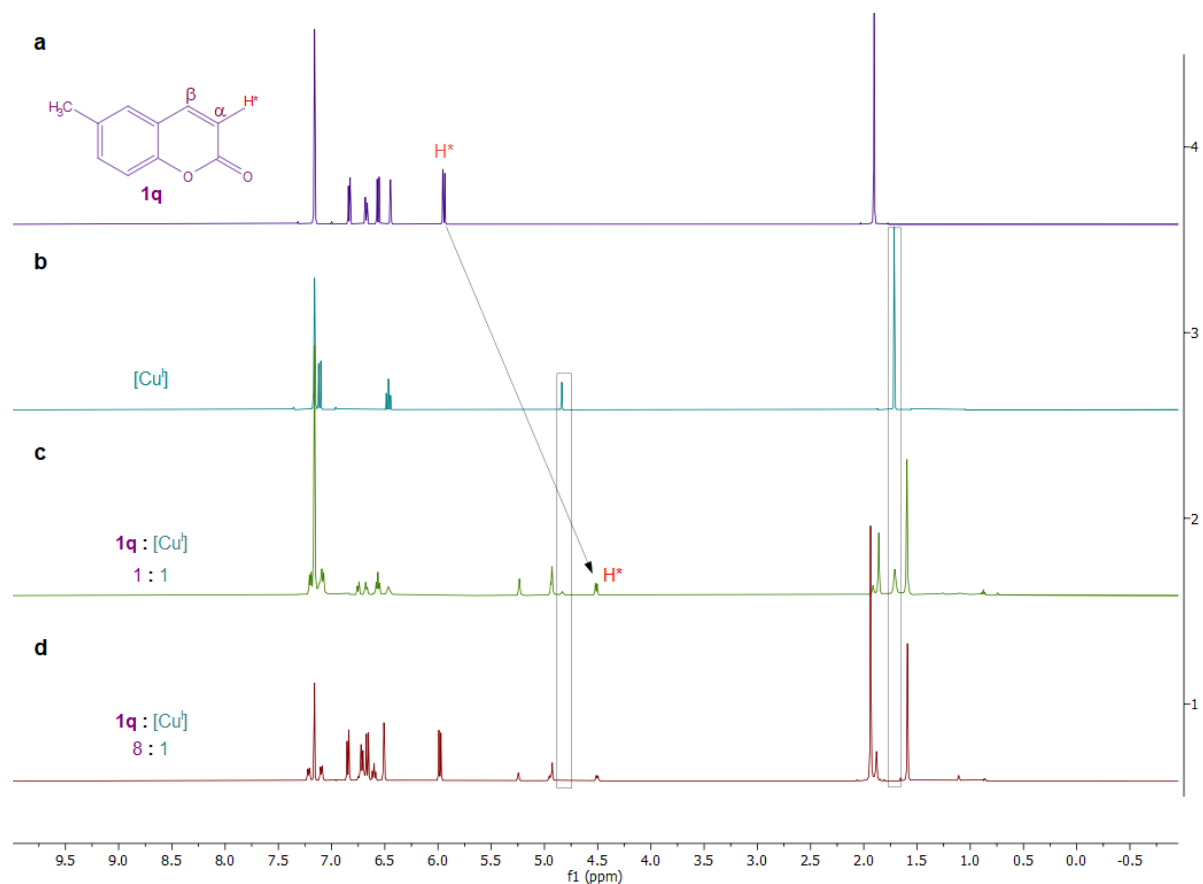
**Figure S4.** $^1$H NMR spectra (500 MHz, C$_6$D$_6$, r.t.) of [Cl$_2$NN]Cu in the presence of C-H substrate 6-methylcoumarin (**1q**). (a) $^1$H NMR spectrum of **1q**. (b) $^1$H NMR spectrum of [Cl$_2$NN]Cu. (c) $^1$H NMR spectrum of 1 : 1 **1q** : [Cl$_2$NN]Cu mixture. (d) $^1$H NMR spectrum of 8:1 **1q** : [Cl$_2$NN]Cu mixture. Boxed signals indicate the chemical shift expected for the β-diketiminato backbone C-H resonance of free [Cl$_2$NN]Cu in C$_6$D$_6$.

**$^1$H NMR study of binding affinity of 2,5-dimethyl-2,4-hexadiene (alkenyl dimer) to [Cl$_2$NN]Cu**

To explore the affinity of the alkenyl dimer Me$_2$C=CH-CH=CMe$_2$ to bind to the [Cl$_2$NN]Cu catalyst, we employed $^1$H NMR spectroscopy with various amount of alkenyl dimer. The NMR samples were stirred for 10 min before the measurement.

**Table S6.** The NMR samples of different molar ratio of alkenyl dimer and [Cl$_2$NN]Cu catalyst.

| Mole ratio Dimer : [Cl$_2$NN]Cu | Dimer | [Cl$_2$NN]Cu | C$_6$D$_6$ |
|---|---|---|---|
| 0.25 : 1 | 0.68 µL, 0.00048 mmol | 10 mg, 0.019 mmol | 0.6 mL |
| 0.5 : 1 | 1.4 µL, 0.0096 mmol | 10 mg, 0.019 mmol | 0.6 mL |
| 1 : 1 | 2.8 µL, 0.019 mmol | 10 mg, 0.019 mmol | 0.6 mL |
| 2.5 :1 | 7.0 µL, 0.048 mmol | 10 mg, 0.019 mmol | 0.6 mL |
| 5:1 | 14 µL, 0.095 mmol | 10 mg, 0.019 mmol | 0.6 mL |
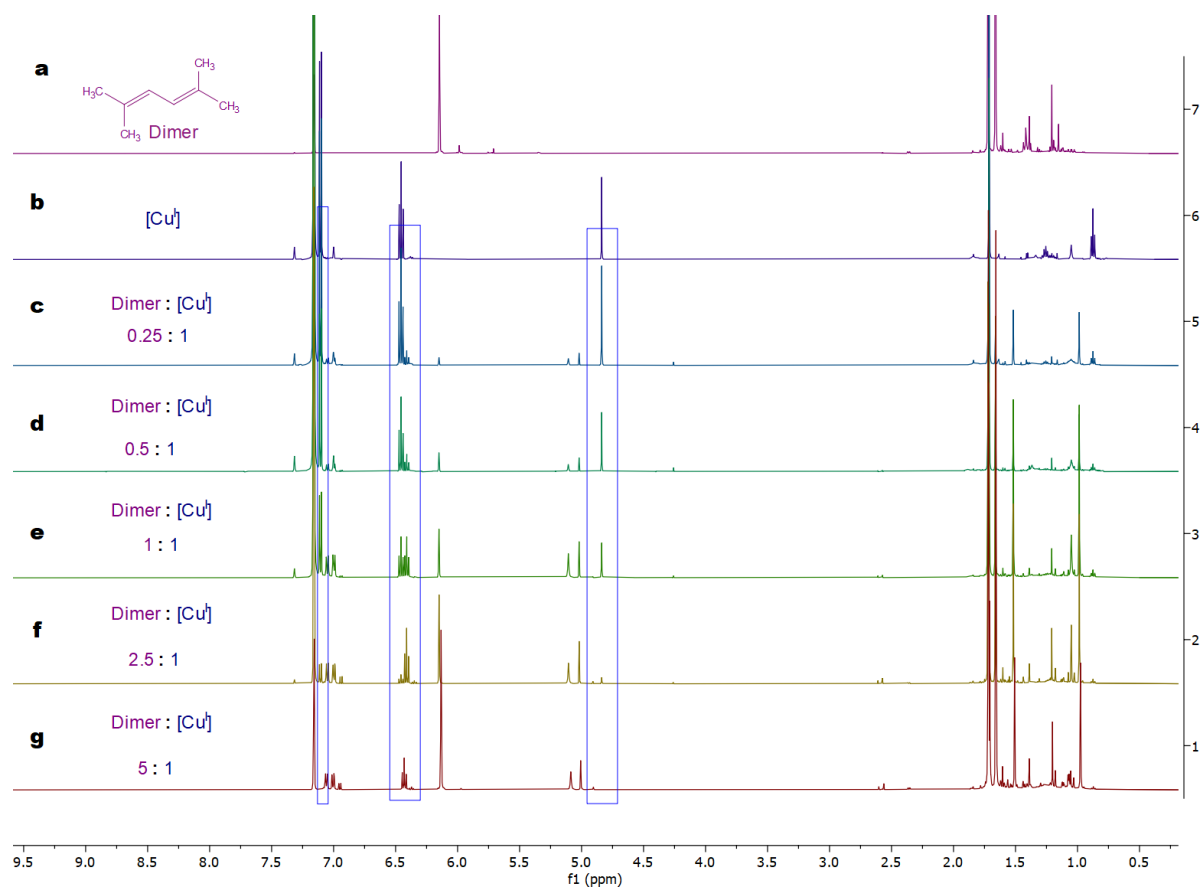
**Figure S5.** The ^{1}H NMR of substrate 2,5-dimethyl-2,4-hexadiene (alkenyl dimer) binds to [Cl$_2$NN]Cu catalyst. (a) ^{1}H NMR of alkenyl dimer in C$_6$D$_6$. (b) ^{1}H NMR of [Cl$_2$NN]Cu in C$_6$D$_6$. (c) ^{1}H NMR of alkenyl dimer: [Cl$_2$NN]Cu = 0.25:1. (d) ^{1}H NMR of alkenyl dimer : [Cl$_2$NN]Cu = 0.5:1. (e) ^{1}H NMR of alkenyl dimer: [Cl$_2$NN]Cu = 1:1. (f) ^{1}H NMR of alkenyl dimer: [Cl$_2$NN]Cu = 2.5:1. (g) ^{1}H NMR of alkenyl dimer: [Cl$_2$NN]Cu = 5:1.  Boxed signals indicate the disappearing signals due to free [Cl$_2$NN]Cu($\eta^2$-benzene).

## 6. Examining the Reactivity of the [Cl$_2$NN]Cu-CH=CMe$_2$ Intermediate

### Synthesis of [Cl$_2$NN]Cu-O$^t$Bu

[Cl$_2$NN]Cu-O$^t$Bu was adapted from a literature procedure.[17] In a nitrogen filled glovebox, $^t$BuOO$^t$Bu (146 μL, 0.76 mmol, 2 equiv.) was added to a suspension of [Cl$_2$NN]Cu (200 mg, 0.38 mmol, 1 equiv.) in pentane (10 mL). The reaction was stirred for 1 h at r.t. The reaction mixture was then filtered through Celite and concentrated under vacuum. The concentrated solution was further recrystallized at -40 °C to give 58 % as a dark red solid of [Cl$_2$NN]Cu-O$^t$Bu.

### Decay of [Cl$_2$NN]Cu-O$^t$Bu upon addition of alkenylboronate (2a)

To a cuvette was added 4.00 mL of a 0.13 mM stock solution of [Cl$_2$NN]Cu-O$^t$Bu ($\varepsilon_{471nm}$ = 4120 M$^{-1}$cm$^{-1}$) in fluorobenzene. After the temperature of the UV-vis cryostat was held at -38 °C for 15 min, **2a** (8.6 μL, 0.534 mmol, 1 equiv. in 0.1 mL fluorobenzene) was added via syringe under nitrogen atmosphere. Immediately after addition of **2a**, decay of [Cl$_2$NN]Cu-O$^t$Bu occurred.
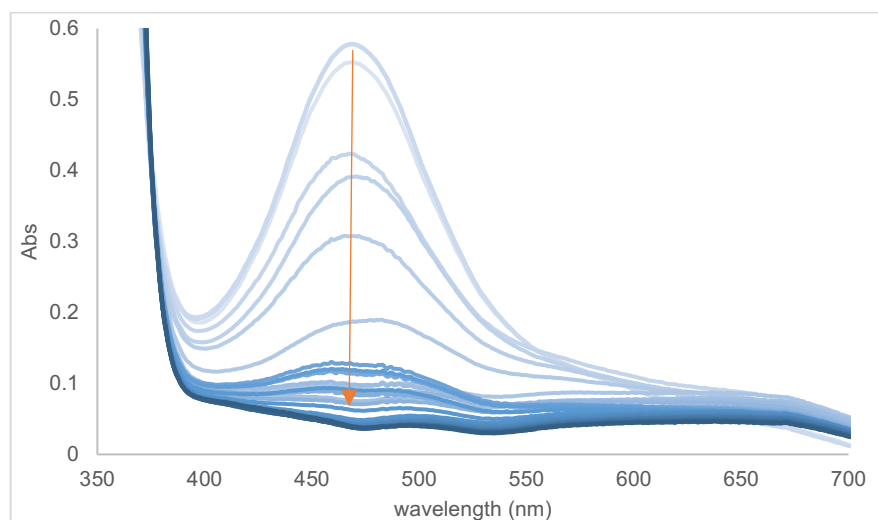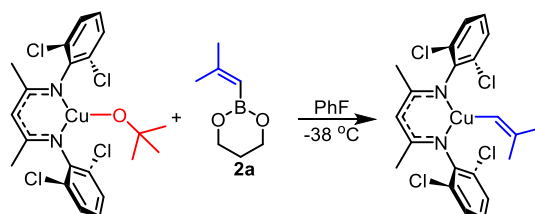




**Figure S6.** Uv-vis spectra recorded in every 30 s during exchange reaction of [Cl$_2$NN]Cu-O$^t$Bu (0.13 mM, 1 equiv.) and **2a** (1 equiv.) in fluorobenzene at – 38 °C over 15 min.

**Dimerization of [Cl₂NN]Cu-CH=CMe₂ intermediate in fluorobenzene**

In a nitrogen filled glovebox, to a stirring solution of [Cl₂NN]Cu-O$^t$Bu (1 equiv., 0.2 mmol, 100 mg) in fluorobenzene (5 mL) was added **2a** (1 equiv., 0.2 mmol, 32 μL). After stirring the reaction mixture for 16 h at -40 °C, the reaction was quenched by exposure to air. 1,2,4,5-tetrachlorobenzene was added to the reaction mixture as an internal standard and the yield of alkenyl dimerization product Me₂C=CH-CH=CMe₂ was 84 % as determined by GCMS analysis.
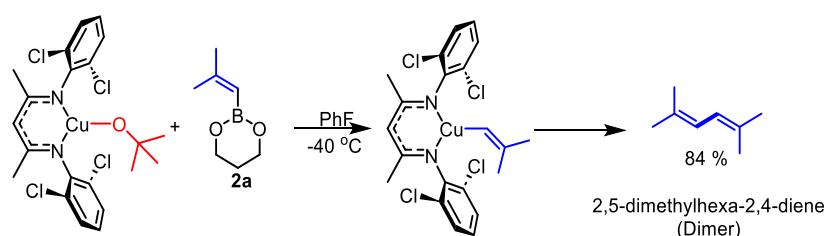


**Illustrating the ability of a 1,3-diene to bind to two copper(I) β-diketiminate complexes: Isolation of {[$^i$Pr₂NN$_{F6}$]Cu}₂(μ-CH₂=CH-CH=CH₂)**
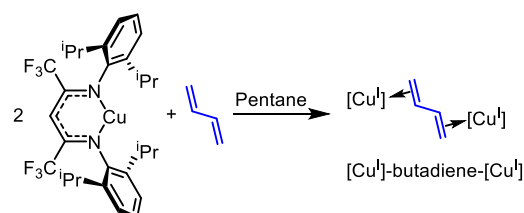


In a nitrogen filled glovebox, [$^i$Pr₂NN$_{F6}$]Cu($\eta^2$-benzene) (200 mg, 0.34 mmol) was dissolved in 15 mL pentane and purged with gaseous 1,3-butadiene for 2 min. Yellow crystals formed immediately. The solution was carefully transferred to a -40 °C freezer which enabled the isolation of X-ray quality crystals in 87% yield. ¹H NMR (500 MHz, C₆D₆) δ 6.93 – 6.90 (m, 4H), 6.86 (d, $J$ = 3.5 Hz, 8H), 6.02 (s, 2H), 4.37 – 4.27 (m, 2H), 2.97 (p, $J$ = 6.9 Hz, 4H), 2.86 (p, $J$ = 6.8 Hz, 3H), 2.44 (d, $J$ = 6.8 Hz, 2H), 1.77 (d, $J$ = 14.0 Hz, 2H), 1.16 (d, $J$ = 6.8 Hz, 12H), 1.11 (d, $J$ = 6.8 Hz, 11H), 1.04 (d, $J$ = 6.9 Hz, 11H), 0.99 (d, $J$ = 6.8 Hz, 12H). ¹³C{¹H} NMR (126 MHz, C₆D₆) δ 146.31, 138.87, 138.66, 125.81, 123.98, 123.77, 102.64, 82.19, 28.54, 28.45, 24.41, 23.98, 23.93, 23.77. ¹⁹F NMR (470 MHz, C₆D₆) δ -60.85. Anal. Calcd for C₆₂H₇₆Cu₂F₁₂N₄: C, 60.43; H, 6.22; N, 4.55. Found: C, 60.16; H, 6.53; N, 4.78. X-ray crystal structure shown in Figure S7.

## [Cl₂NN]Cu-CH=CMe₂ intermediate radical capture experiment
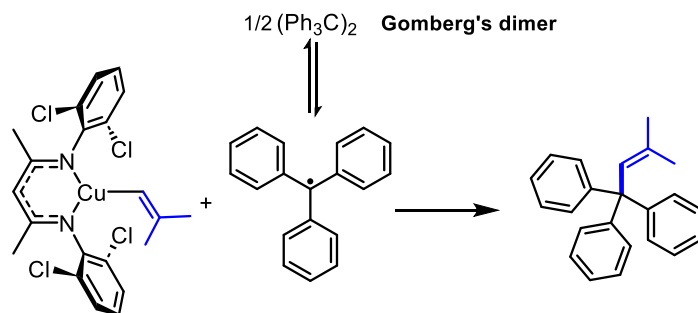


Gomberg's dimer was prepared according to literature reported methods.[17] In a nitrogen filled glovebox, **2a** (32 µL, 0.2 mmol, 1 equiv.) and Gomberg's dimer (49 mg, 0.1 mmol, 0.5 equiv.) were dissolved in 1 mL of benzene. Then the mixture solution was slowly added into a solution of [Cl₂NN]Cu-O$^t$Bu (100 mg, 0.2 mmol, 1 equiv. in 4 mL of benzene) under r.t. for 30 minutes. After the reaction was done, the reaction was quenched by exposure to air. The radical capture product was isolated via flash column chromatography (100 % hexane). Isolated yield was 35 %.
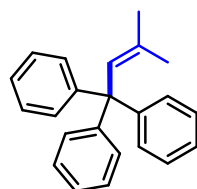


(3-methylbut-2-ene-1,1,1-triyl)tribenzene

$^1$H NMR (500 MHz, CDCl₃): δ 7.29 (m, 12H), 7.18 (m, 3H), 6.24 (s, 1H), 1.90 (d, $J$ = 1.5 Hz, 3H), 1.87 (d, $J$ = 1.4 Hz, 3H). $^{13}$C{$^1$H} NMR (126 MHz, CDCl₃) δ 147.07, 144.40, 137.83, 136.06, 128.40, 128.06, 127.80, 127.36, 124.76, 27.14, 19.66. HRMS (CI) m/z calcd. For C₂₃H₂₁$^+$ 297.1643, found 297.1632.

## Reactivity of [Cl₂NN]Cu-CH=CMe₂ in toluene

In a nitrogen filled glovebox, **2a** (32 µL, 0.2 mmol, 1 equiv.) was added to a stirring solution of [Cl₂NN]Cu-O$^t$Bu (100 mg, 0.2 mmol, 1 equiv.) in toluene (5 mL) and stirred for 16 h at -40 °C. The reaction was quenched by exposure to air. The Cu catalyst was removed by passing through 2 inches height of silica before analyzed by GCMS. 1,2,4,5-tetrachlorobenzene was added to the reaction mixture as an internal standard. Determined by GCMS analysis, the alkenyl dimerization product Me₂C=CH-CH=CMe₂ yield was 58% and the C-H alkenylation yield of **3a** was 3 %.
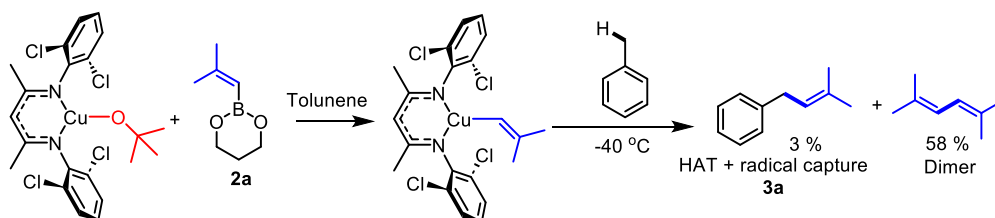
## 7. Crystallographic Details

X-ray data for compound [Cl$_2$NN]Cu-**2a** (CCDC: 2268882) and {[$^i$Pr$_2$NN$_{F6}$]Cu}$_2$(µ-CH$_2$=CH-CH=CH$_2$) (CCDC: 2329536) were collected at Michigan State University. A single crystal was selected and mounted on a nylon loop with paratone oil on a XtaLAB Synergy, Dualflex, HyPix diffractometer. The crystal was kept at a steady T = 100 K during data collection. The data was measured using $w$ scans using Cu K$_\alpha$ radiation (micro-focus sealed X-ray tube, 50 kV, 1 mA). The total number of runs and images was based on the strategy calculation from the program CrysAlisPro 1.171.42.93a (Rigaku OD, 2023).[18] The achieved resolution was 0.78 (Å). The structure was solved with the ShelXT 2018/2 (Sheldrick, 2018)[19] solution program using dual methods solution program using direct methods and by using Olex2 1.5 (Dolomanov et al., 2009) as the graphical interface.[20] The model was refined with ShelXL 2018/3 (Sheldrick, 2015)[21] using full matrix least squares minimization on F$^2$.
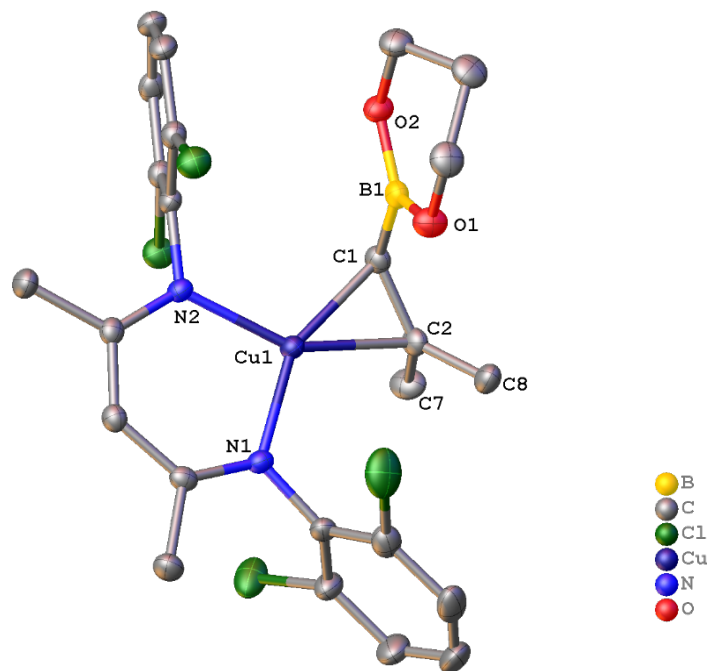


**Figure S7.** X-ray structure of [Cl$_2$NN]Cu($\eta^2$-**2a**) (CCDC: 2268882). The thermal ellipsoid plots are drawn at the 50% probability level. Hydrogen atoms were omitted for clarity. Selected bond distances (Å) and angles (°): Cu1-N1: 1.929(5), Cu1-N2: 1.948(2), Cu-C1: 2.000(1), Cu1-C2: 2.082(1), C1-C2: 1.397(1), N1-Cu-N2: 97.45(4).
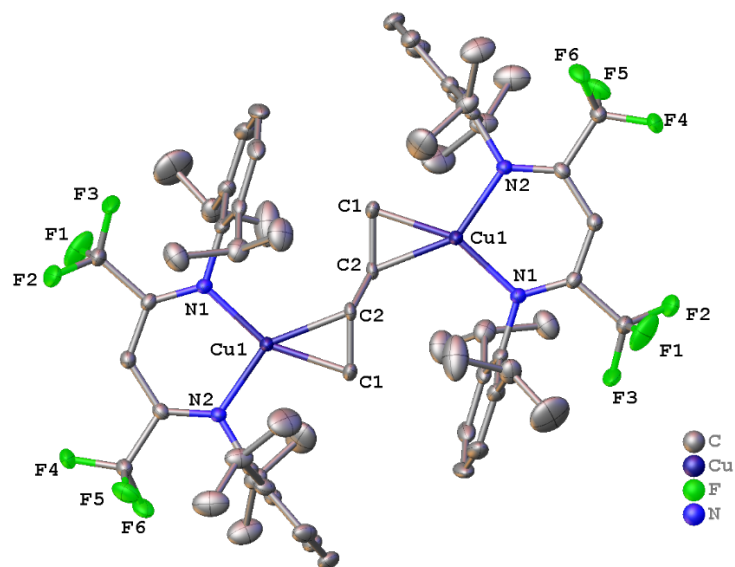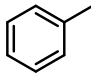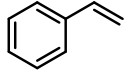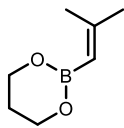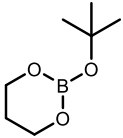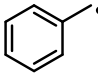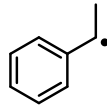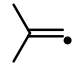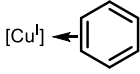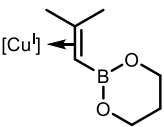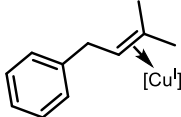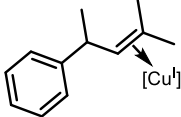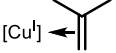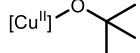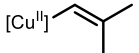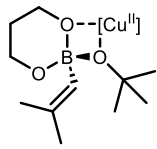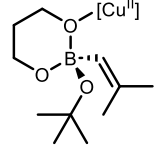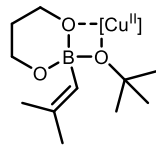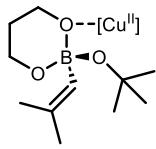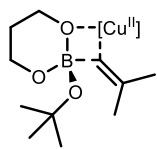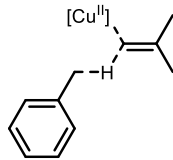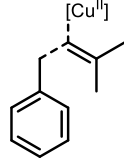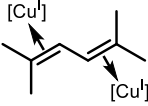
**Figure S8.** X-ray structure of {[$^i$Pr$_2$NN$_{F6}$]Cu}$_2$($\mu$-CH$_2$=CH-CH=CH$_2$) (CCDC: 2329536). The thermal ellipsoid plots were drawn at the 50% probability level. Hydrogen atoms were omitted for clarity. Selected bond distances (Å) and angles (°): Cu1-N1: 1.944(2), Cu1-N2: 1.953(5), Cu-C1: 2.035(1), Cu1-C2: 2.116(2), C1-C2: 1.390(5), C2-C2: 1.459(5), N1-Cu-N2: 98.42(2).

## 8. Computational Methods and Results

All computational results were done by the Gaussian 16 program.[22] Chemcraft 1.6 and Chimera were used to visualize structures and molecular orbitals. Calculations were performed adopting the BP86 functional,[23,24] and the 6-311++G(d,p) basis set for structure optimizations, single point geometries calculations, and free energy calculations. Calculations were conducted on closed-shell singlet and open-shell doublet spin states. Geometry optimizations were also performed without symmetry constraints at 298.15 K and 1 atmosphere with unscaled vibrational frequencies. Single point calculation of the optimized geometry also included solvent (SMD-benzene)[25] and dispersion (GD3BJ)[26] correction.

**Table S7.** Free energies for computed compounds in Hartrees at 298.15 K in benzene. [Cu$^I$] corresponds to the $\beta$-diketiminato [Cl$_2$NN]Cu fragment.

|  | C$_6$H$_6$ | C$_6$H$_5$CH$_3$ | C$_6$H$_5$CH$_3$ | **2a** | $^t$BuO-boronate |
|---|---|---|---|---|---|
| charge | 0 | 0 | 0 | 0 | 0 |
| spin state | 1 | 1 | 1 | 1 | 1 |
| free energy (Hartrees) | -232.2537094 | -271.5634419 | -309.6534893 | -449.9549335 | -526.4440753 |

|  | PhCH(•) | PhCH(•) | (CH$_3$)$_2$C=CH(•) | [Cu$^I$](C$_6$H$_6$) | [Cu$^I$]($\eta^2$-**2a**) |
|---|---|---|---|---|---|
| charge | 0 | 0 | 0 | 0 | 0 |
| spin state | 2 | 2 | 2 | 1 | 1 |
| free energy (Hartrees) | -270.9224698 | -310.2307259 | -156.5253654 | -4479.32959 | -4696.934112 |

|  | [Cu$^I$]($\eta^2$-**3a**) | [Cu$^I$]($\eta^2$-**3j**) | [Cu$^I$]($\eta^2$-CH$_2$=CMe$_2$) | [Cu$^{II}$]-O$^t$Bu | [Cu$^{II}$]-CH=CMe$_2$ |
|---|---|---|---|---|---|
| charge | 0 | 0 | 0 | 0 | 0 |
| spin state | 1 | 1 | 1 | 2 | 2 |
| free energy (Hartrees) | -4674.650066 | -4713.947558 | -4404.283445 | -4480.112795 | -4403.629456 |

|  | in$_A$ | in$_B$ | TS$_A$ | TS$_B$ |
|---|---|---|---|---|
| charge | 0 | 0 | 0 | 0 |
| spin state | 2 | 2 | 2 | 2 |
| free energy (Hartrees) | -4930.053516 | -4930.05341 | -4930.050742 | -4930.046292 |

|  | TS$_C$ | TS$_{HAT}$ | TS$_{RC}$ | dimer |
|---|---|---|---|---|
| charge | 0 | 0 | 0 | 0 |
| spin state | 2 | 2 | 3 | 1 |
| free energy (Hartrees) | -4930.050759 | -4675.172402 | -4674.535757 | -8807.374072 |

S29
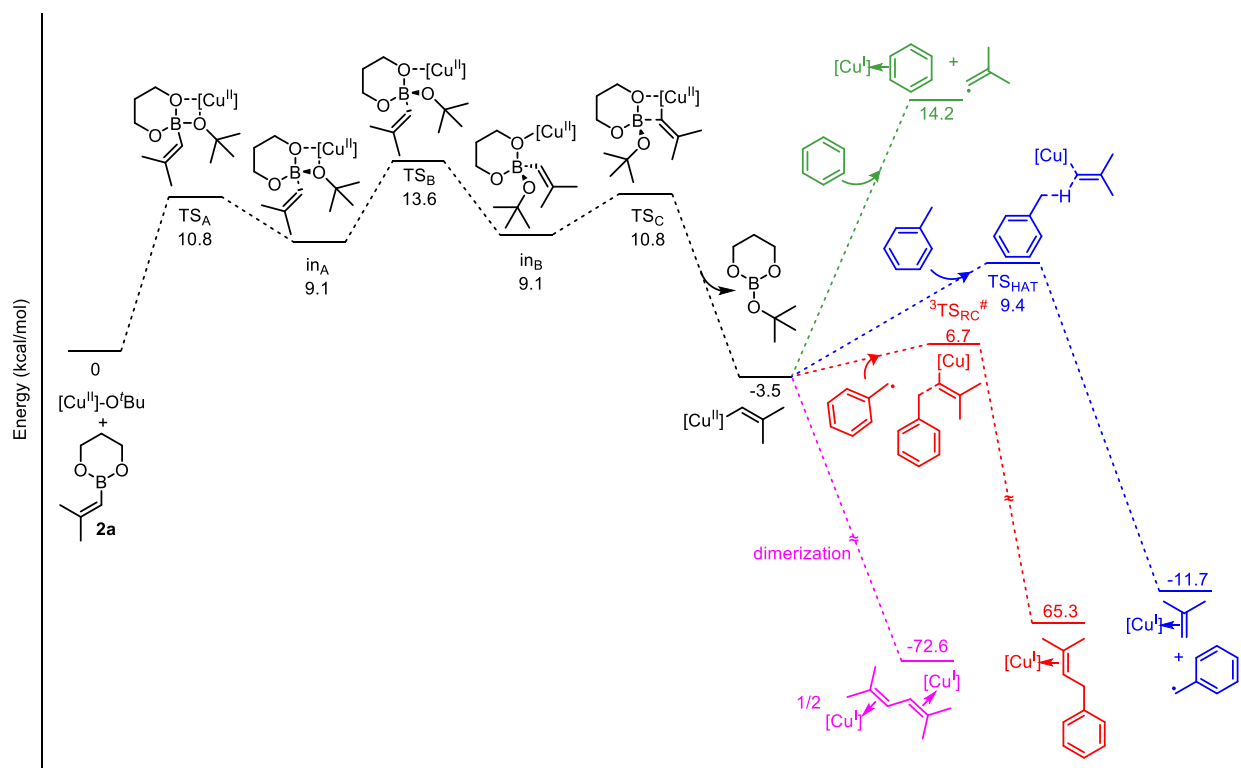
**Scheme S3.** Reaction coordinate and energy diagram for the reaction of alkenyl boronate **2a** with [Cu$^{II}$]-O$^t$Bu to form [Cu$^{II}$]-CH=CMe$_2$ (black). Subsequent steps illustrate reactivity of [Cu$^{II}$]-CH=CMe$_2$: loss of •CH=CMe$_2$ via displacement by benzene (green), H-atom abstraction of toluene to form PhCH$_2$• and [Cu$^I$]($\eta^2$-CH$_2$=CMe$_2$) (blue), capture of PhCH$_2$• to form [Cu$^I$]($\eta^2$-Me$_2$C=CHCH$_2$Ph) (red), and dimerization to form [Cu$^I$]$_2$($\mu$-Me$_2$C=CH-CH=CMe$_2$) (magenta). Free energies indicated in kcal/mol at 298.15 K. $^{\#3}$TS$_{RC}$ was optimized under triplet state ($\Delta$G$^{\ddagger}$= 10.2 kcal/mol) and suggests that radical coupling via the singlet state would have an even smaller reaction barrier.

[Cu$^I$] exhibits a higher affinity for binding with the reactant **2a** (ΔG = 7.5 kcal/mol) and a lower affinity with the product **3a** (ΔG = 5.9 kcal/mol) (Scheme S4a, b). Thus, dissociating the [Cu$^I$]($\eta^2$-**3a**) adduct is easier compared to [Cu$^I$]($\eta^2$-**2a**). Even if the unreacted **2a** replaces the **3a** in [Cu$^I$]($\eta^2$-**3a**) (ΔG = -1.6 kcal/mol, Scheme S4c), the newly formed [Cu$^I$]($\eta^2$-**2a**) can still dissociate under mild heating conditions (Scheme S4a), initiating the next cycle of the catalytic process.
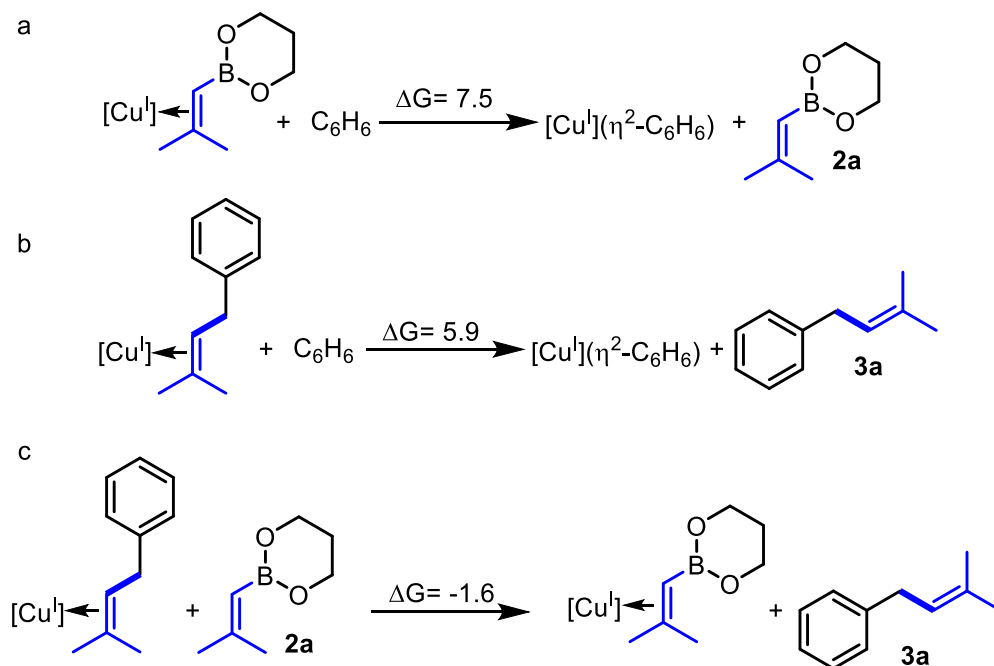


**Scheme S4.** DFT calculation of (a) [Cu$^I$] binds to **2a**, (b) [Cu$^I$] binds to **3a**, (c) [Cu$^I$]-**3a** displacement with **2a**. Free energies indicated in kcal/mol at 298.15 K.

Since the reaction intermediate [Cu<sup>II</sup>]-CH=C(Me)$_2$ exhibits H-atom abstraction reactivity (Scheme S3 and manuscript Figure 5civ), we considered the competition between radical capture of a 2° ethylbenzene radical to form a sp3-sp3 C-C bond in [Cu<sup>I</sup>](η²-**3l**) (ΔG = -55 kcal/mol) or undergo a HAT at the β-H position, producing styrene (ΔG = -48.3 kcal/mol) (Scheme S5). Both pathways are highly thermodynamically favorable, aligning with experimental results that show a ratio of PhCH(CH=Me$_2$)Me (**3l**) : styrene of 37% : 23%.
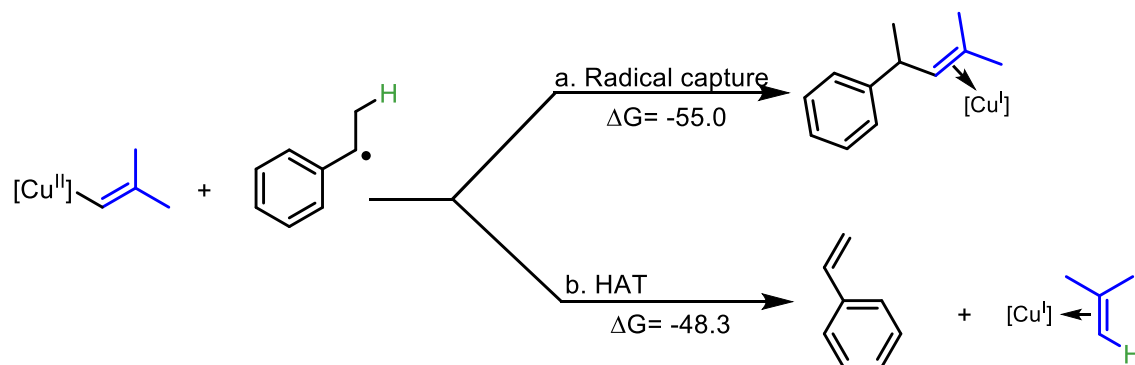


**Scheme S5.** DFT calculation of ethylbenzene radical reacts with [Cu<sup>II</sup>]-CH=C(Me)$_2$ via (a) radical capture, and (b) HAT. Free energies indicated in kcal/mol at 298.15 K.
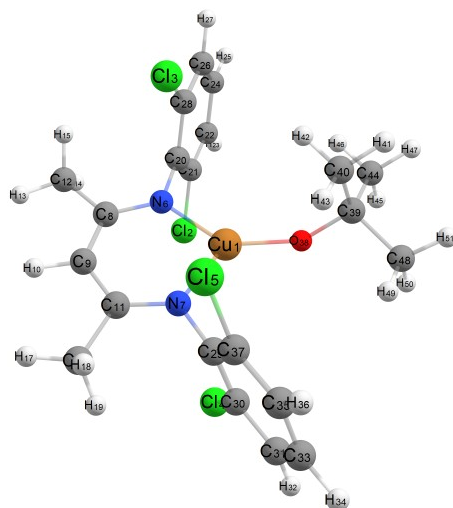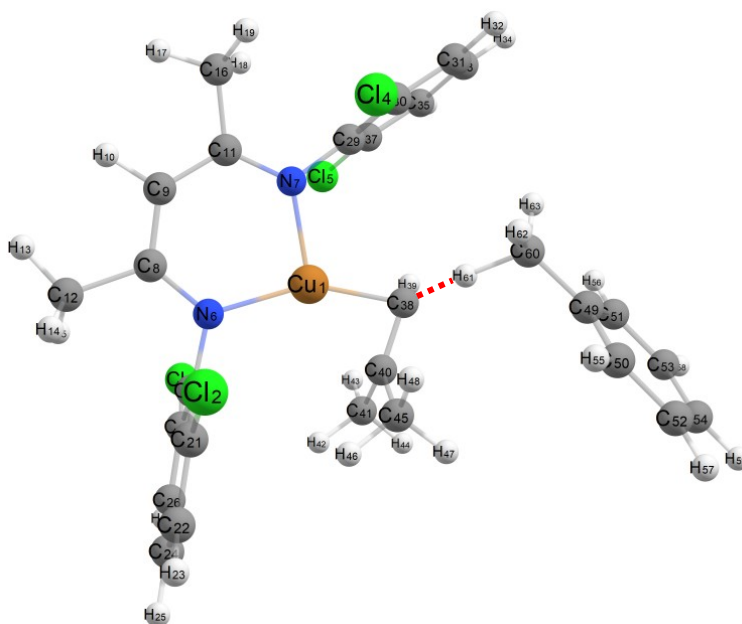


**Figure S9.** Geometry optimized structure of [Cl$_2$NN]Cu-O<sup>t</sup>Bu with charge = 0, multiplicity = 2. Selected calculated bond distances (Å) and angles (°) for [Cl$_2$NN]Cu(O-<sup>t</sup>Bu): Cu1-N6: 1.934; Cu1-N7: 1.934; Cu1-O38: 1.816; O38-C39: 1.421; N6-Cu1-N7: 96.20; N6-Cu1-O38: 131.68; N7-Cu1-O38: 131.68; Cu1-O38-C39: 132.602.
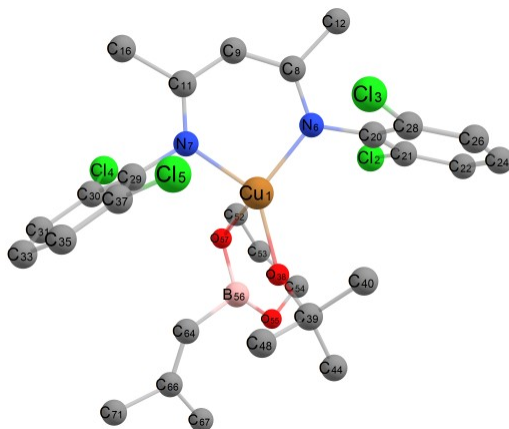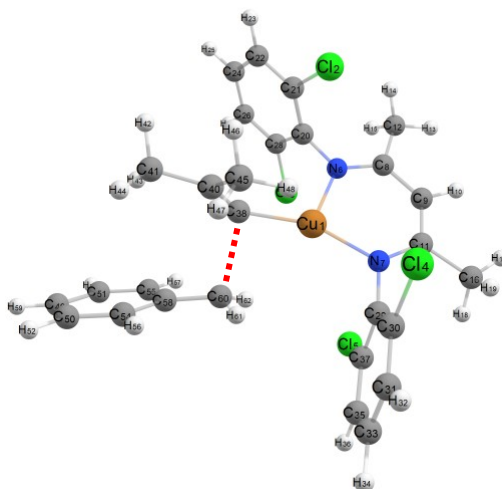
**Figure S10.** Geometry optimized structure of TS$_A$ with charge = 0, multiplicity = 2. Hydrogen atoms were omitted for clarity. Selected calculated bond distances (Å) and angles (º) for TS$_A$: Cu1-N6: 1.980; Cu1-N7: 1.957; Cu1-O38: 1.911; Cu1-O57: 2.364; Cu1-C64: 3.751; N6-Cu1-N7: 95.07; O38-Cu1-O57: 68.58; O38-B56-O57: 92.22; Cu1-O38-C39: 132.602.
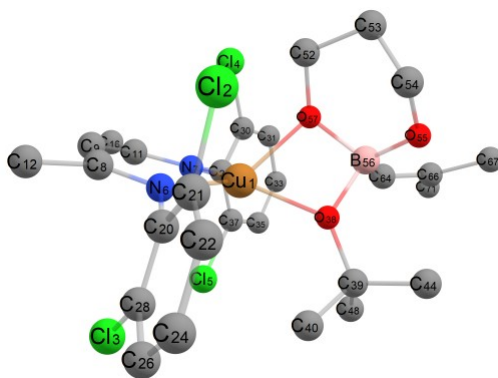


**Figure S11.** Geometry optimized structure of In$_A$ with charge = 0, multiplicity = 2. Hydrogen atoms were omitted for clarity. Selected calculated bond distances (Å) and angles (º) for In$_A$: Cu1-N6: 1.993; Cu1-N7: 1.972; Cu1-O38: 2.027; Cu1-O57: 2.091; Cu1-C64: 3.717; N6-Cu1-N7: 94.76; O38-Cu1-O57: 68.26; O38-B56-O57: 94.90.
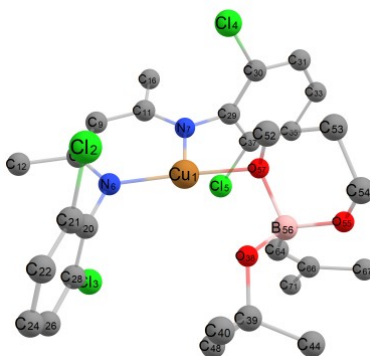
**Figure S12.** Geometry optimized structure of TS$_B$ with charge = 0, multiplicity = 2. Hydrogen atoms were omitted for clarity. Selected calculated bond distances (Å) and angles (°) for TS$_B$: Cu1-N6: 1.914; Cu1-N7: 1.994; Cu1-O38: 2.936; Cu1-O57: 1.933; Cu1-C64: 3.258; N6-Cu1-N7: 96.98; O38-Cu1-O57: 53.20; O38-B56-O57: 98.95.
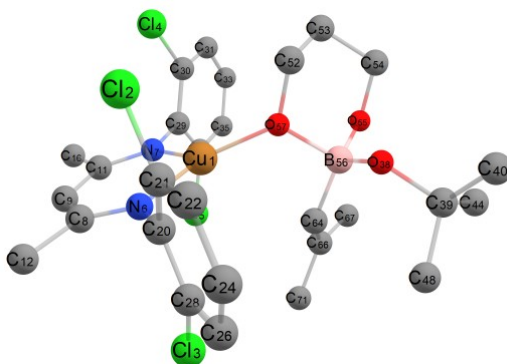


**Figure S13.** Geometry optimized structure of In$_B$ with charge = 0, multiplicity = 2. Hydrogen atoms were omitted for clarity. Selected calculated bond distances (Å) and angles (°) for In$_B$: Cu1-N6: 1.937; Cu1-N7: 1.926; Cu1-O38: 3.967; Cu1-O57: 1.888; Cu1-C64: 3.002; N6-Cu1-N7: 96.99; C64-Cu1-O57: 57.68; O38-B56-O57: 100.35.
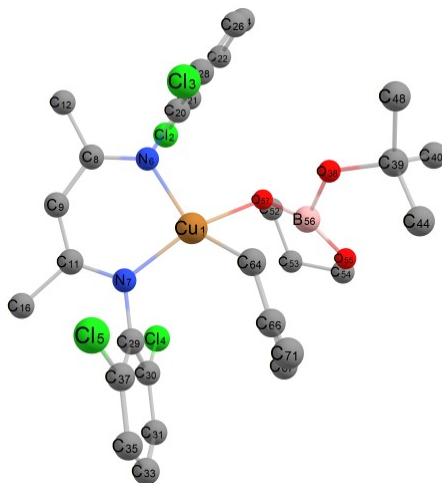


**Figure S14.** Geometry optimized structure of TS$_C$ with charge = 0, multiplicity = 2. Hydrogen atoms were omitted for clarity. Selected calculated bond distances (Å) and angles (°) for TS$_C$: Cu1-N6: 2.019; Cu1-N7: 1.984; Cu1-O57: 2.053; Cu1-C64: 2.051; C64-B56: 2.033; O38-B56: 1.409; N6-Cu1-N7: 94.84; C64-Cu1-O57: 81.42; O38-B56-O57: 110.18.
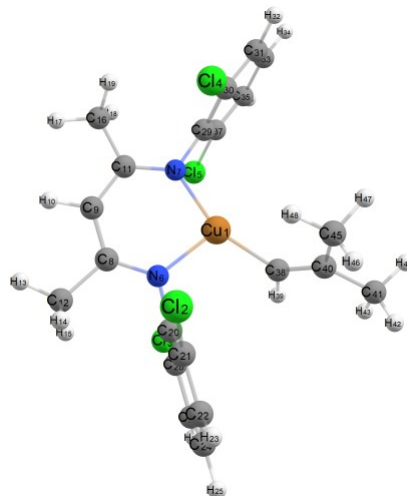
**Figure S15.** Geometry optimized structure of [Cu$^{II}$]-CH=CMe$_2$ with charge = 0, multiplicity = 2. Selected calculated bond distances (Å) and angles (°) for [Cu$^{II}$]-CH=CMe$_2$: Cu1-N6: 1.968; Cu1-N7: 1.934; Cu1-C38: 1.907; Cu1-C64: 2.051; N6-Cu1-N7: 96.03; N7-Cu1-C38: 155.40; O38-B56-O57: 108.43; Cu1-C38-C40: 127.18; Cu1-C38-H39: 115.43.



**Figure S16.** Geometry optimized structure of TS$_{HAT}$ with charge = 0, multiplicity = 2. Selected calculated bond distances (Å) and angles (°) for TS$_{HAT}$ : Cu1-N6: 1.958; Cu1-N7: 1.971; Cu1-C38: 1.947; C38-H61: 1.479; C60-H61: 1.269; N6-Cu1-N7: 96.95; N6-Cu1-C38: 153.29; N7-Cu1-C38: 109.57; C38-H61-C60: 170.91; Cu1-C38-C40: 79.63. The dotted red line represents the H61 atom movement during HAT. Imaginary frequency: -1037.07 cm$^{-1}$.
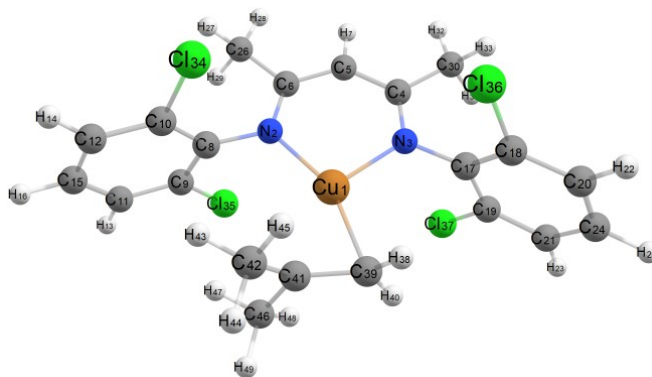
**Figure S17.** Geometry optimized structure of $[Cu^I](\eta^2\text{-CH}_2=\text{CMe}_2)$ with charge = 0, multiplicity = 1. Selected calculated bond distances (Å) and angles (°) for $[Cu^I](\eta^2\text{-CH}_2=\text{CMe}_2)$: Cu1-N2: 1.952; Cu1-N3: 1.965; Cu1-C39: 2.004; C39-C41: 1.399; C39-H38: 1.097; C39-H40: 1.097; N2-Cu1-N3: 97.60; N2-Cu1-C39: 155.80; C41-C39-Cu1: 74.67; H38-C39-H40: 115.68; C41-C39-H38: 120.64.



**Figure S18.** Geometry optimized structure of TS$_{RC}$ with charge = 0, multiplicity = 3. Selected calculated bond distances (Å) and angles (°) for TS$_{RC}$: Cu1-N6: 1.970; Cu1-N7: 1.937; Cu1-C38: 1.926; C38-C60: 2.221; N6-Cu1-N7: 96.18; N7-Cu1-C38: 156.92; C58-C60-C38: 106.61; C60-C38-C40: 111.22; C60-C38-H39: 90.13. The dotted red line represents the C38 and C60 atom movement during radical capture. Imaginary frequency: -362.4334 cm$^{-1}$.
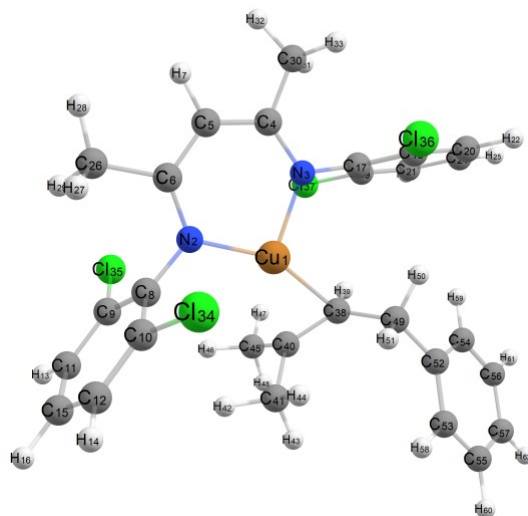
**Figure S19.** Geometry optimized structure of $[Cu^I](\eta^2$-$Me_2C$=$CHCH_2Ph$) with charge = 0, multiplicity = 1. Selected calculated bond distances ($\text{Å}$) and angles ($^o$) for $[Cu^I]$ ($\eta^2$-$Me_2C$=$CHCH_2Ph$): Cu1-N2: 1.962; Cu1-N3: 1.974; Cu1-C38: 2.037; Cu1-C40: 2.104; C40-C38: 1.404; N2-Cu1-N3: 97.27; N2-Cu1-C38: 153.76; C49-C38-C40: 125.54; H39-C38-C49: 114.02.
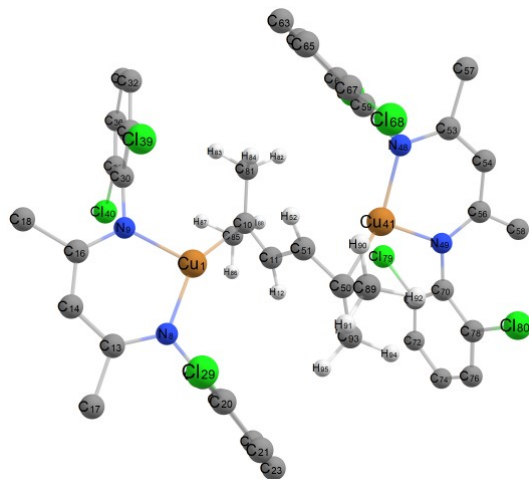


**Figure S20.** Geometry optimized structure of $[Cu^I]_2(\mu$-$Me_2C$=$CH$-$CH$=$CMe_2$) with charge = 0, multiplicity = 1. Hydrogen atoms on ligands were omitted for clarity. Selected calculated bond distances (Å) and angles ($^o$) for $[Cu^I]_2(\mu$-$Me_2C$=$CH$-$CH$=$CMe_2$): Cu1-N8: 1.986; Cu1-N9: 1.986; Cu1-C10: 2.095; Cu1-C11: 2.113; C10-C11: 2.113; C11-C51: 1.478; N8-Cu1-N9: 97.03; C10-Cu1-C11: 39.08; C51-C11-C10: 126.50.
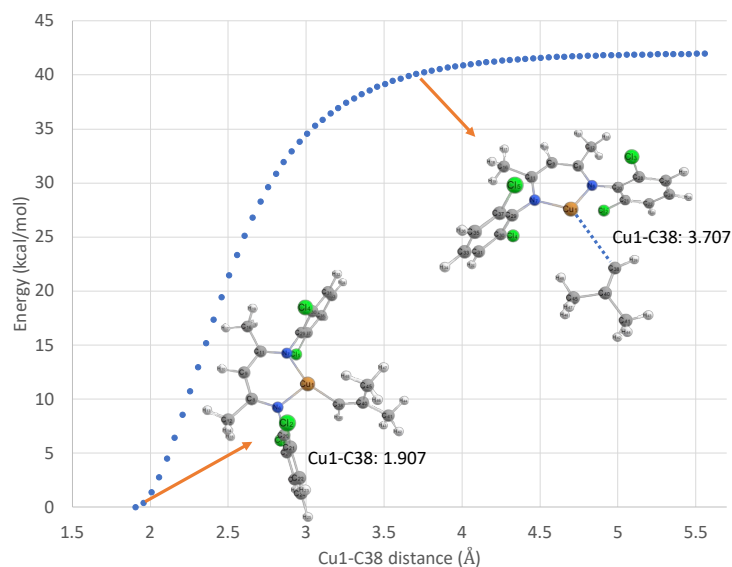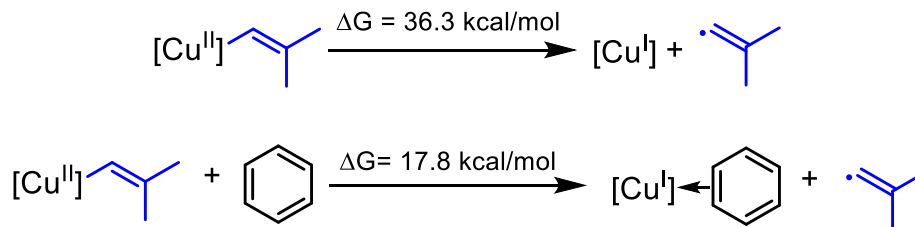
**Figure S21.** The free energy change calculated for alkenyl radical separation from [Cl$_2$NN]Cu-CH=CMe$_2$ in benzene solvent, both considering simple dissociative loss and associative displacement by benzene (top). A relaxed energy scan for alkenyl group dissociation from [Cl$_2$NN]Cu considers the electronic energy as the Cu-C distance is lengthened (bottom). Each step increment distance was +0.05 Å. The relaxed energy scan were performed adopting the BP86 functional, and the 6-31+G(d) basis set in gas phase.
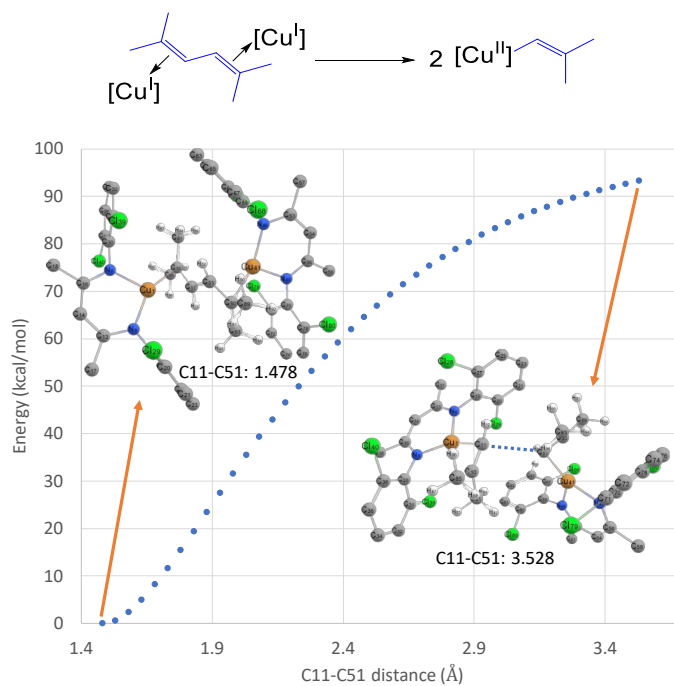
**Figure S22.** Relaxed energy scan of dimerization product [Cu$^I$]$_2$($\mu$-Me$_2$C=CH-CH=CMe$_2$) along the Me$_2$C=CH-CH=CMe$_2$ C-C single bond vector. Each step increment distance was +0.05 Å. This relaxed energy scan reveals that C-C bond formation from separated [Cu$^{II}$]-CH=CMe$_2$ species was extremely favored with a low (if any) barrier. Calculations were performed adopting the BP86 functional, and the 6-31+G(d) basis set in gas phase.
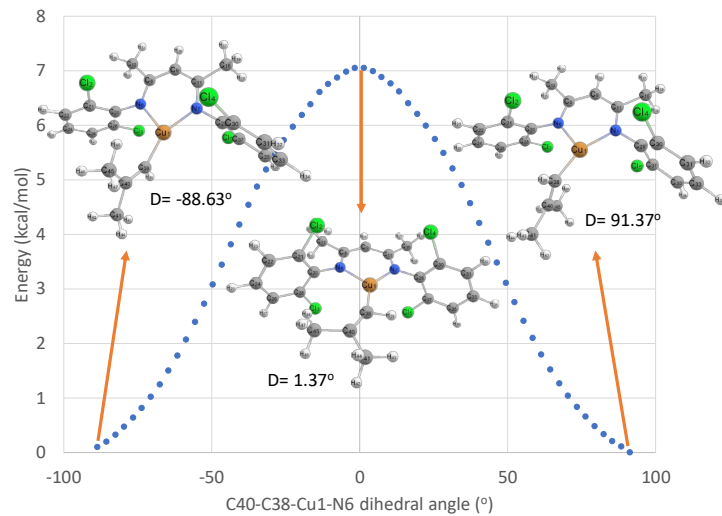
**Figure S23.** A relaxed energy scan illustrating rotation of the N-Cu-C=CMe$_2$ vector of [Cu$^{II}$]-CH=CMe$_2$ indicating a low barrier for Cu-C bond rotation. Each step increment distance was +3.0°. Calculations were performed adopting the BP86 functional, and the 6-31+G(d) basis set in gas phase.

### 9. Construction the Chemical Space Diagram for Benzylic CH₃ Substrates

The search was performed on Reaxys® on September 20, 2023.

Examining our substrate scope, we identified the compatibility of our catalytic conditions with ketones, ethers, and aryl halides. We further investigated the extent to which our substrate scope covers the chemical space diagram for commercially available benzylic CH₃ substrates.

Initial search:

Using "ARY-CH₃" as a model molecule in Reaxy, we got 3,996,213 substrates as the initial result. To further minimize the substrate pool to fit our substrate table, we add additional filters including "Molecular weight <= 185", "Number of fragments= 1", "commercial substances", available "NMR spectroscopy", available "Boiling point", available "Melting point", "Hydrogen bond donors= 0", "no alkyl halide", "no ester", "no Sulfer, Nitrogen, Phospher, Boron", and "no alkene and alkyne". The filtered search minimizes the substrate pool to 655 molecules, and the result was exported to a smile file.

Annotated Jupyter notebook

```python
#!/usr/bin/env python
# coding: utf-8

# In[1]:


from rdkit import Chem
from rdkit import DataStructs
from rdkit.Chem import Descriptors
from rdkit.Chem.MolStandardize import rdMolStandardize
# rdkit.Chem.MolStandardize.rdMolStandardize


import re, tqdm, sys, copy
import sklearn.decomposition, sklearn.manifold, lmfit
import numpy as np
import pandas as pd

import matplotlib.pyplot as plt
import matplotlib.cm as cm
import matplotlib

import plotly.express as px
import molplotly
```

```python
# make matplotlib look good
plt.rc('font', size=8, family="serif")
plt.rc('axes', titlesize=10, labelsize=10)
plt.rc(['xtick', 'ytick'], labelsize=8)
plt.rc('legend', fontsize=10)
plt.rc('figure', titlesize=12)
get_ipython().run_line_magic('matplotlib', 'inline')
get_ipython().run_line_magic('config', "InlineBackend.figure_format='svg'")


# In[2]:


class BenCH3:

    def __init__(self, smiles):
        self.smiles = smiles
        self.mol = Chem.MolFromSmiles(self.smiles)
        self.fingerprint = None

    def __repr__(self):
        return f"BenCH3({self.smiles})"

    def get_fingerprint(self):
        if self.fingerprint is None:
            self.fingerprint = Chem.RDKFingerprint(self.mol, maxPath=7,
branchedPaths=False)

        return self.fingerprint


# In[3]:


class BenCH3:

    def __init__(self, smiles):
        self.smiles = smiles
        self.mol = Chem.MolFromSmiles(self.smiles)
        self.fingerprint = None

    def __repr__(self):
        return f"BenCH3({self.smiles})"

    def get_fingerprint(self):
        if self.fingerprint is None:
```

```python
        self.fingerprint = Chem.RDKFingerprint(self.mol, maxPath=7,
branchedPaths=False)

        return self.fingerprint

    def get_molecular_weight(self):

        return Descriptors.MolWt(self.mol)

# In[4]:


mols = []
with open("BenCH3.smi", "r") as f:
    for smiles_string in tqdm.tqdm(f.readlines(), total=660, ncols=100):
        mols.append(BenCH3(smiles_string))

# mols = []
# with open("aryl_bromide.smi", "r") as f:
#     for smiles_string in tqdm.tqdm(f.readlines(), total=1557, ncols=100):
#         mol = BenCH3(smiles_string)
#         molecular_weight = mol.get_molecular_weight()
#         if 100 <= molecular_weight <= 1500:
#             mols.append(mol)


# In[5]:


mol_nums = []

for i, m in enumerate(mols):
    mol_nums.append(i+1)
    try: fp = m.get_fingerprint()
    except: print(f"Problematic structure at index {i}: {m.smiles}")

len(mol_nums)


# In[6]:


X = np.stack([m.get_fingerprint() for m in mols])
print(X.shape)

pca = sklearn.decomposition.PCA(n_components=2)
```

```
Xpca = pca.fit_transform(X)
print(Xpca.shape)


# In[8]:


def plot_df_interactive(df, xlabel, ylabel, port, color=None):
    # to make color optional, we'll use some kwargs magic
    bonus_px_kwargs = {}
    bonus_mp_kwargs = {}
    if color is not None:
        bonus_px_kwargs["color"] = color
        bonus_mp_kwargs["color_col"] = color

    # generate a scatter plot in plotly
    fig = px.scatter(
        df,
        x=xlabel,
        y=ylabel,
        width=550,
        height=550,
        template="simple_white",
        **bonus_px_kwargs
    )

    # add molecules to the plotly graph - returns a Dash app
    app = molplotly.add_molecules(
        fig=fig,
        df=df,
        smiles_col='smiles',
        title_col='smiles',
        **bonus_mp_kwargs
    )

    # run Dash app inline in notebook (or in an external server)
    app.run_server(mode='inline', port=port, height=600)
    # app.run_server()


# In[11]:


df = pd.DataFrame([m.smiles for m in mols], columns=["smiles"])
df["pca_1"] = Xpca[:, 0]
```

```python
df["pca_2"] = Xpca[:, 1]

plot_df_interactive(df, "pca_1", "pca_2", port=8053)


# In[21]:


# tsne = sklearn.manifold.TSNE(n_components=2, learning_rate='auto',
init='random', metric='jaccard', perplexity=20)
# Xtsne = tsne.fit_transform(X)
# print(Xtsne.shape)


# In[22]:


# df["tsne_1"] = Xtsne[:, 0]
# df["tsne_2"] = Xtsne[:, 1]

# plot_df_interactive(df, "tsne_1", "tsne_2")


# In[23]:


Xumap = umap.UMAP(
    n_components=2,
    n_neighbors=30,
    min_dist=0.3,
    metric="jaccard"
).fit_transform([m.get_fingerprint() for m in mols])


# In[20]:


# add umap to df
df["umap_1"] = Xumap[:,0]
df["umap_2"] = Xumap[:,1]

# and now we plot
plot_df_interactive(df, "umap_1", "umap_2", port=8090)
```
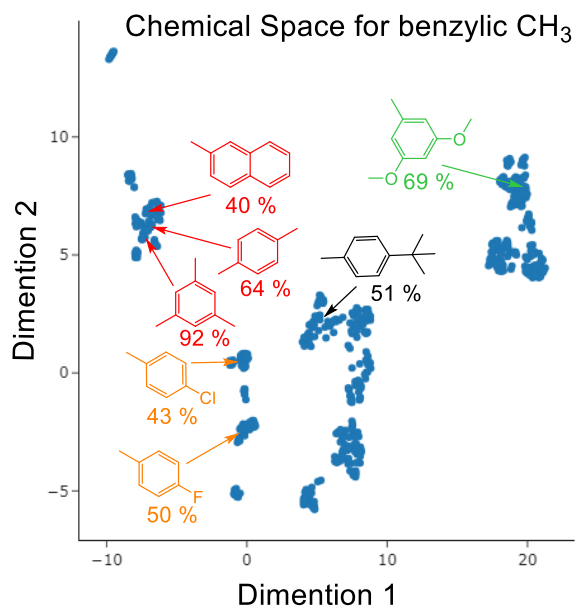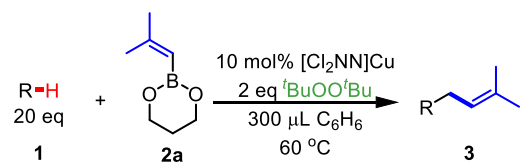
**Figure S24.** Chemical space diagram of benzylic CH₃ substrates by using uniform manifold approximation and projection (UMAP) with molecular fingerprints from a Reaxys search.

## 10. NMR spectra

$^1$H NMR spectrum of **2a** (500 MHz, CDCl$_3$).
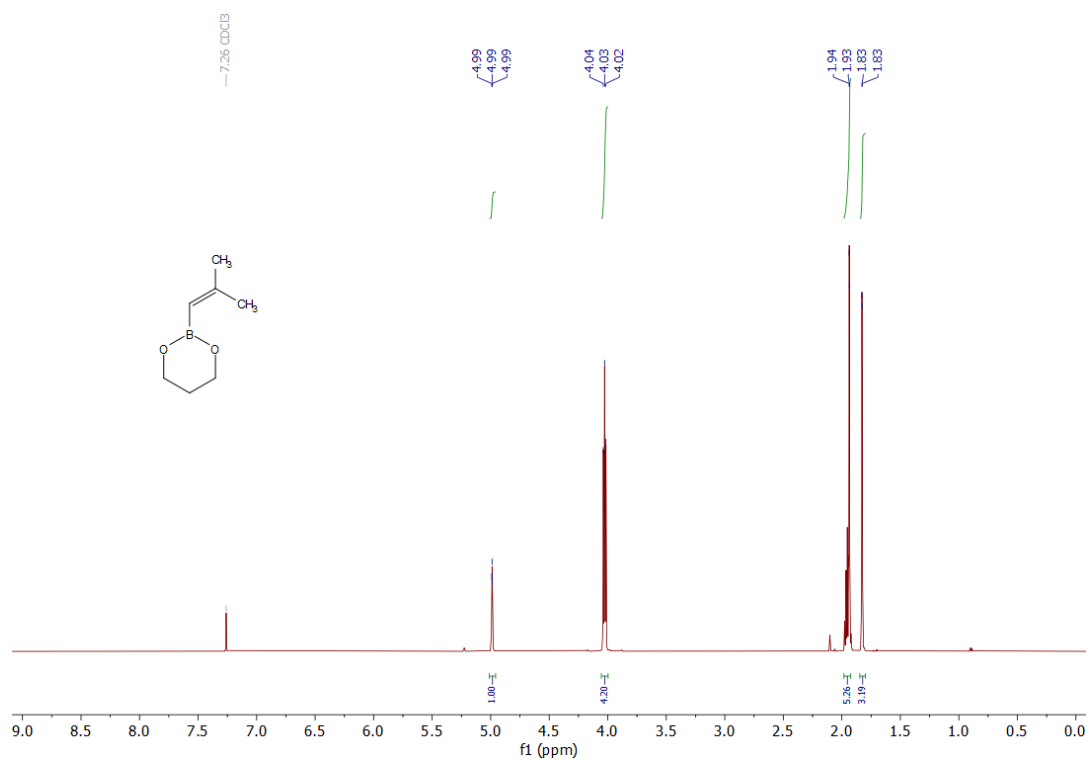


$^{13}$C{$^1$H} NMR spectrum of **2a** (500 MHz, CDCl$_3$).
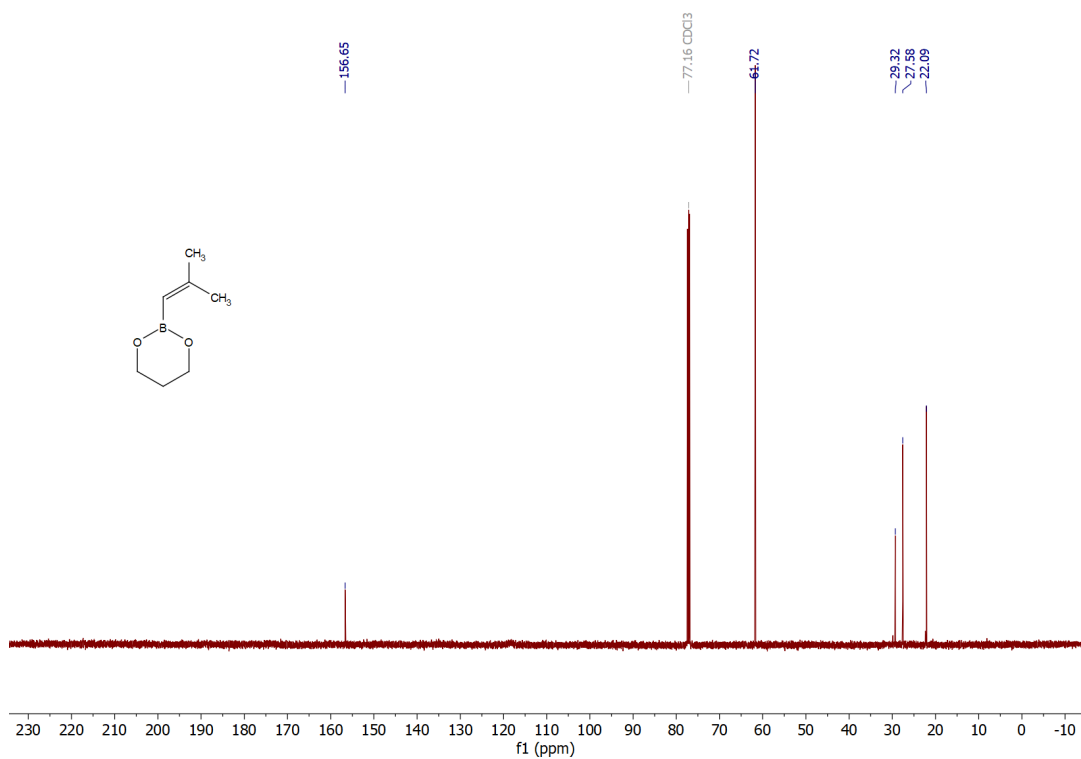
<sup>11</sup>B NMR spectrum of **2a** (500 MHz, CDCl<sub>3</sub>). BF<sub>3</sub>·OEt<sub>2</sub> serves as the internal standard (δ = 0.0 ppm).
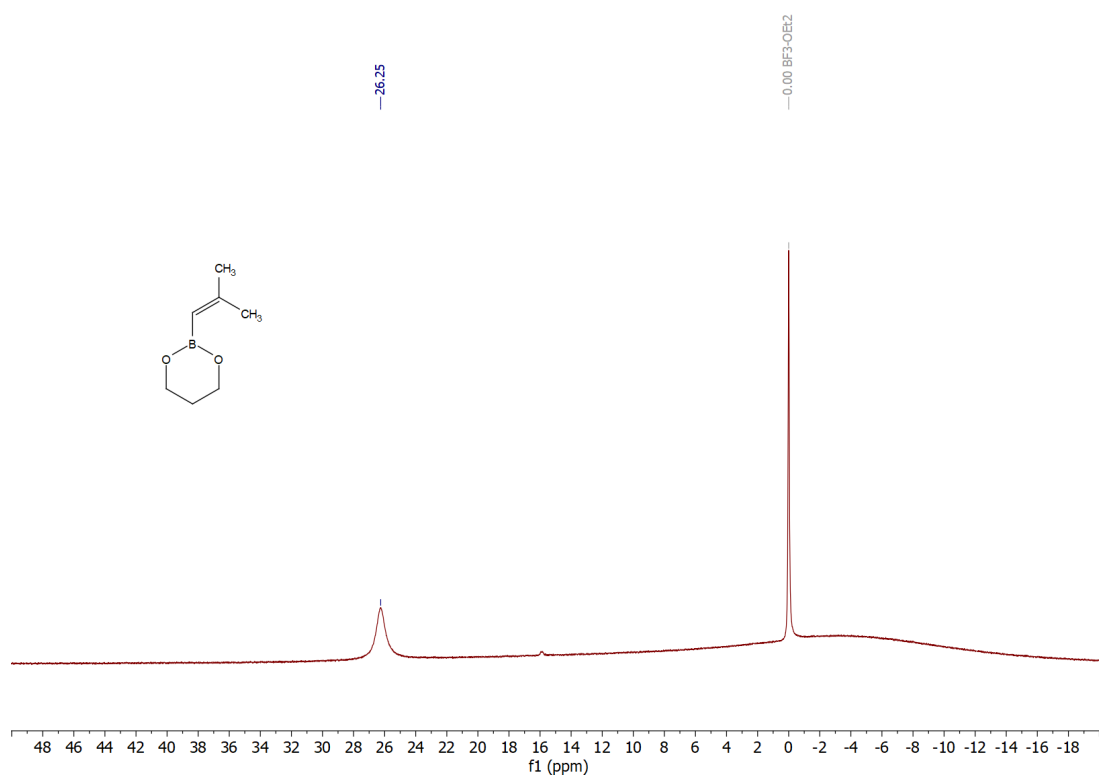
# ¹H NMR spectrum of **2b** (500 MHz, CDCl₃).
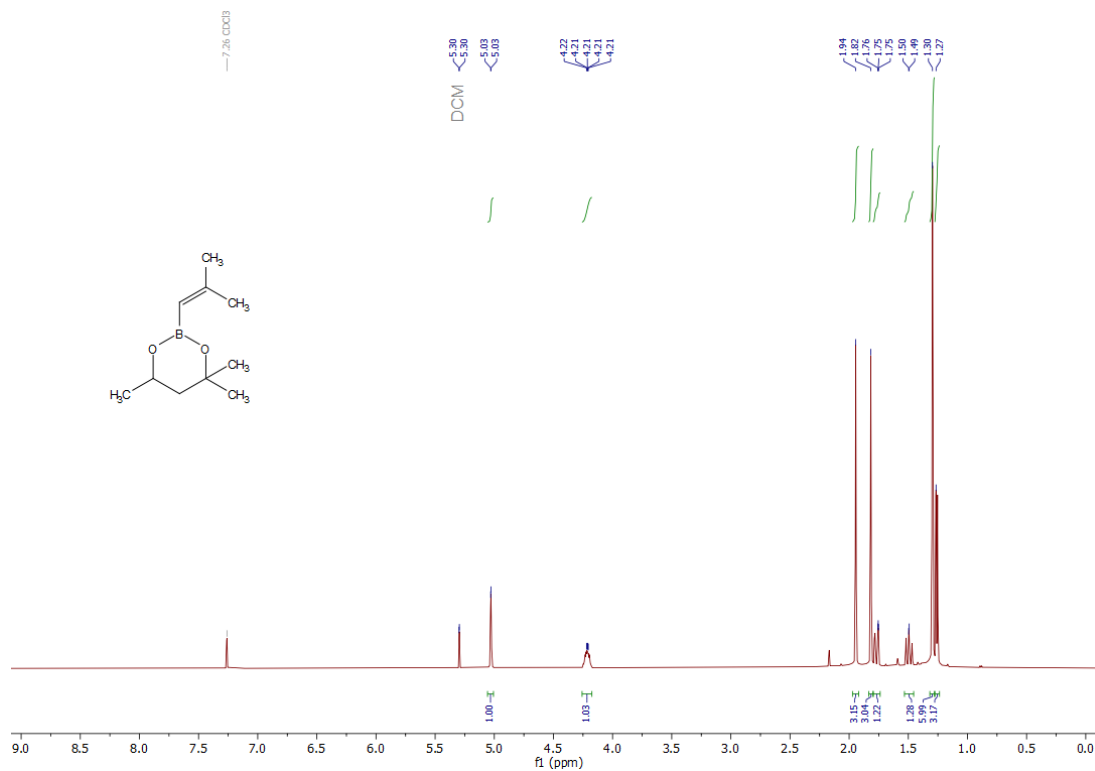


# ¹³C{¹H} NMR spectrum of **2b** (500 MHz, CDCl₃).
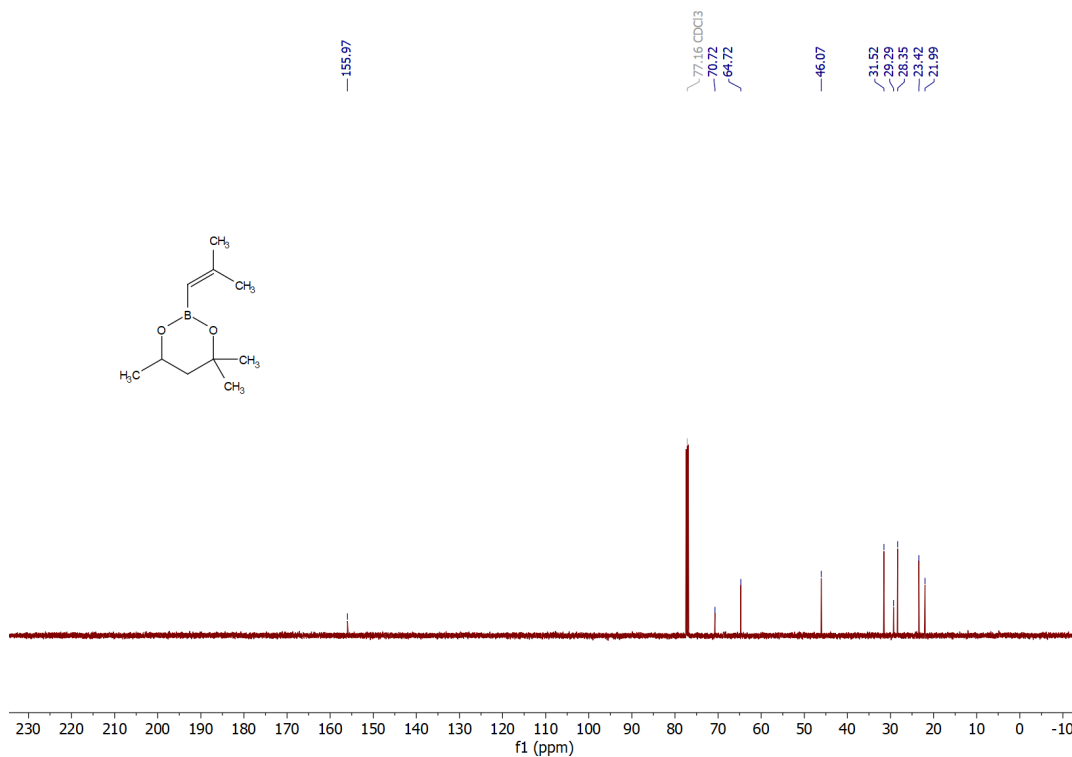
<sup>11</sup>B NMR spectrum of **2b** (500 MHz, CDCl$_3$). BF$_3$·OEt$_2$ serves as the internal standard ($\delta$ = 0.0 ppm). The broad peak at -4.3 ppm belongs to borosilicate from the NMR tube.
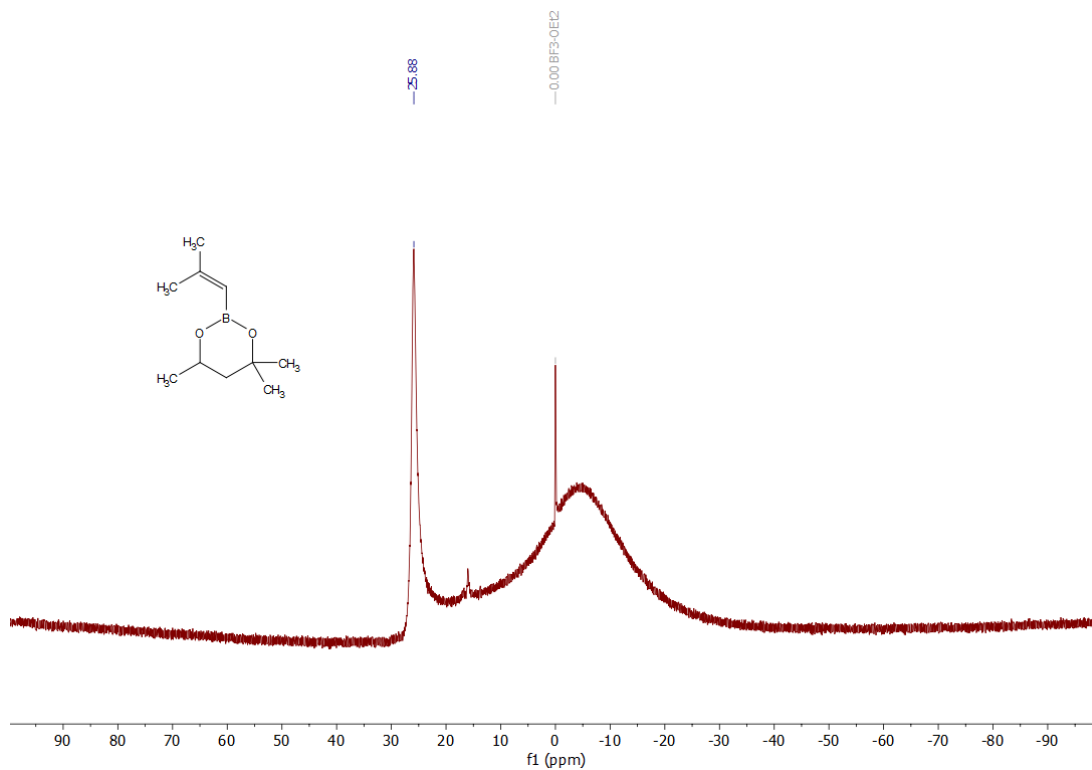
<sup>1</sup>H NMR spectrum of benzyl t-butyl ether from independent synthesis via acid-catalyzed etherification (500 MHz, CDCl<sub>3</sub>).
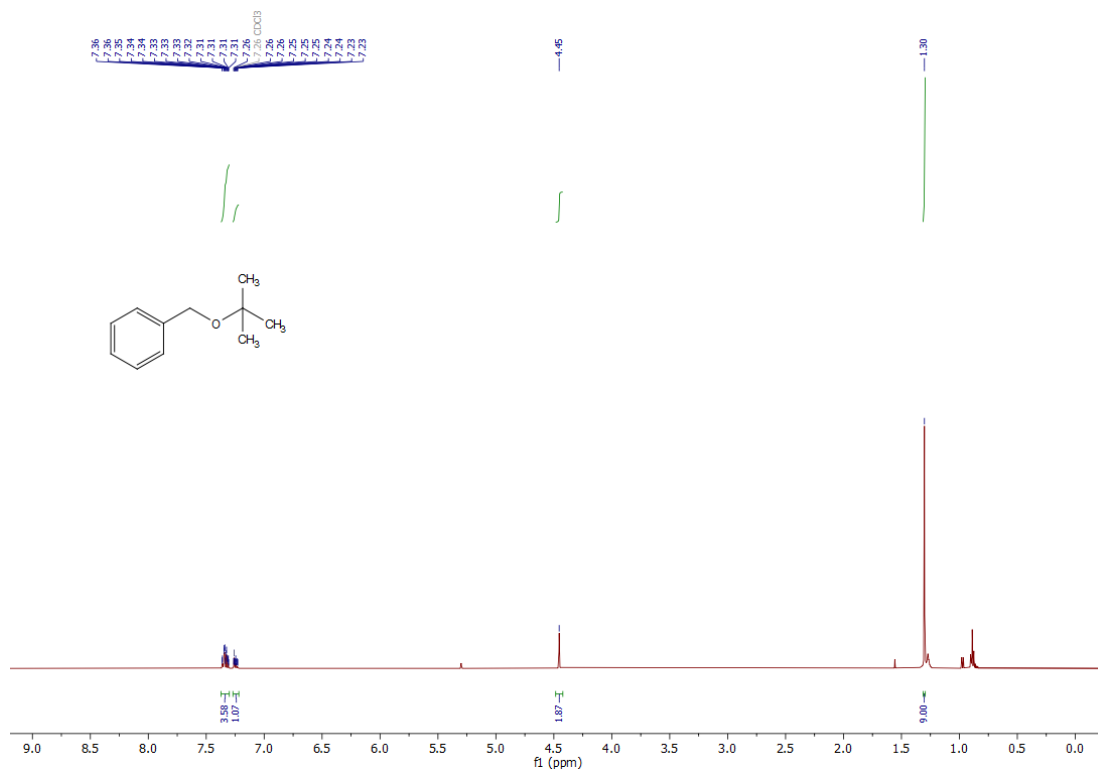
¹H NMR spectrum of **3a** from independent synthesis via Wittig reaction (500 MHz, CDCl₃).
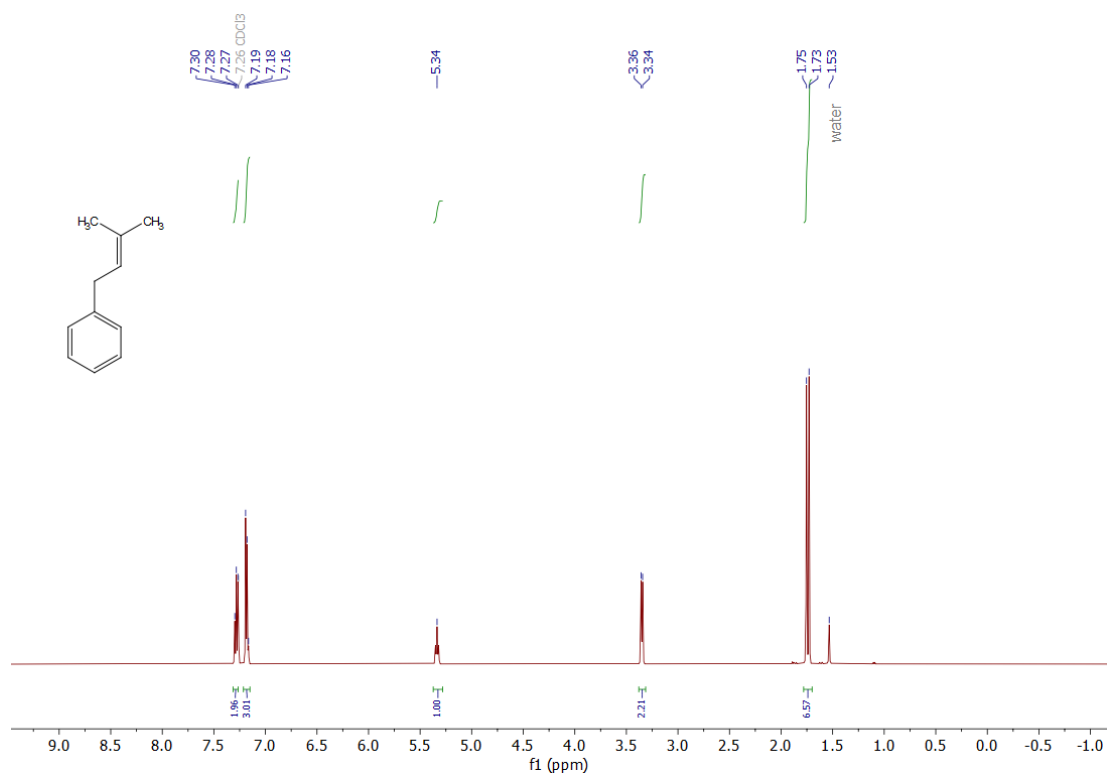


¹³C{¹H} NMR spectrum of **3a** from independent synthesis via Wittig reaction (500 MHz, CDCl₃).
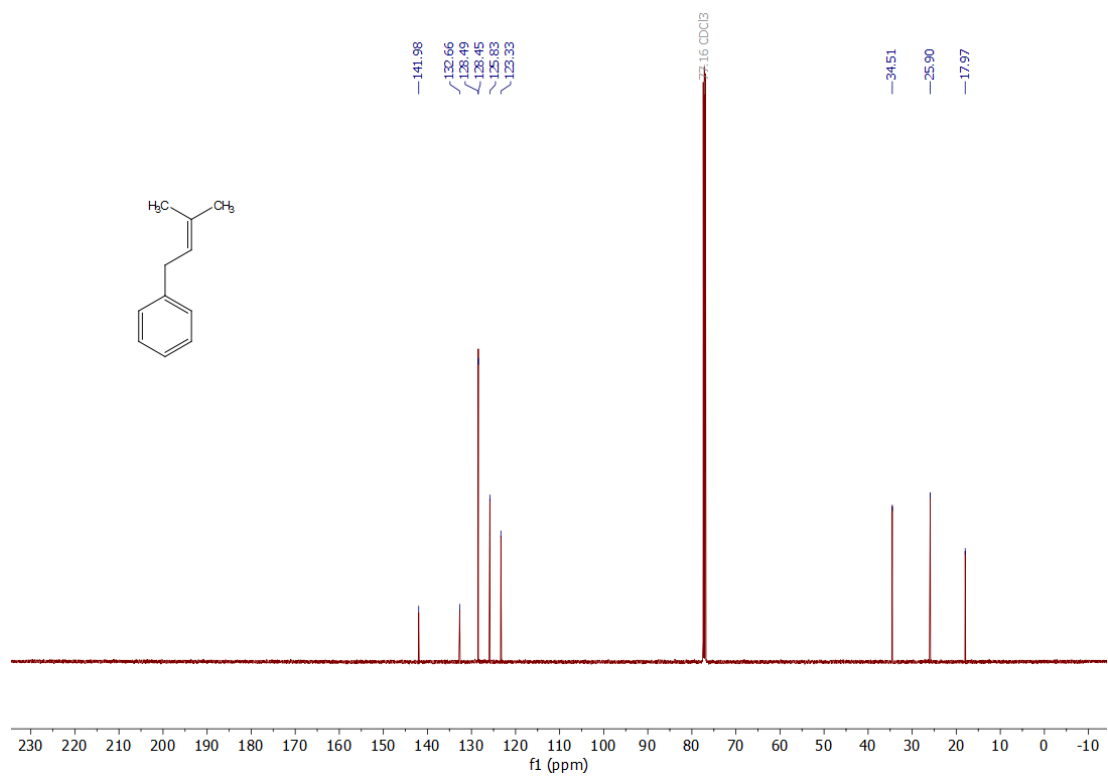
# ¹H NMR spectrum of **3b** (500 MHz, CDCl₃).
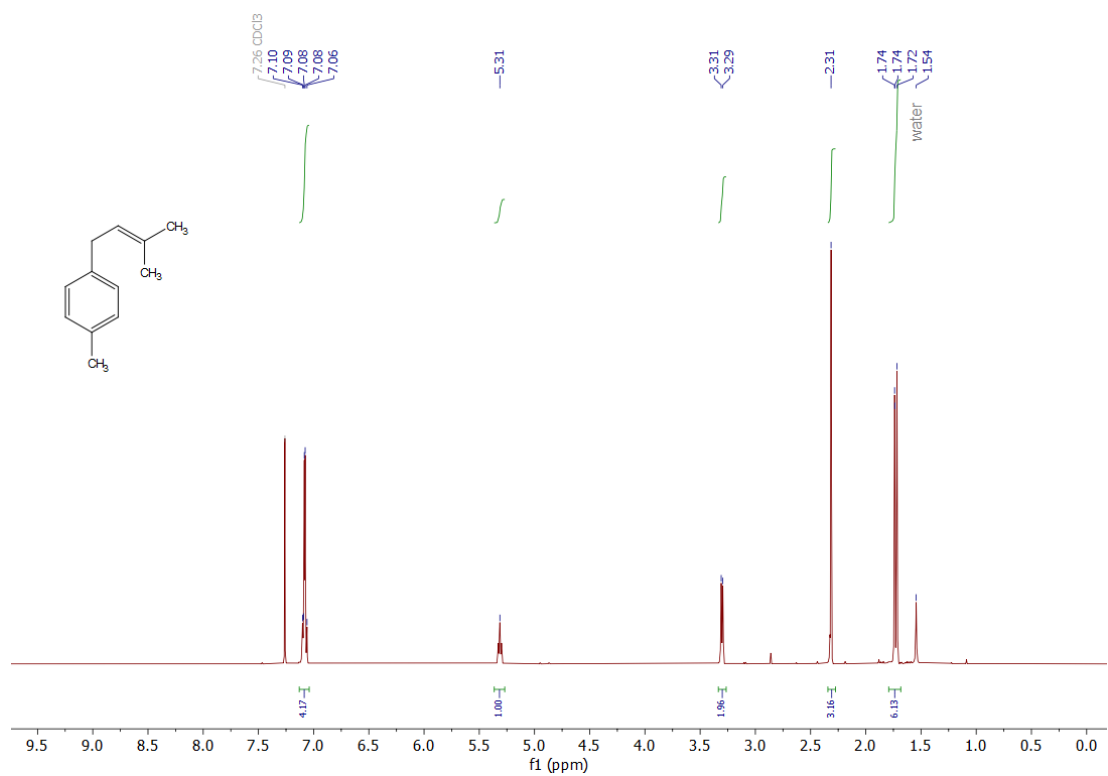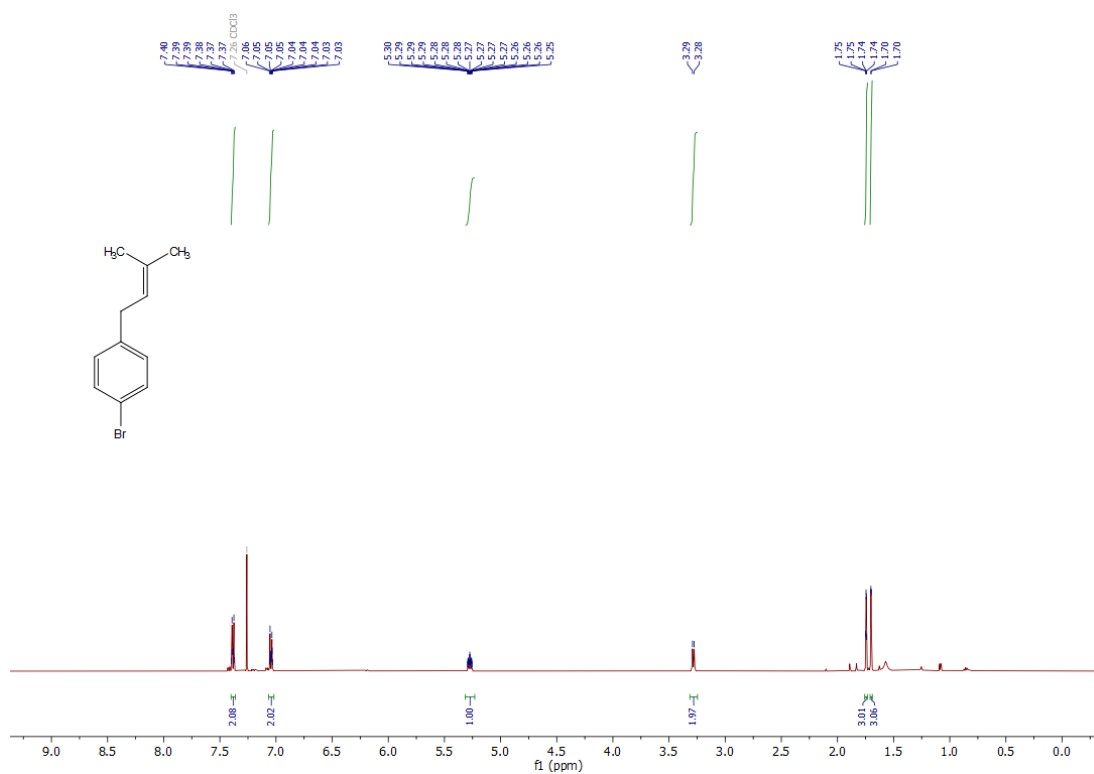


# ¹³C{¹H} NMR spectrum of **3b** (126 MHz, CDCl₃).
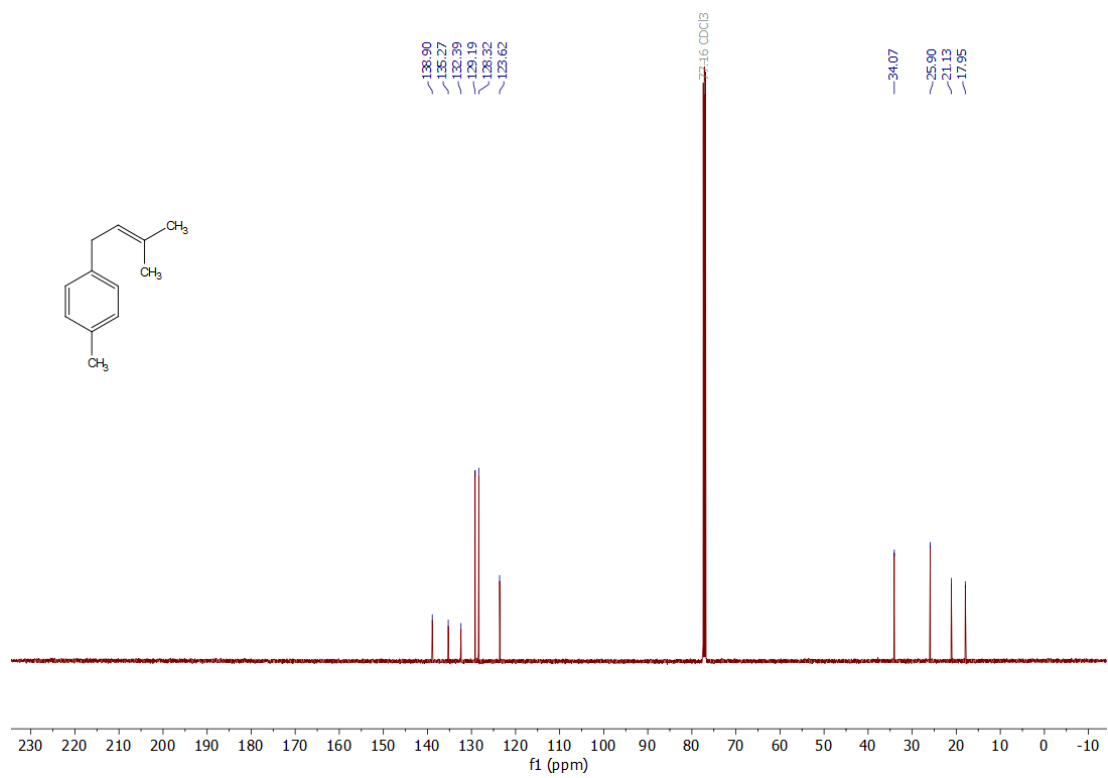
# $^1$H NMR spectrum of **3c** (500 MHz, CDCl$_3$).
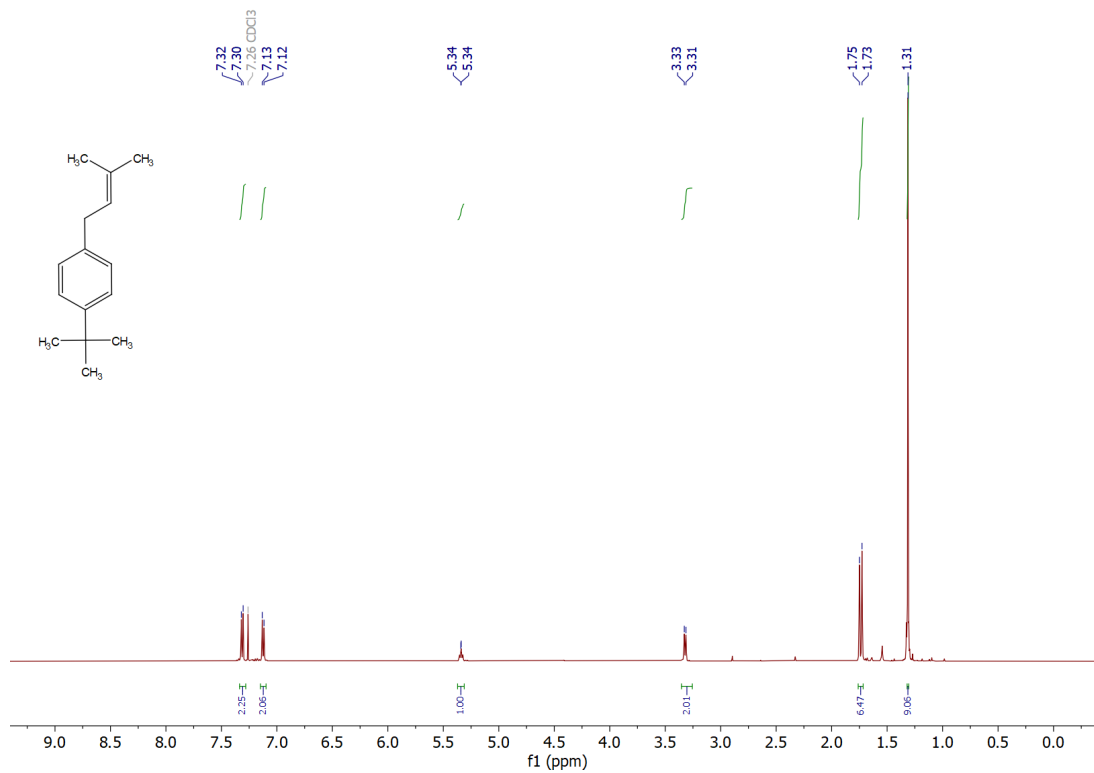


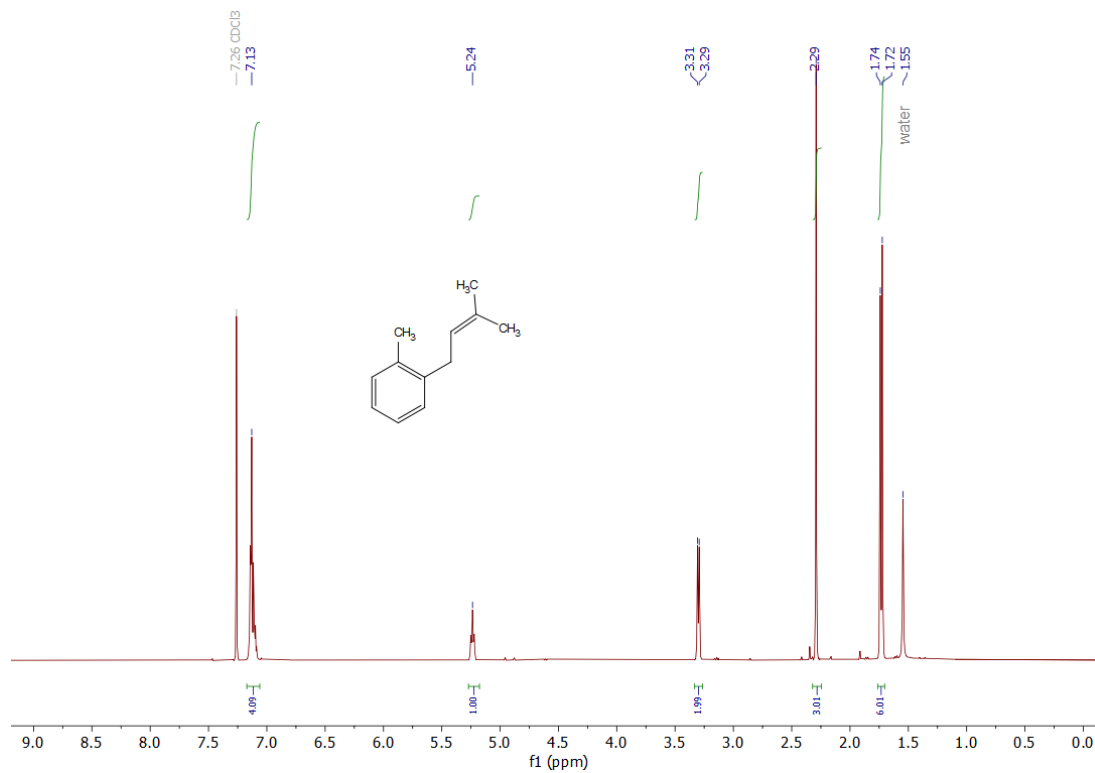# $^{13}$C{$^1$H} NMR spectrum of **3c** (126 MHz, CDCl$_3$).
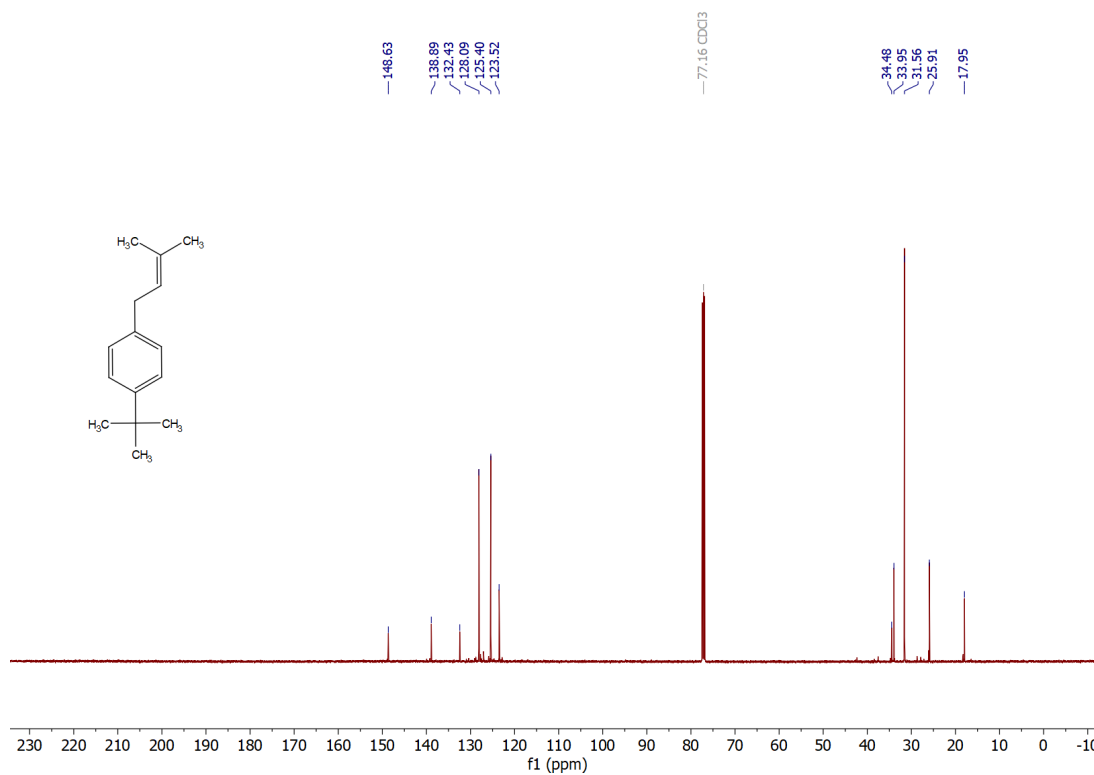
## $^1$H NMR spectrum of **3d** (500 MHz, CD$_2$Cl$_2$).
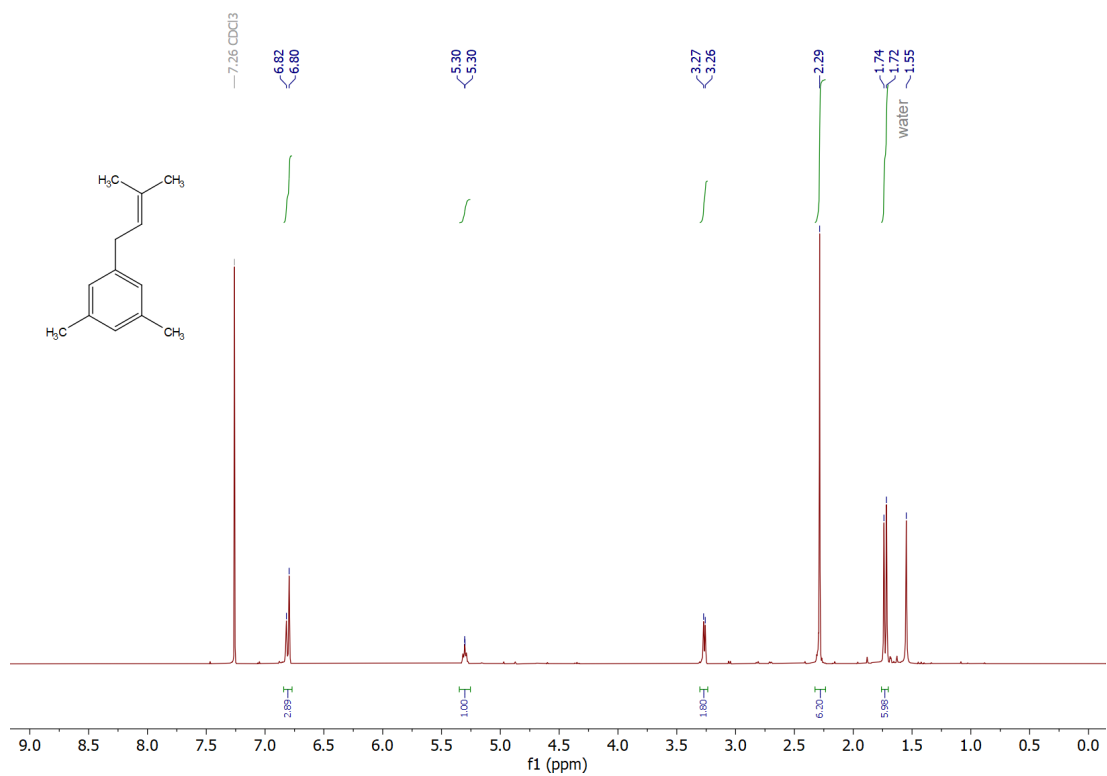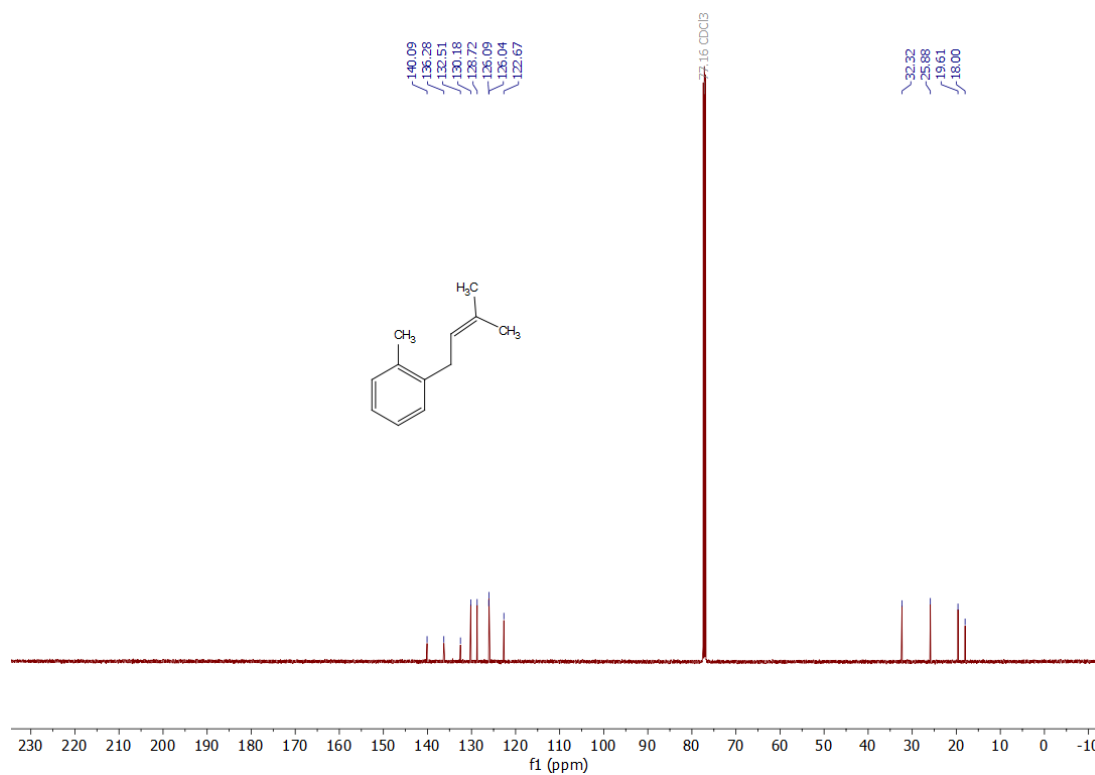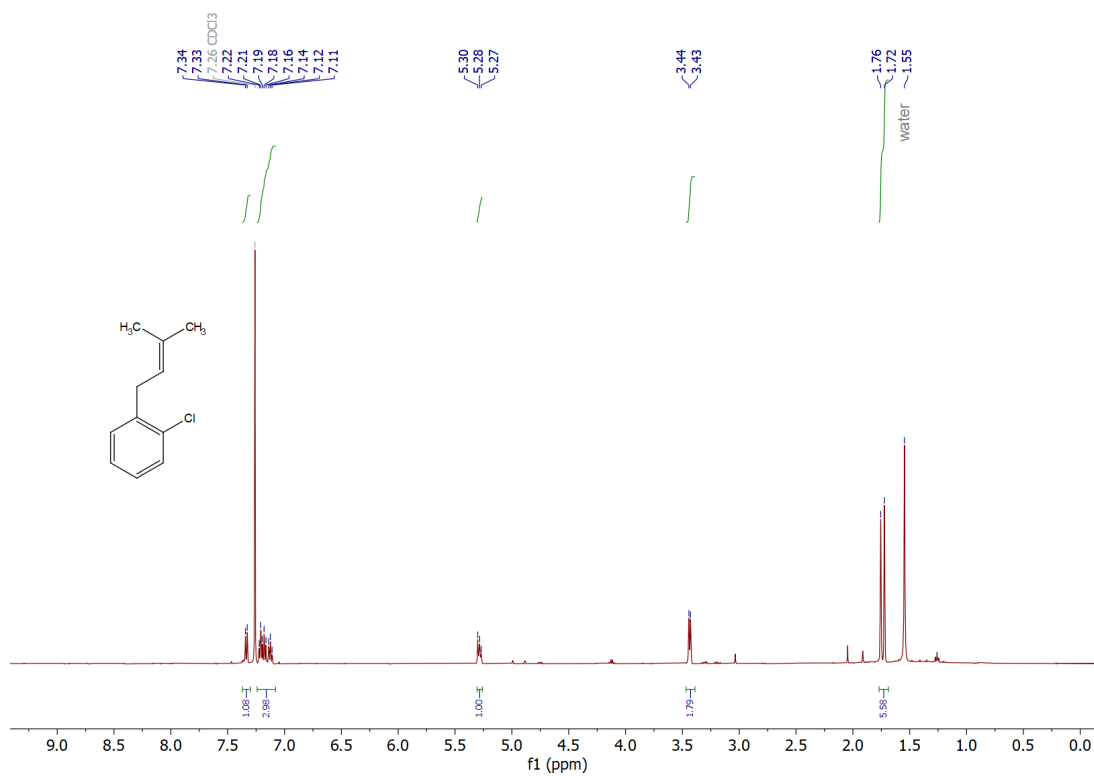


## $^{13}$C{$^1$H} NMR spectrum of **3d** (126 MHz, CD$_2$Cl$_2$).
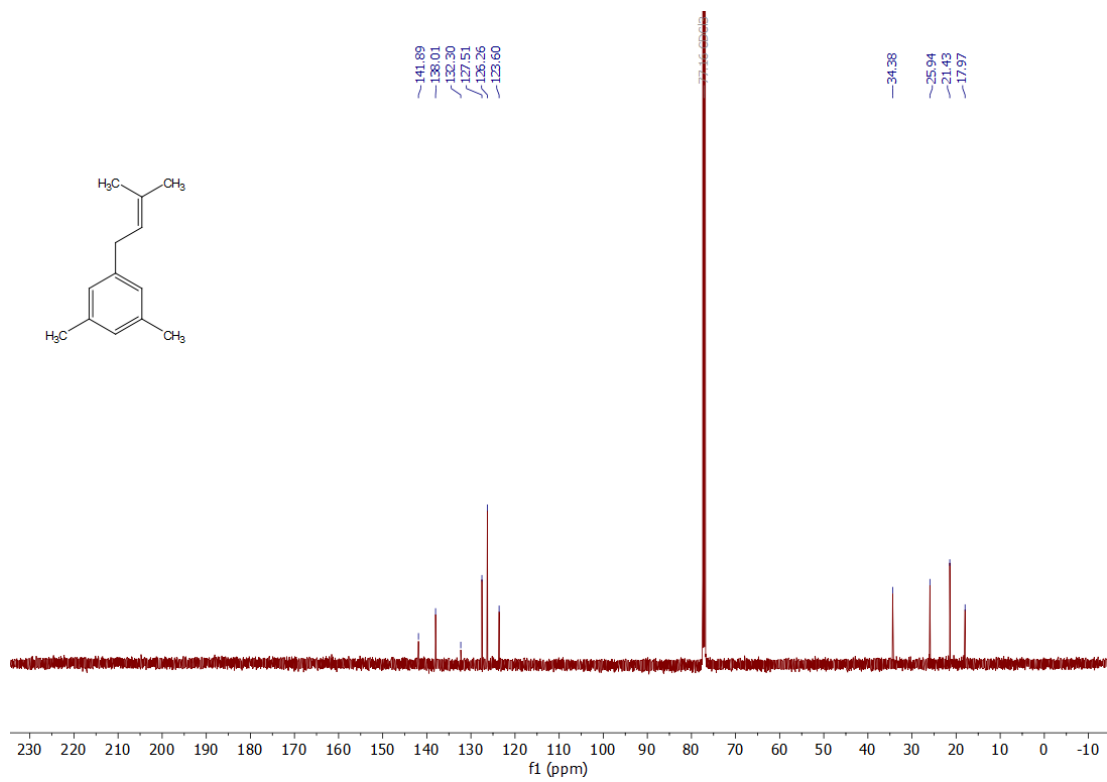
<sup>1</sup>H NMR spectrum of **3e** (500 MHz, CDCl<sub>3</sub>). Due to the separation challenges, a significant amount of R-H substrate (1,3-dimethoxy-5-methylbenzene) could not be removed. (# note as 1,3-dimethoxy-5-methylbenzene.)
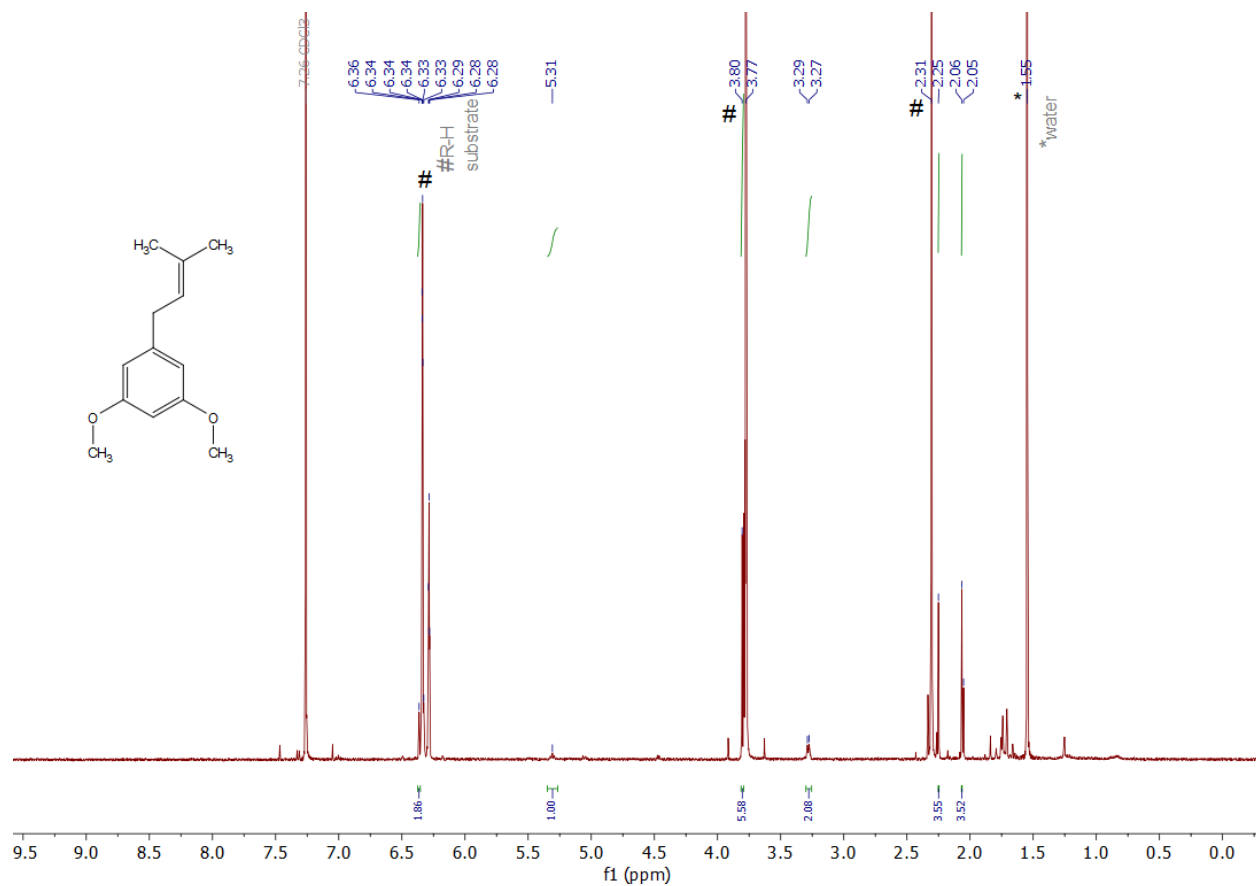
$^1$H NMR spectrum of **3f** (500 MHz, CDCl$_3$). Due to the low volatility of **3f**, trace amount of hexane could not be removed completely which appears in the $^1$H and $^{13}$C{$^1$H} NMR spectra. (*note as hexane.)
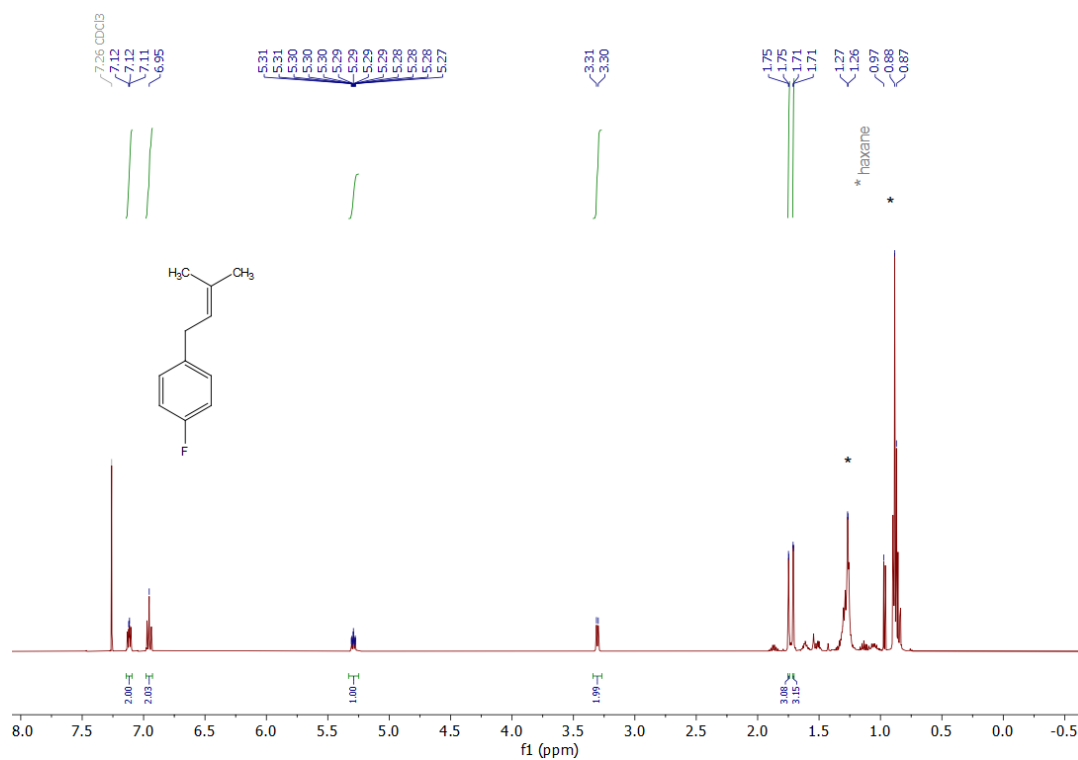


$^{13}$C{$^1$H} NMR spectrum of **3f** (126 MHz, CDCl$_3$).

<sup>1</sup>H NMR spectrum of **3g** (500 MHz, CDCl₃).
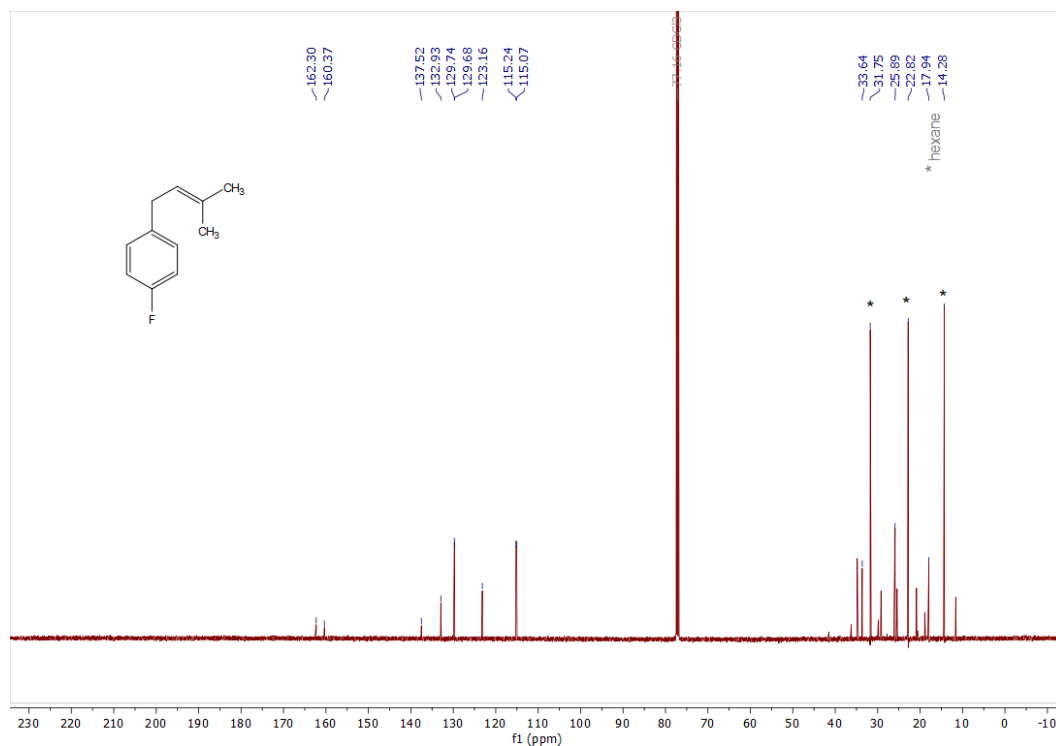
1H NMR spectrum of **3g** (500 MHz, CDCl₃).
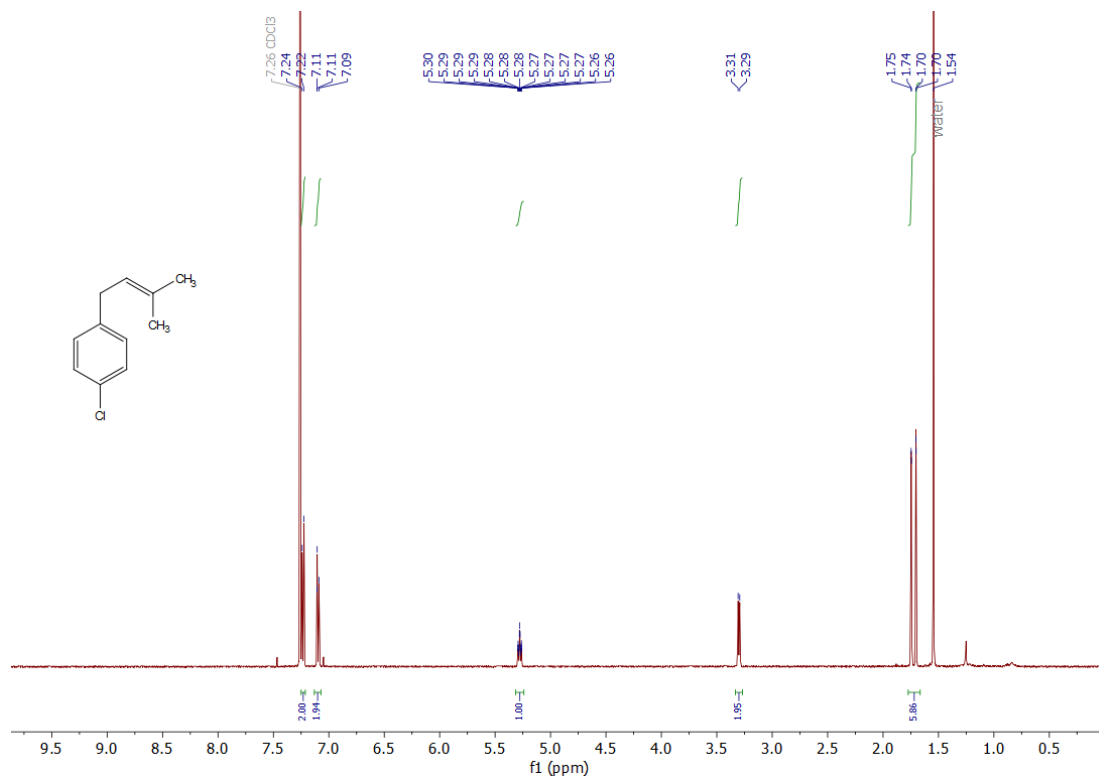


<sup>13</sup>C{<sup>1</sup>H} NMR spectrum of **3g** (126 MHz, CDCl₃).
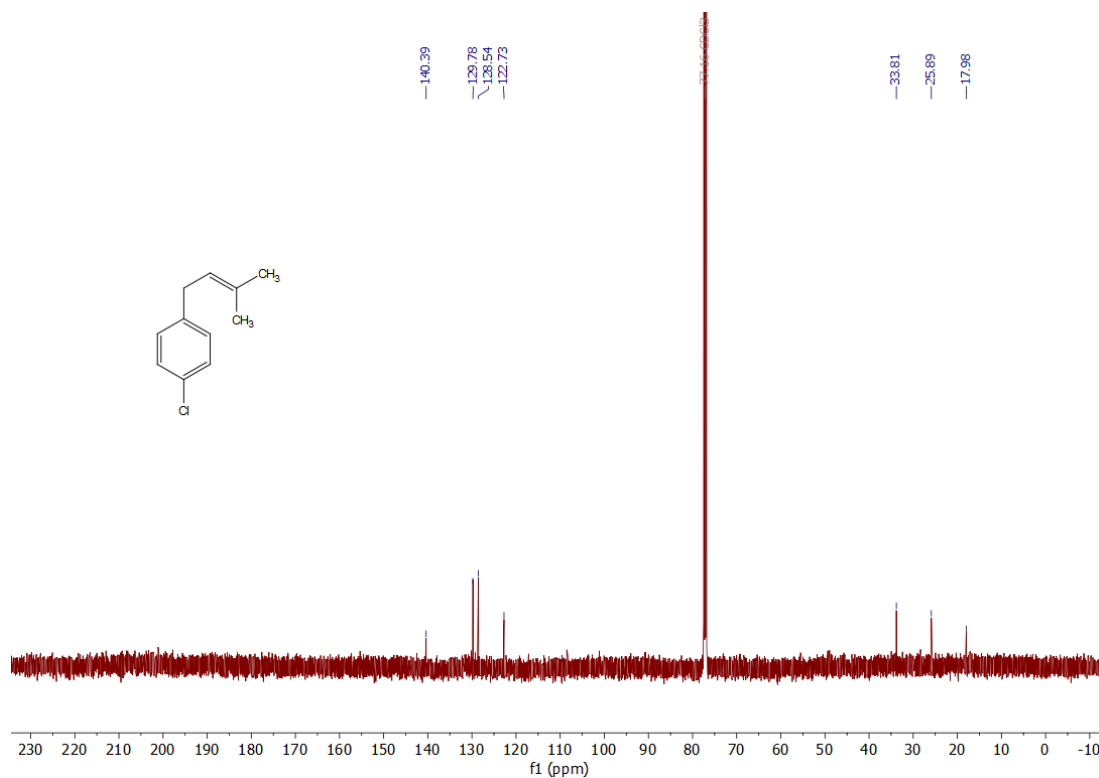
## $^1$H NMR spectrum of **3h** (500 MHz, CDCl$_3$).



## $^{13}$C{$^1$H} NMR spectrum of **3h** (126 MHz, CDCl$_3$).
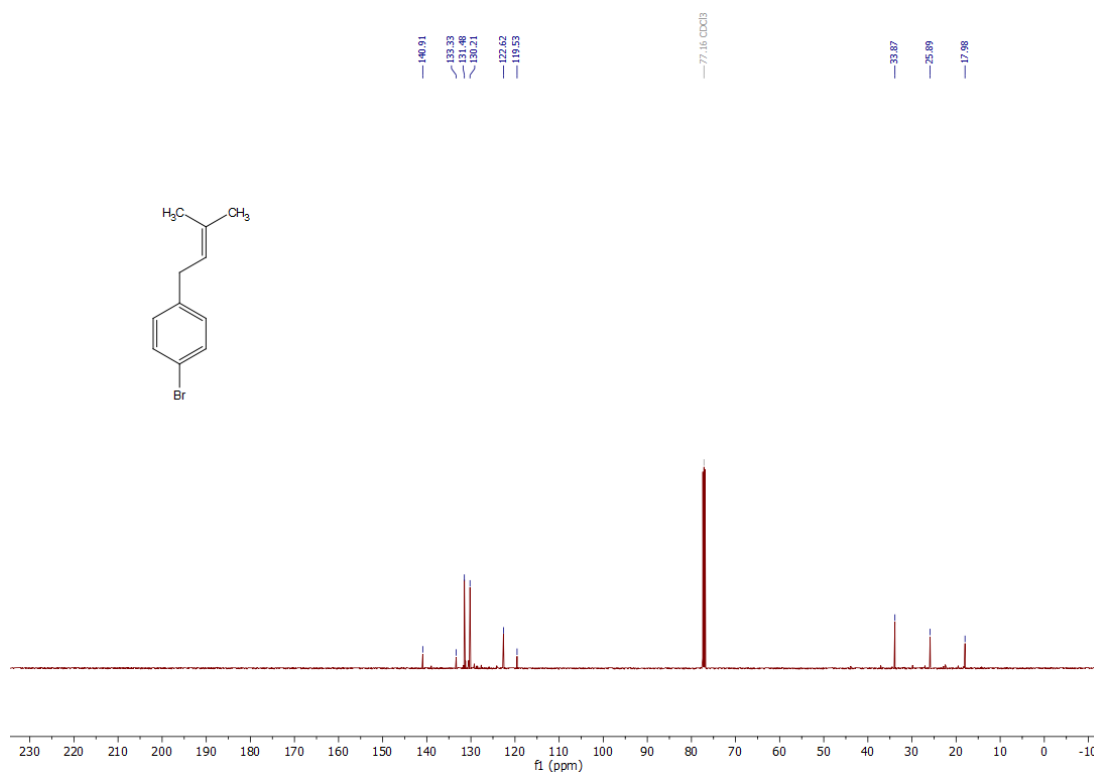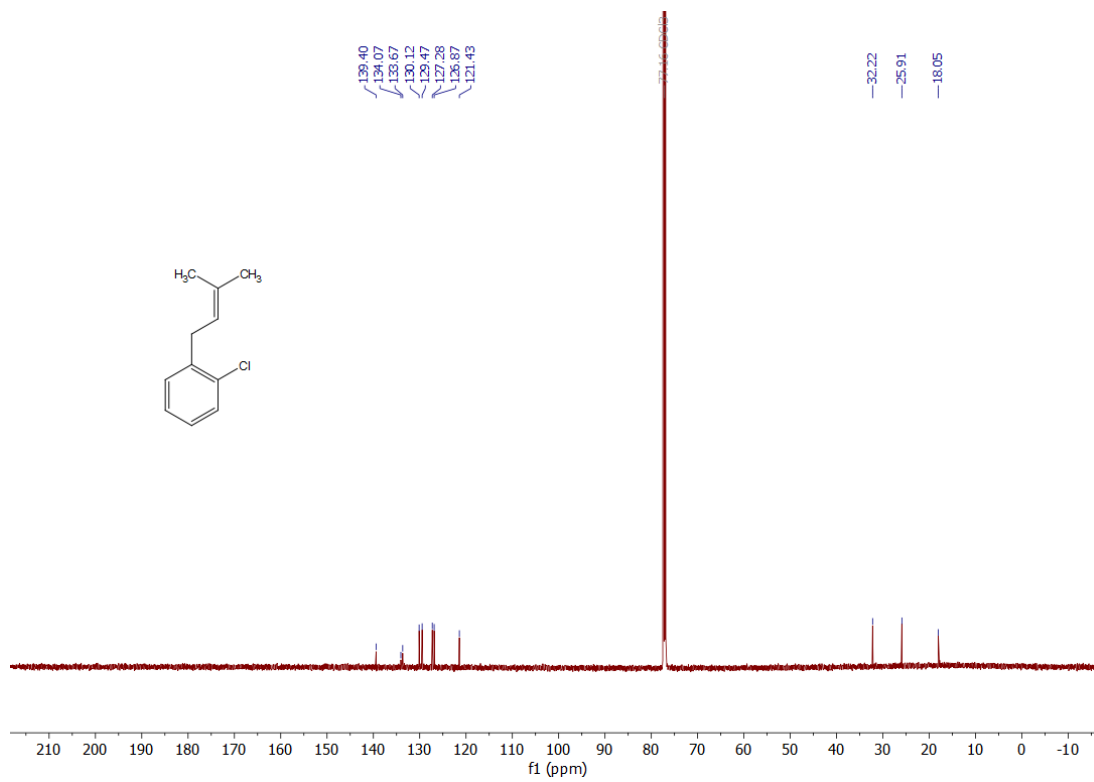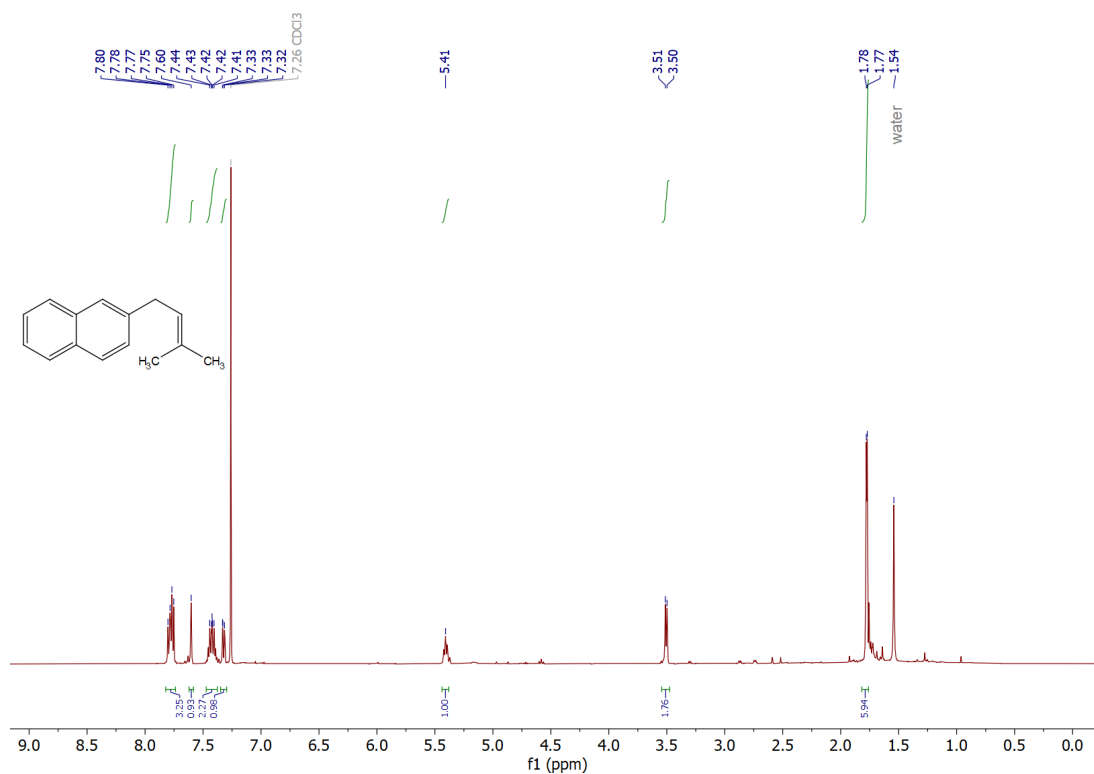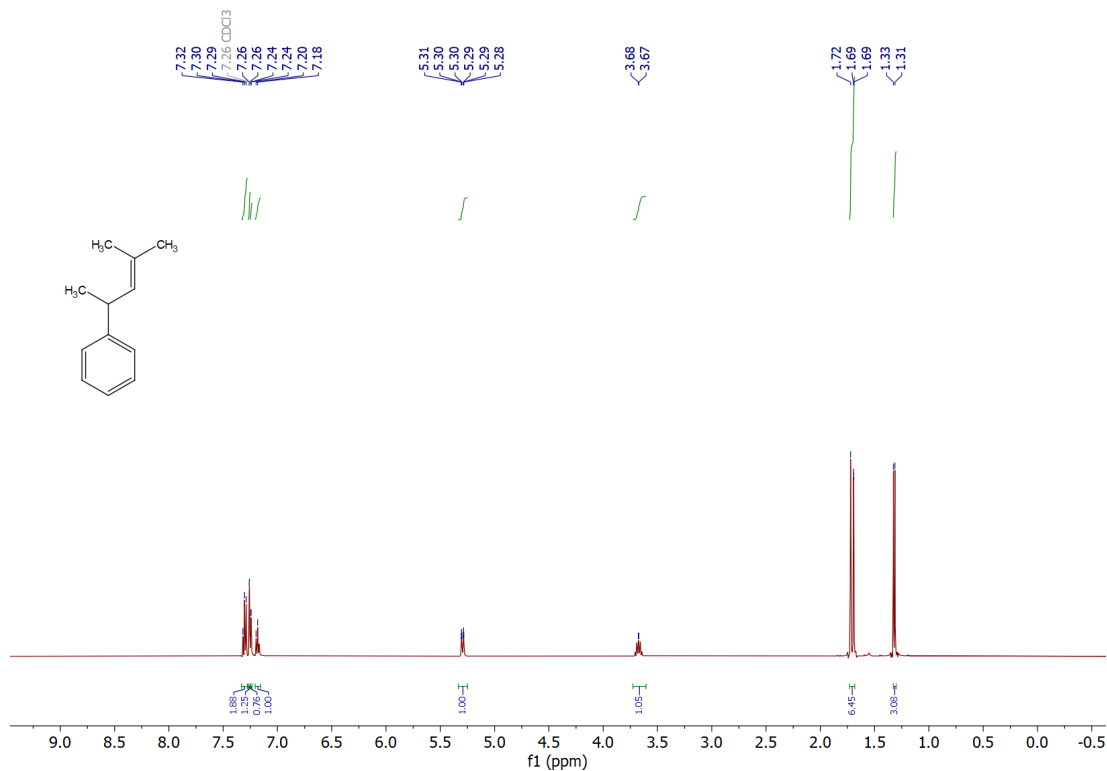
¹H NMR spectrum of **3i** (500 MHz, CDCl₃).



¹³C{¹H} NMR spectrum of **3i** (126 MHz, CDCl₃).

## ¹H NMR spectrum of **3j** (500 MHz, CDCl₃).



## ¹³C{¹H} NMR spectrum of **3j** (126 MHz, CDCl₃).

## $^1$H NMR spectrum of **3k** (500 MHz, CDCl$_3$).



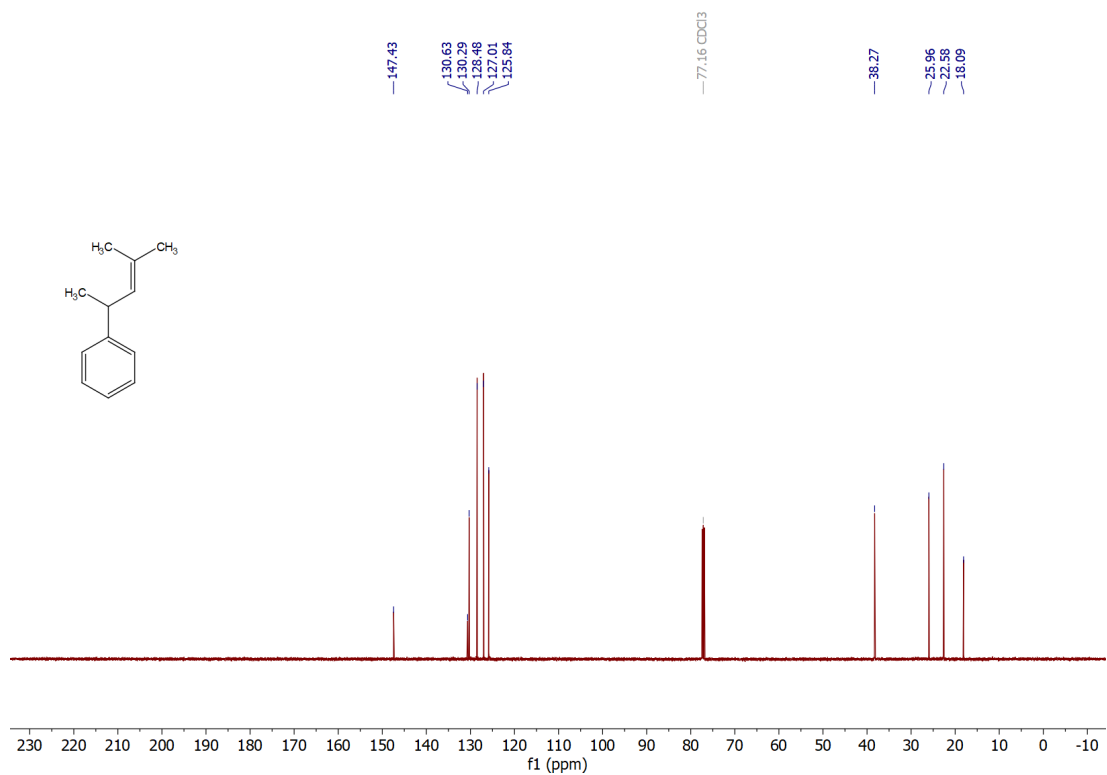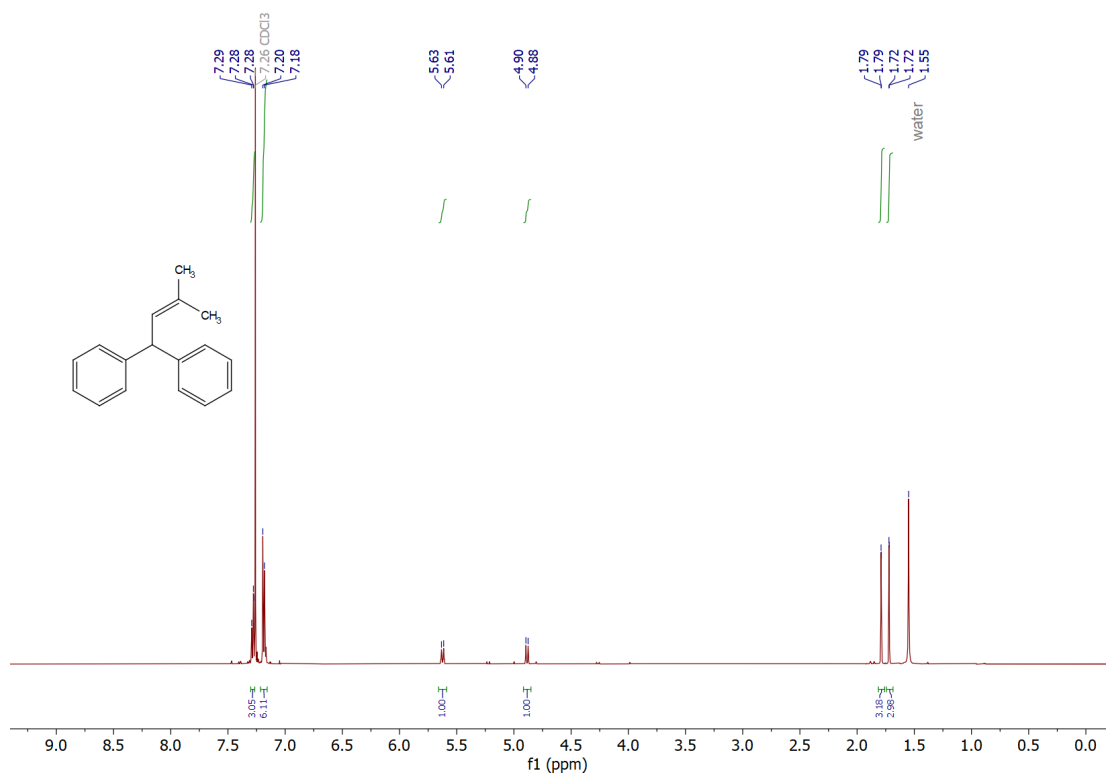## $^{13}$C{$^1$H} NMR spectrum of **3k** (126 MHz, CDCl$_3$).
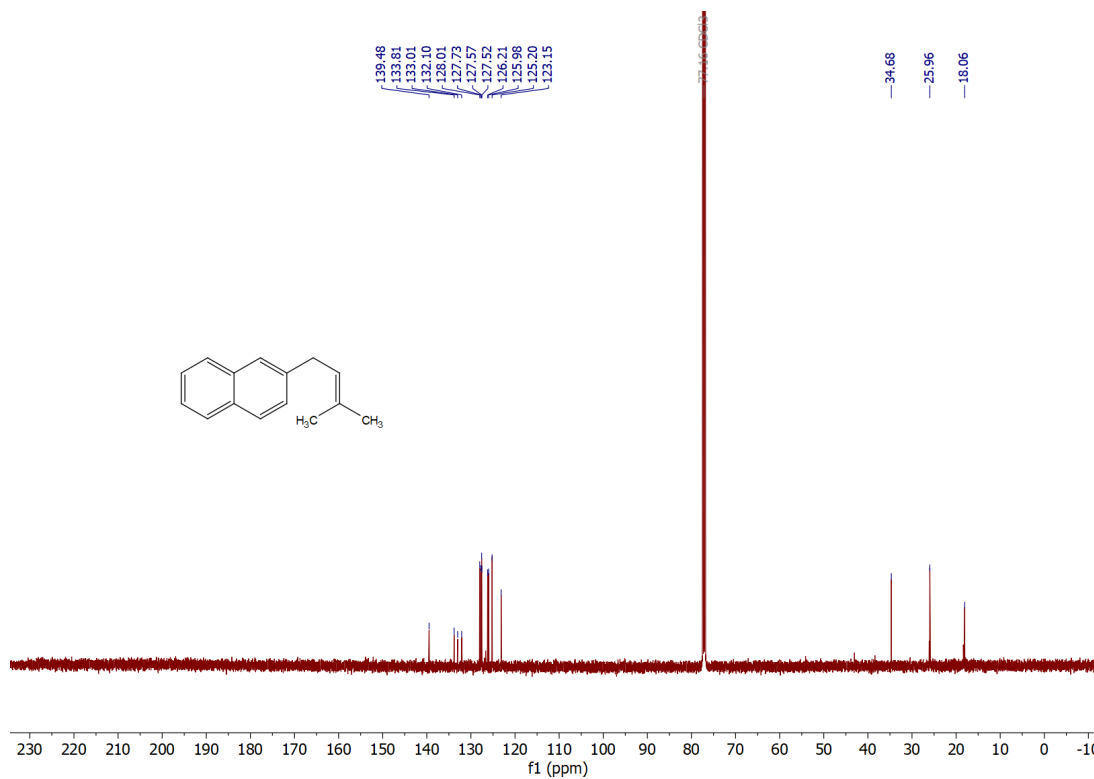
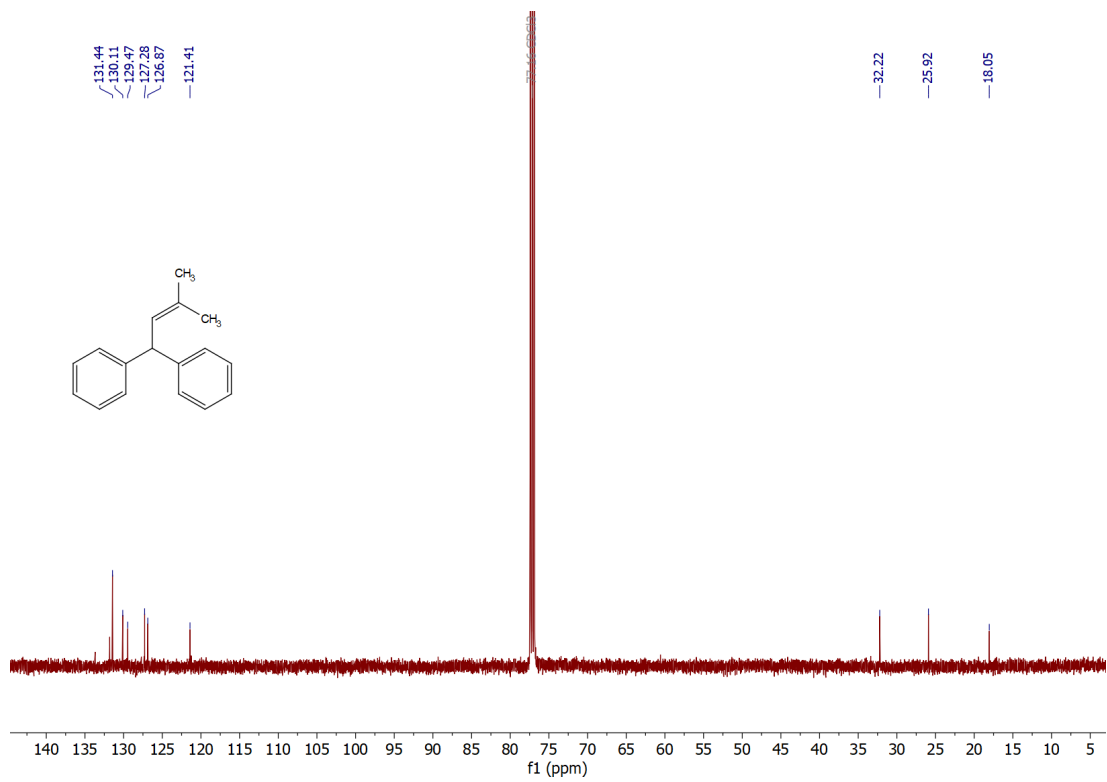<sup>1</sup>H NMR spectrum of **3l** from independent synthesis via Wittig reaction (500 MHz, CDCl<sub>3</sub>).



<sup>13</sup>C{<sup>1</sup>H} NMR spectrum of **3l** from independent synthesis via Wittig reaction (500 MHz, CDCl<sub>3</sub>).
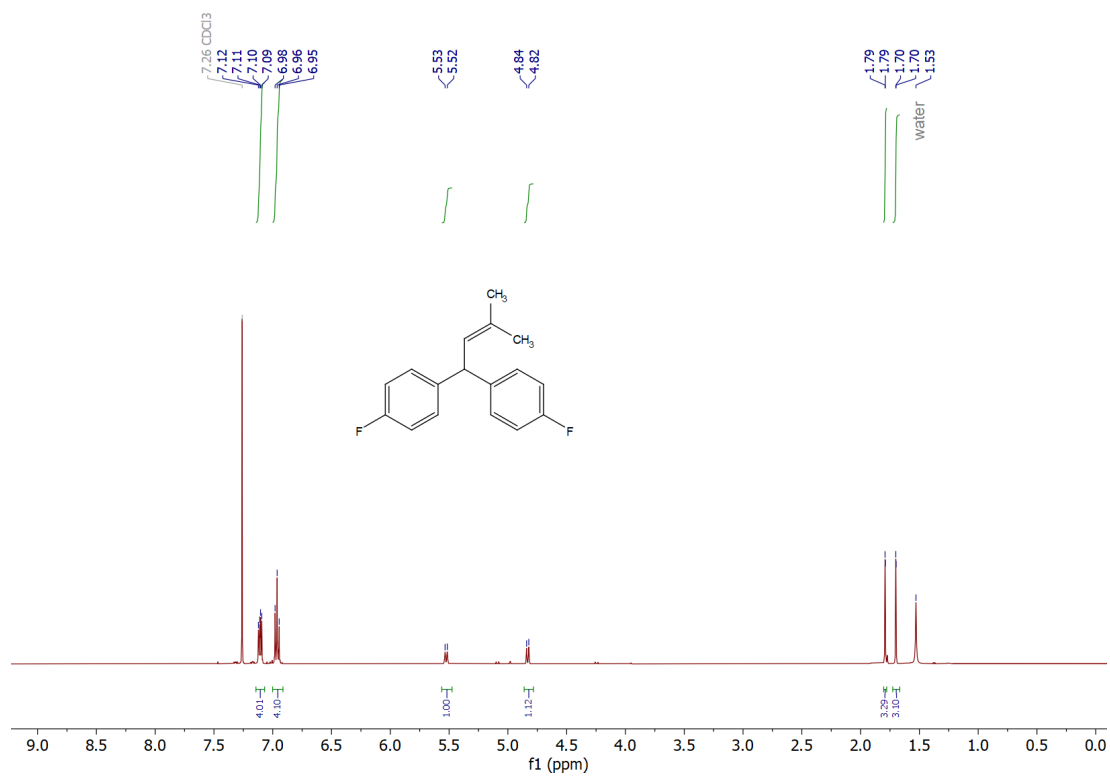
## $^1$H NMR spectrum of **3m** (500 MHz, CDCl$_3$).
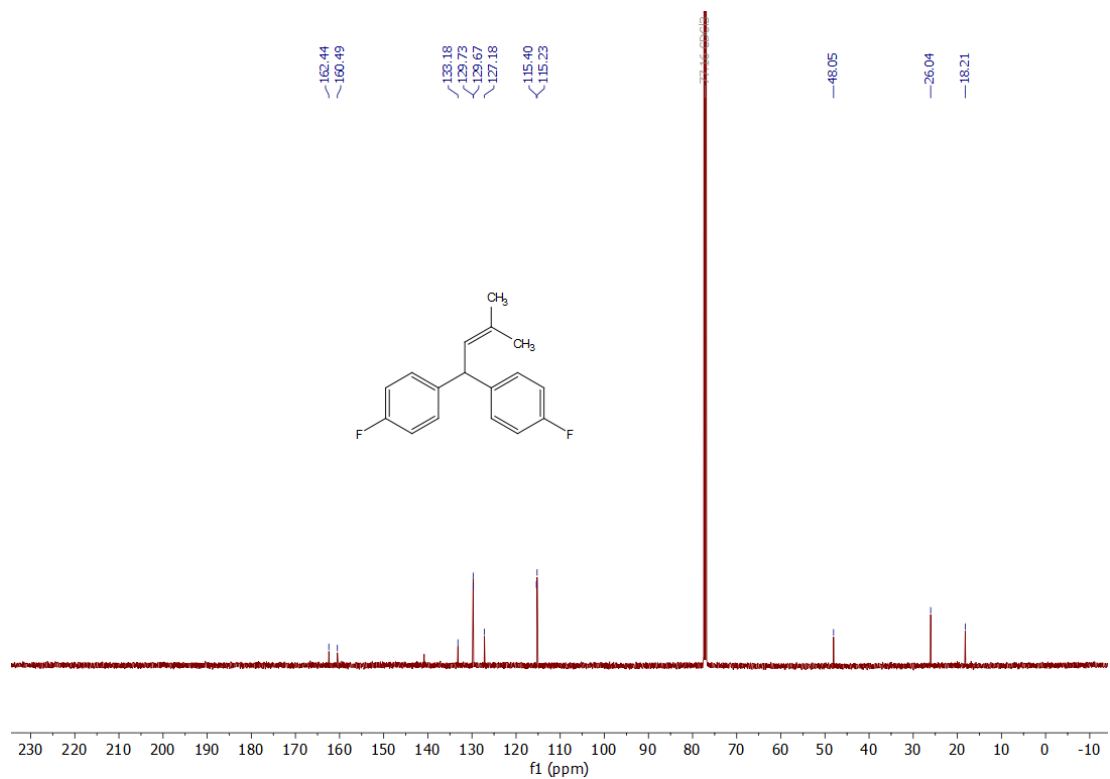


## $^{13}$C{$^1$H} NMR spectrum of **3m** (126 MHz, CDCl$_3$).

<sup>1</sup>H NMR spectrum of **3n** (500 MHz, CDCl$_3$).



<sup>13</sup>C{<sup>1</sup>H} NMR spectrum of **3n** (126 MHz, CDCl$_3$).

$^{19}$F{$^1$H} NMR spectrum of **3n** (126 MHz, CDCl$_3$). Fluorobenzene serves as the internal standard (δ = -113.15 ppm).
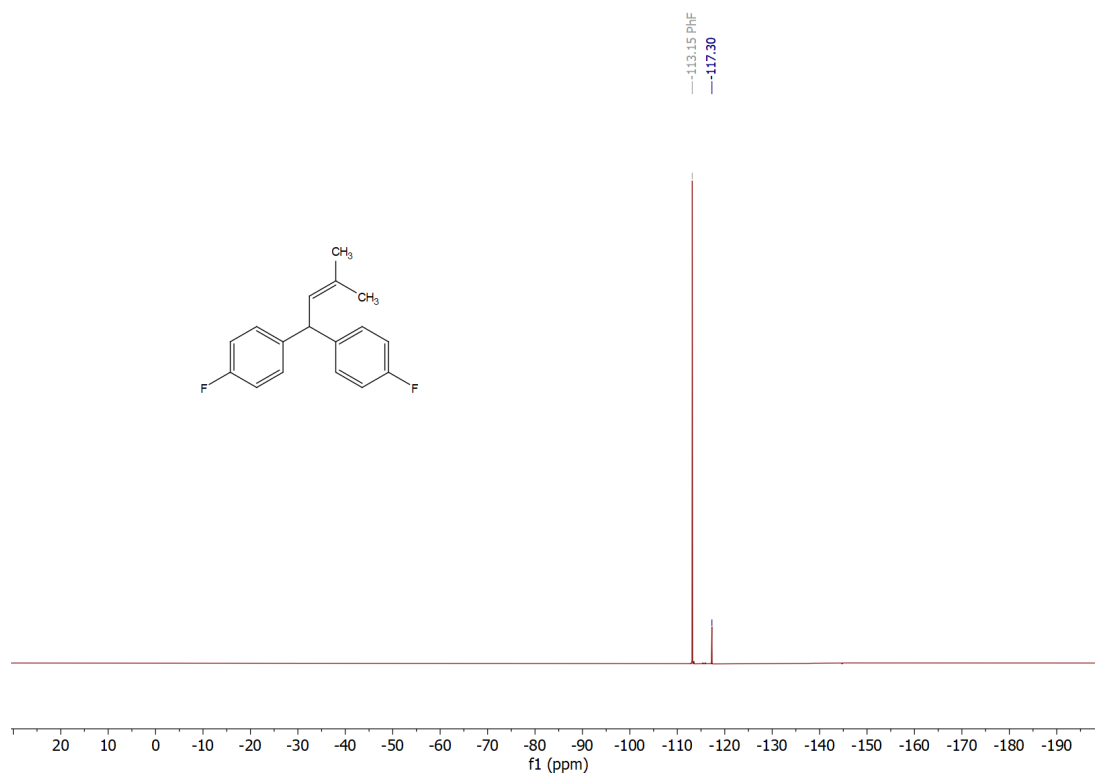
<sup>1</sup>H NMR spectrum of **3o** (500 MHz, CDCl<sub>3</sub>). Due to the separation challenge of **3m**, a significant amount of R-H substrate (N,N-dimethylaniline) could not be removed completely in <sup>1</sup>H NMR. (*note as R-H substrate).
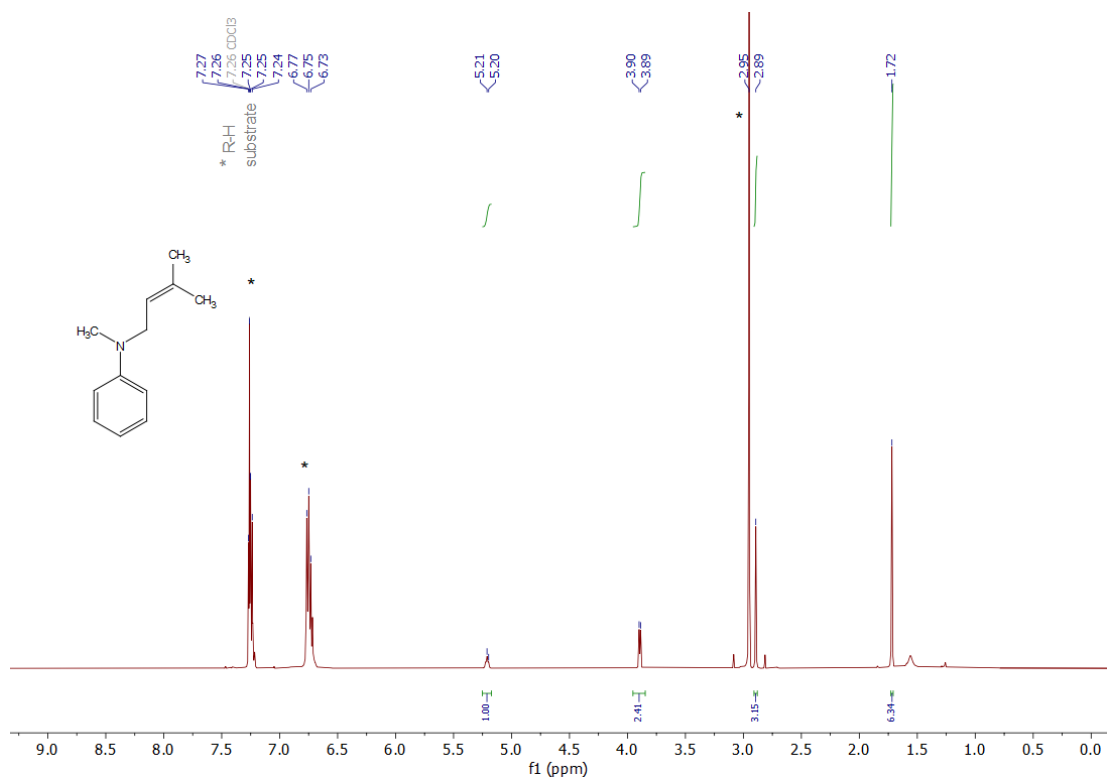
## ¹H NMR spectrum of **3p** (500 MHz, CDCl₃).
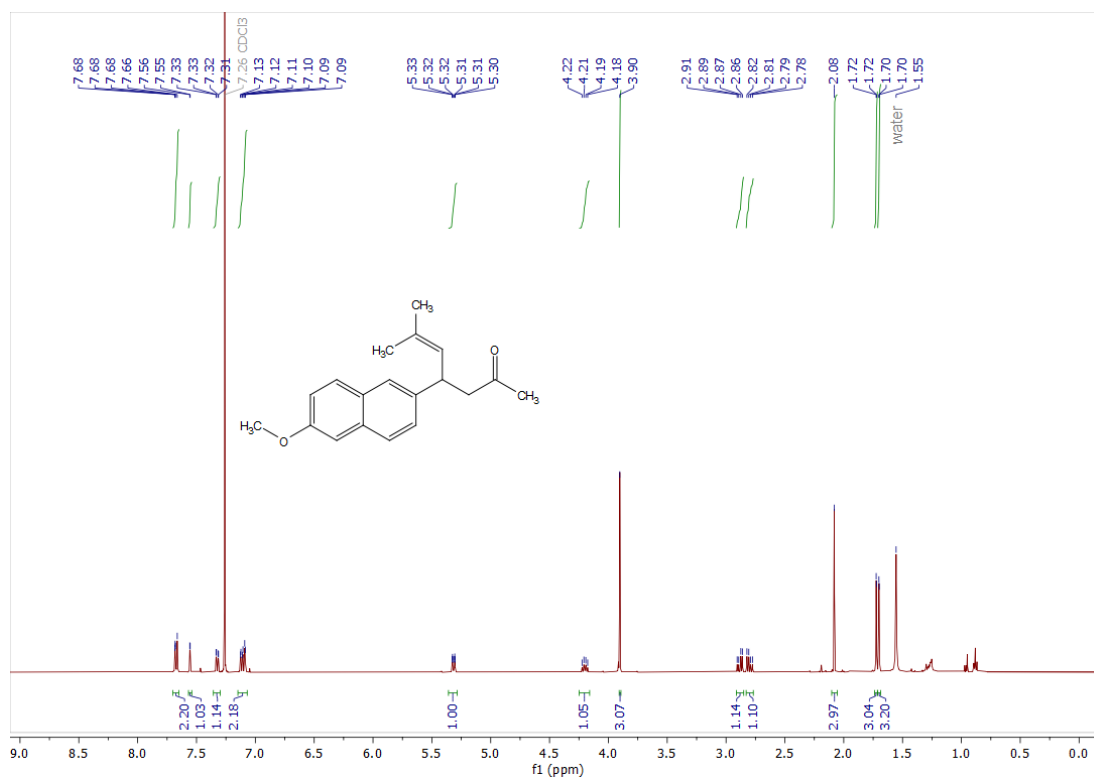


## ¹³C{¹H} NMR spectrum of **3p** (126 MHz, CDCl₃).
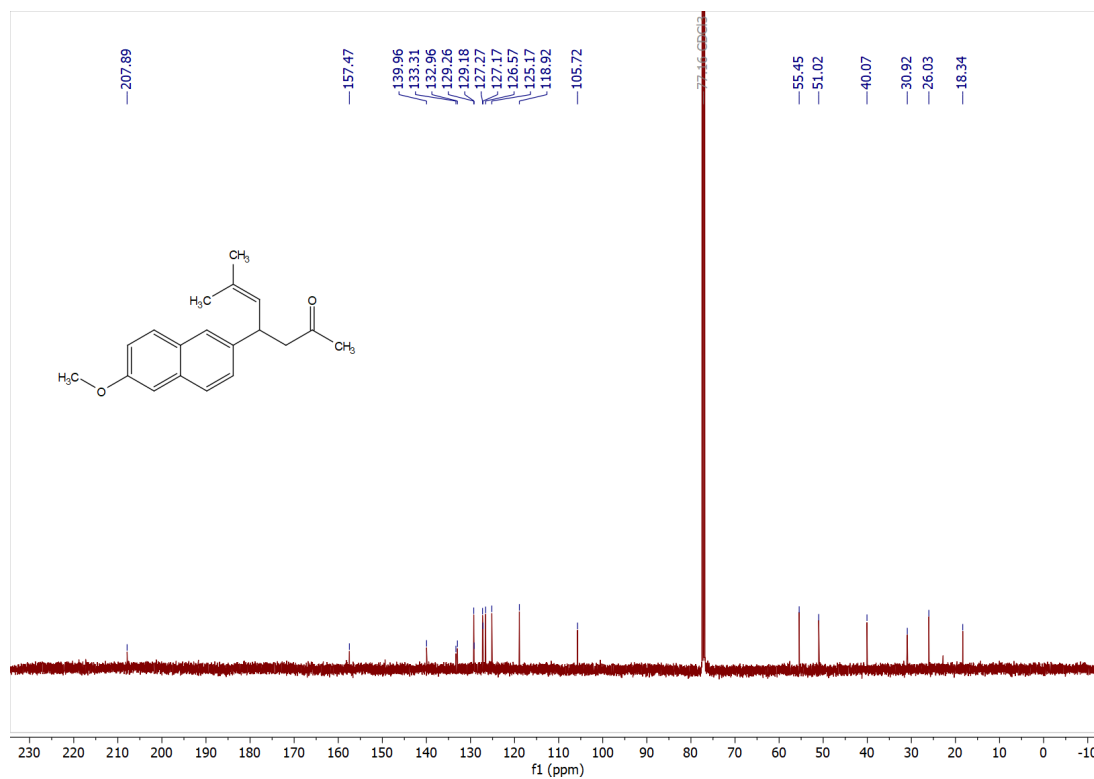
# <sup>1</sup>H NMR spectrum of **3q** (500 MHz, CD<sub>2</sub>Cl<sub>2</sub>).
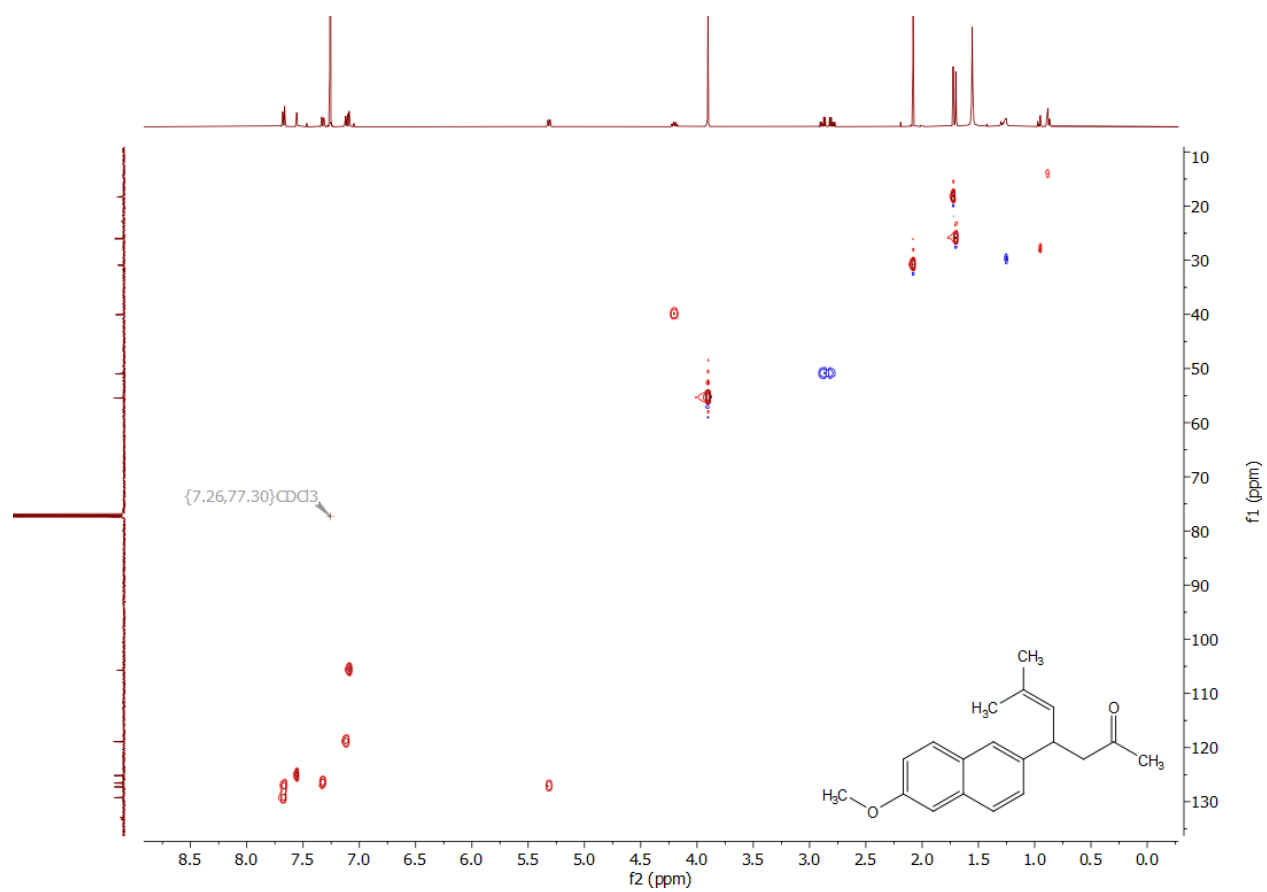
¹H NMR spectrum of **3q** (500 MHz, CD₂Cl₂).
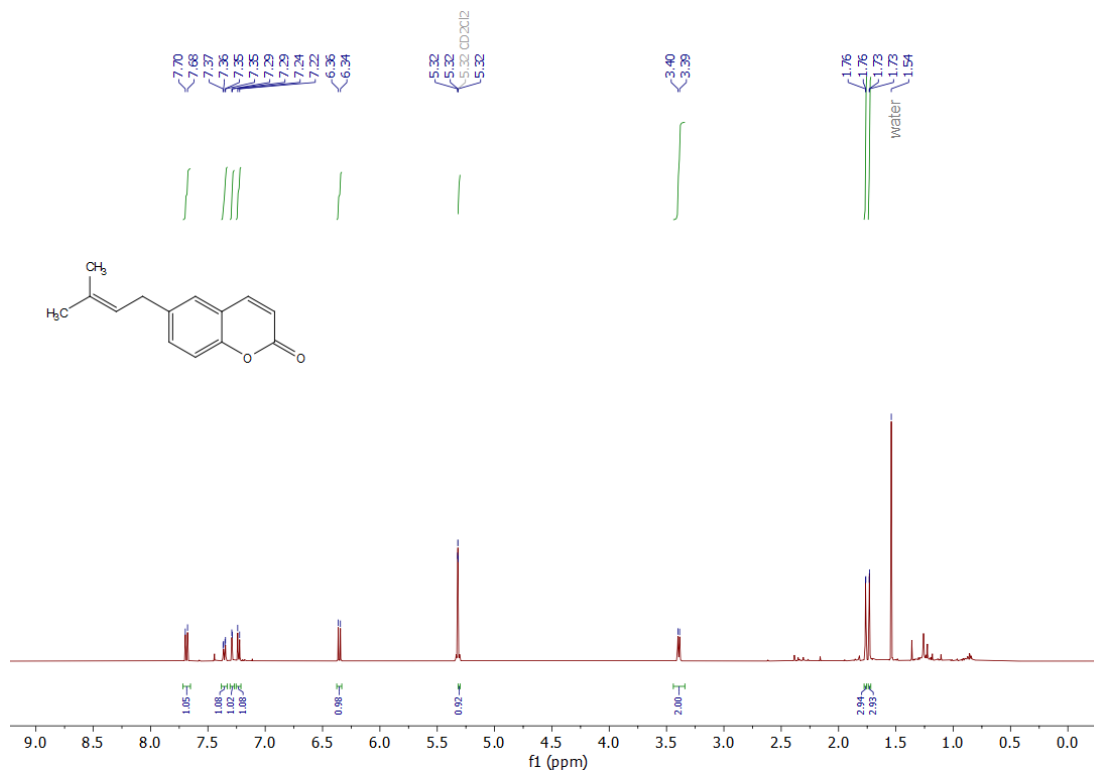


¹³C{¹H} NMR spectrum of **3q** (126 MHz, CD₂Cl₂).
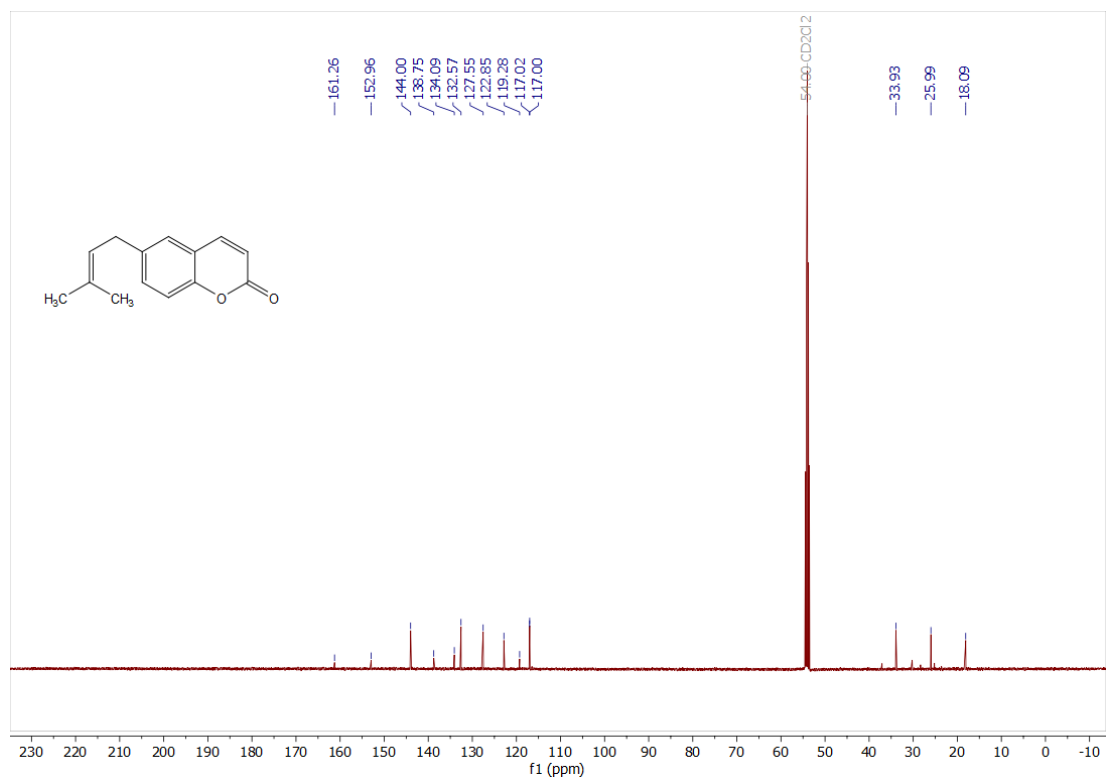
<sup>1</sup>H NMR spectrum of **3r** (500 MHz, CDCl₃).
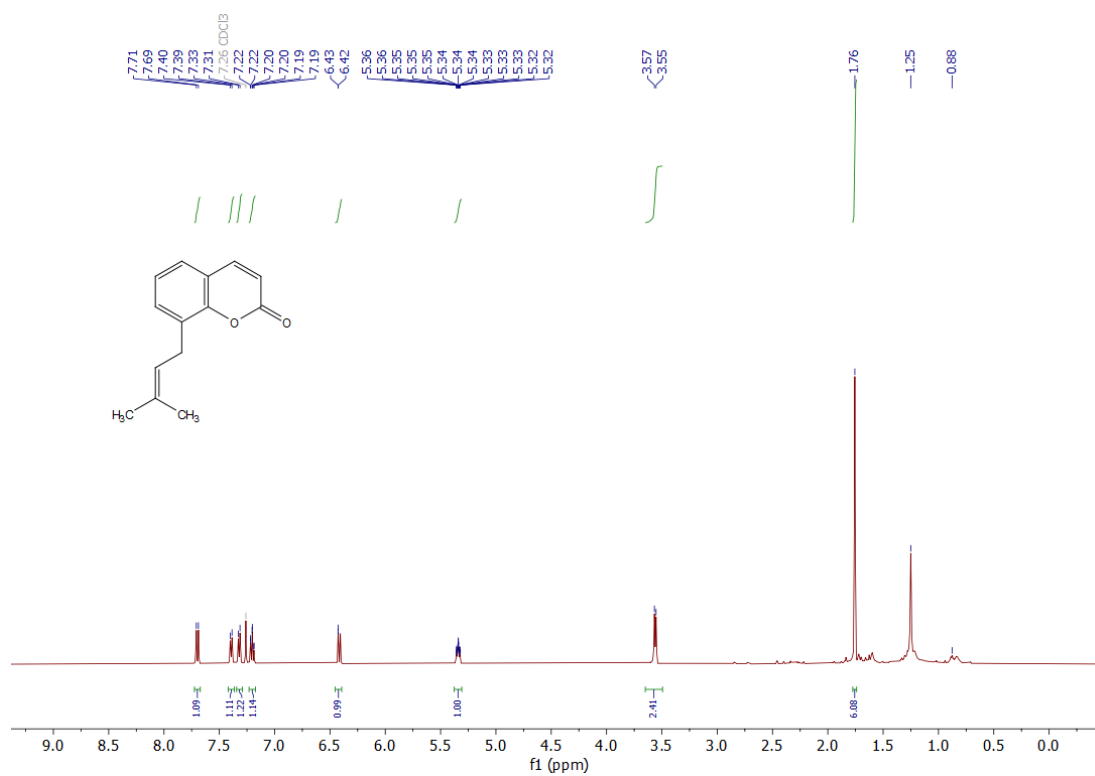


<sup>13</sup>C{<sup>1</sup>H} NMR spectrum of **3r** (126 MHz, CDCl₃).
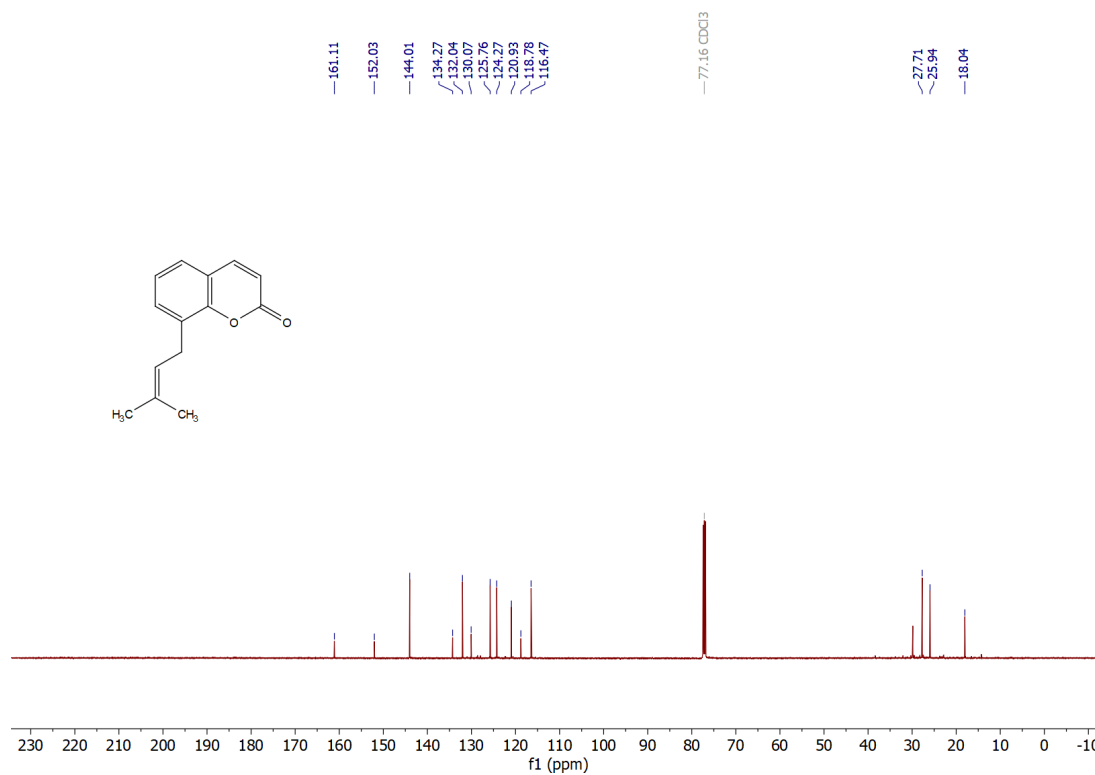
¹H NMR spectrum of (3-methylbut-2-ene-1,1,1-triyl)tribenzene (500 MHz, CDCl₃).



¹³C{¹H} NMR spectrum of (3-methylbut-2-ene-1,1,1-triyl)tribenzene (126 MHz, CDCl₃).

## 11. References

(1)    Badiei, Y. M.; Dinescu, A.; Dai, X.; Palomino, R. M.; Heinemann, F. W.; Cundari, T. R.; Warren, T. H. Copper–Nitrene Complexes in Catalytic C-H Amination. *Angew. Chem. Int. Ed.* **2008**, *47*, 9961–9964. https://doi.org/10.1002/anie.200804304.

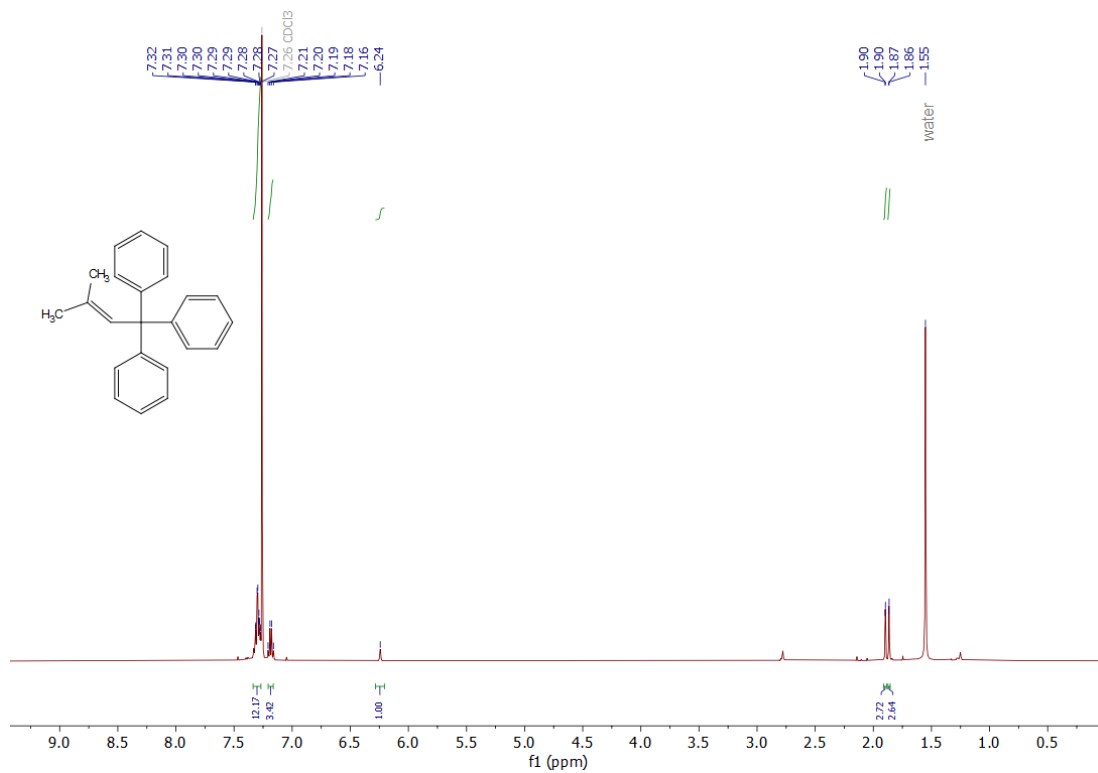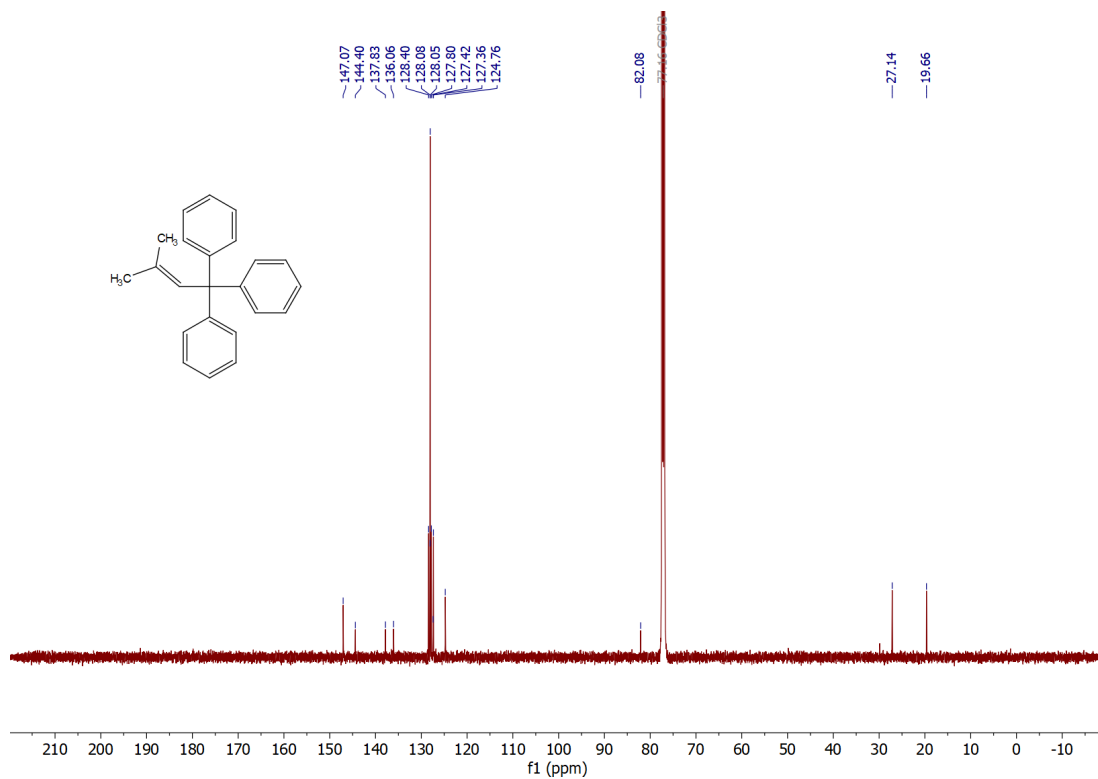(2)    Badiei, Y. M.; Warren, T. H. Electronic Structure and Electrophilic Reactivity of Discrete Copper Diphenylcarbenes. *J. Organomet. Chem* **2005**, *690*, 5989–6000. https://doi.org/10.1016/j.jorganchem.2005.07.098.

(3)    Bakhoda, A. (Gus); Jiang, Q.; Badiei, Y. M.; Bertke, J. A.; Cundari, T. R.; Warren, T. H. Copper-Catalyzed C(Sp3)–H Amidation: Sterically Driven Primary and Secondary C–H Site-Selectivity. *Angew. Chem. Int. Ed.* **2019**, *58*, 3421–3425. https://doi.org/10.1002/anie.201810556.

(4)    Sakhaei, Z.; Kundu, S.; Donnelly, J. M.; Bertke, J. A.; Kim, W. Y.; Warren, T. H. Nitric Oxide Release via Oxygen Atom Transfer from Nitrite at Copper(II). *Chem. Commun.* **2017**, *53*, 549–552. https://doi.org/10.1039/C6CC08745K.

(5)    Salvador, T. K.; Arnett, C. H.; Kundu, S.; Sapiezynski, N. G.; Bertke, J. A.; Raghibi Boroujeni, M.; Warren, T. H. Copper Catalyzed Sp3 C–H Etherification with Acyl Protected Phenols. *J. Am. Chem. Soc.* **2016**, *138*, 16580–16583. https://doi.org/10.1021/jacs.6b09057.

(6)    Vasilopoulos, A.; Zultanski, S. L.; Stahl, S. S. Feedstocks to Pharmacophores: Cu-Catalyzed Oxidative Arylation of Inexpensive Alkylarenes Enabling Direct Access to Diarylalkanes. *J. Am. Chem. Soc.* **2017**, *139*, 7705–7708. https://doi.org/10.1021/jacs.7b03387.

(7)    Xu, W.-L.; Zhang, H.; Hu, Y.-L.; Yang, H.; Chen, J.; Zhou, L. Metal-Free Dehydrogenative Diels–Alder Reactions of Prenyl Derivatives with Dienophiles via a Thermal Reversible Process. *Org. Lett.* **2018**, *20*, 5774–5778. https://doi.org/10.1021/acs.orglett.8b02469.

(8)    Tzeng, Y. L.; Yang, P. F.; Mei, N. W.; Yuan, T. M.; Yu, C. C.; Luh, T. Y. NiCl2(Dppe)-Catalyzed Geminal Dialkylation of Dithioacetals and Trimethylation of Ortho Thioesters. *J. Org. Chem.* **1991**, *56*, 5289–5293. https://doi.org/10.1021/jo00018a016.

(9)    Wright, S. W.; Hageman, D. L.; Wright, A. S.; McClure, L. D. Convenient Preparations of T-Butyl Esters and Ethers from t-Butanol. *Tetrahedron Lett.* **1997**, *38*, 7345–7348. https://doi.org/10.1016/S0040-4039(97)01792-9.

(10)   Delolo, F. G.; Fessler, J.; Neumann, H.; Junge, K.; dos Santos, E. N.; Gusevskaya, E. V.; Beller, M. Cobalt-Catalysed Reductive Etherification Using Phosphine Oxide Promoters under Hydroformylation Conditions. *Chem. Eur. J.* **2022**, *28*, e202103903. https://doi.org/10.1002/chem.202103903.

(11)   Rathnayake, M. D.; Weaver, J. D. A General Photocatalytic Route to Prenylation. *Eur. J. Org. Chem.* **2020**, *2020*, 1433–1438. https://doi.org/10.1002/ejoc.201900356.

(12)   Meimetis, L. G.; Nodwell, M.; Yang, L.; Wang, X.; Wu, J.; Harwig, C.; Stenton, G. R.; Mackenzie, L. F.; MacRury, T.; Patrick, B. O.; Ming-Lum, A.; Ong, C. J.; Krystal, G.; Mui, A. L.-F.; Andersen, R. J. Synthesis of SHIP1-Activating Analogs of the Sponge Meroterpenoid Pelorol. *Eur. J. Org. Chem.* **2012**, *2012*, 5195–5207. https://doi.org/10.1002/ejoc.201200631.

(13)   Suga, T.; Takahashi, Y.; Ukaji, Y. One-Shot Radical Cross Coupling Between Benzyl Alcohols and Alkenyl Halides Using Ni/Ti/Mn System. *Adv. Synth. Catal.* **2020**, *362*, 5622–5626. https://doi.org/10.1002/adsc.202000945.

(14)   Gansäuer, A.; Hildebrandt, S.; Michelmann, A.; Dahmen, T.; von Laufenberg, D.; Kube, C.; Fianu, G. D.; Flowers II, R. A. Cationic Titanocene(III) Complexes for Catalysis in Single-Electron Steps. *Angew. Chem. Int. Ed.* **2015**, *54*, 7003–7006. https://doi.org/10.1002/anie.201501955.

(15)   Tamura, S.; Fujitani, T.; Kaneko, M.; Murakami, N. Prenylcoumarin with Rev-Export Inhibitory Activity from Cnidii Monnieris Fructus. *Bioorg. Med. Chem. Lett.* **2010**, *20*, 3717–3720. https://doi.org/10.1016/j.bmcl.2010.04.081.

(16) Gephart, R. T. I.; McMullin, C. L.; Sapiezynski, N. G.; Jang, E. S.; Aguila, M. J. B.; Cundari, T. R.; Warren, T. H. Reaction of CuI with Dialkyl Peroxides: CuII-Alkoxides, Alkoxy Radicals, and Catalytic C–H Etherification. *J. Am. Chem. Soc.* **2012**, *134*, 17350–17353. https://doi.org/10.1021/ja3053688.

(17) Jang, E. S.; McMullin, C. L.; Käß, M.; Meyer, K.; Cundari, T. R.; Warren, T. H. Copper(II) Anilides in Sp3 C-H Amination. *J. Am. Chem. Soc.* **2014**, *136*, 10930–10940. https://doi.org/10.1021/ja5026547.

(18) CrysAlisPro Software System. Rigaku Oxford Diffraction, 2023.

(19) Sheldrick, G. M. SHELXT – Integrated Space-Group and Crystal-Structure Determination. *Acta Cryst A* **2015**, *71*, 3–8. https://doi.org/10.1107/S2053273314026370.

(20) Dolomanov, O. V.; Bourhis, L. J.; Gildea, R. J.; Howard, J. A. K.; Puschmann, H. OLEX2: A Complete Structure Solution, Refinement and Analysis Program. *J. Appl. Crystallogr.* **2009**, *42*, 339–341. https://doi.org/10.1107/S0021889808042726.

(21) Sheldrick, G. M. Crystal Structure Refinement with SHELXL. *Acta Cryst C* **2015**, *71*, 3–8. https://doi.org/10.1107/S2053229614024218.

(22) *Citation | Gaussian.com*. https://gaussian.com/citation/ (accessed 2023-11-17).

(23) Becke, A. D. Density-Functional Exchange-Energy Approximation with Correct Asymptotic Behavior. *Phys. Rev. A* **1988**, *38*, 3098–3100. https://doi.org/10.1103/PhysRevA.38.3098.

(24) Perdew, J. P. Density-Functional Approximation for the Correlation Energy of the Inhomogeneous Electron Gas. *Phys. Rev. B* **1986**, *33*, 8822–8824. https://doi.org/10.1103/PhysRevB.33.8822.

(25) Marenich, A. V.; Cramer, C. J.; Truhlar, D. G. Universal Solvation Model Based on Solute Electron Density and on a Continuum Model of the Solvent Defined by the Bulk Dielectric Constant and Atomic Surface Tensions. *J. Phys. Chem. B* **2009**, *113*, 6378–6396. https://doi.org/10.1021/jp810292n.

(26) Grimme, S.; Ehrlich, S.; Goerigk, L. Effect of the Damping Function in Dispersion Corrected Density Functional Theory. *J. Comput. Chem.* **2011**, *32*, 1456–1465. https://doi.org/10.1002/jcc.21759.